November 2012

contact: qualif@mercator-ocean.fr

QuO Va Dis?
Quarterly Ocean Validation Display #10

Validation bulletin for July-August-September (JAS) 2012

Edition:
Marie Drévillon, Charly Régnier, Bruno Levier, Charles Desportes
(MERCATOR OCEAN/Production Dep./Products Quality)

Contributions :
Eric Greiner (CLS)
Jean-Michel Lellouche, Olivier Le Galloudec, Anne Daudin (MERCATOR OCEAN/ Production Dep./R&D)

Credits for validation methodology and tools:
Eric Greiner, Mounir Benkiran, Nathalie Verbrugge, Hélène Etienne (CLS)
Fabrice Hernandez, Laurence Crosnier (MERCATOR OCEAN)
Nicolas Ferry, Gilles Garric, Jean-Michel Lellouche (MERCATOR OCEAN)
Jean-Marc Molines (CNRS), Sébastien Theeten (Ifremer), Mélanie Juza (IMEDEA), the DRAKKAR and NEMO groups.
Nicolas Pene (ex-AKKA), Silvana Buarque (Météo-France), the BCG group (Météo-France, CERFACS)

Information on input data:
Christine Boone, Stéphanie Guinehut, Gaël Nicolas (CLS/ARMOR team)

Abstract

*This bulletin gives an estimate of the accuracy of MERCATOR OCEAN's analyses and forecast for the season of **July-August-September 2012**. It also provides a summary of useful information on the context of the production for this period. Diagnostics will be displayed for the global 1/12° (PSY4), global ¼° (PSY3), the Atlantic and Mediterranean zoom at 1/12° (PSY2), and the Iberia-Biscay-Ireland (IBI) monitoring and forecasting systems currently producing daily 3D temperature, salinity and current products. Surface Chlorophyll concentrations from the BIOMER biogeochemical monitoring and forecasting system are also displayed and compared with simultaneous observations.*

Table of contents

I Executive summary 4
II Status and evolutions of the systems 6
II.1. Short description and current status of the systems 6
II.2. Incidents in the course of JAS 2012 9
III Summary of the availability and quality control of the input data 10
III.1. Observations available for data assimilation 10
III.1.1. In situ observations of T/S profiles 10
III.1.2. Sea Surface Temperature 11
III.1.3. Sea level anomalies along track 11
III.2. Observations available for validation 12
IV Information on the large scale climatic conditions 12
V Accuracy of the products 15
V.1. Data assimilation performance 15
V.1.1. Sea surface height 15
V.1.2. Sea surface temperature 17
V.1.3. Temperature and salinity profiles 20
V.2. Accuracy of the daily average products with respect to observations 29
V.2.1. T/S profiles observations 29
V.2.2. SST Comparisons 38
V.2.3. Drifting buoys velocity measurements 39
V.2.4. Sea ice concentration 42
V.2.5. Closer to the coast with the IBI36V2 system: multiple comparisons 44
V.2.5.1. Comparisons with SST from CMS 44
V.2.5.2. Comparisons with in situ data from EN3/ENSEMBLE for JAS 2012 45
V.2.5.3. MLD Comparisons with in situ data 47
V.2.5.4. Comparisons with moorings and tide gauges 48
V.2.6. Biogeochemistry validation: ocean colour maps 50
VI Forecast error statistics 52
VI.1. General considerations 52
VI.2. Forecast accuracy: comparisons with observations when and where available 52
VI.2.1. North Atlantic region 52
VI.2.2. Mediterranean Sea 53
VI.2.3. Tropical Oceans, Indian, Global: what system do we choose in JAS 2012? 55
VI.3. Forecast verification: comparison with analysis everywhere 58
VII Monitoring of ocean and sea ice physics 61
VII.1. Global mean SST and SSS 61
VII.2. Surface EKE 62
VII.3. Mediterranean outflow 63
VII.4. Sea Ice extent and area 65
I Annex A 66
I.1. Table of figures 66

II Annex B 70
II.1. Maps of regions for data assimilation statistics 70
II.1.1. Tropical and North Atlantic 70
II.1.2. Mediterranean Sea 71
II.1.3. Global ocean 72
III Annex C 73
III.1. Quality control algorithm for the Mercator Océan drifter data correction (Eric Greiner) 73

I Executive summary

The Mercator Ocean global monitoring and forecasting system (MyOcean V1 global MFC) is evaluated for the **period July-August-September 2012**. The system's description of the **ocean water masses is very accurate on global average** and almost everywhere between the bottom and 200m. Between 0 and 500m departures from *in situ* observations **rarely exceed 1 °C and 0.2 psu** (mostly in high variability regions like the Gulf Stream or the Eastern Tropical Pacific). During this northern hemisphere summer season the systems display stratification weaknesses in the North Atlantic and North Pacific (resulting in cold biases in the surface layer especially in the global ¼° PSY3V3R1).

A **cold SST** (and 3DT) bias of 0.1 °C on average is observed all year long in the **high resolution global at 1/12°** (PSY4V1R3) which does not yet benefit from the bias correction scheme that is implemented in PSY3V3R1 and PSY2V4R2.

The temperature and salinity forecast have **significant skill** in many regions of the ocean in the 0-500m layer, but the signal is noisy.

The monitoring systems are generally very close to altimetric observations (global average of 6 cm residual RMS error). Future updates of the Mean Dynamic Topography will correct the local biases that are currently observed for instance in the Banda Sea, and hopefully will prevent the **degradation of the subsurface currents at the Equator**. The latter are unrealistic in both global systems, especially in the warm pools in the western equatorial Pacific and Atlantic.

The **surface currents** are underestimated in the mid latitudes and overestimated at the equator with respect to *in situ* measurements of drifting buoys (drifter velocities are corrected of windage and slippage with a method developed by Mercator Océan). The underestimation ranges from 20% in strong currents up to 60% in weak currents. On the contrary the orientation of the current vectors is well represented**. The 1/12° global currents are slightly closer to drifters' observations than ¼° global currents**, especially in equatorial countercurrents.

The high resolution North East Atlantic at 1/36° (IBI36V1) with no data assimilation is accurate on average. **Tidal and residual sea surface elevations are well represented**. Zones of intense tidal mixing are less accurate. The mixed layer is too shallow in the Bay of Biscay (the thermocline is too diffusive). The upwelling along the Iberian coasts is underestimated.

The sea ice concentrations are overestimated in the Arctic all year round in the global 1/12° PSY4V1R3 (unrealistic rheology). PSY3V3R1 **global ¼° sea ice concentrations are realistic** but there is still too much accumulation of ice in the Arctic, especially in the Beaufort Sea. The sea ice concentration is underestimated in the Barents Sea. Antarctic sea ice concentration is underestimated in austral winter (including JAS 2012) due to atmospheric forcing problems in PSY3V3R1. The global 1/12° PSY4V1R3 sea ice concentration is overestimated all year round in the Antarctic because of rheology problems.

The **large scale structures corresponding to specific biogeographic regions** (double-gyres, ACC, etc…) **are well reproduced** by the global biogeochemical model at 1° BIOMER. However there are **serious discrepancies especially in the Tropical band** due to overestimated vertical velocities. The latter are the source of anomalous levels of nitrates in the equatorial surface layer. O2, however, is close to climatological estimations. The seasonal cycle is realistic in most parts of the ocean. However **the timing of the blooms is not yet in phase with observations**.

II Status and evolutions of the systems

II.1. Short description and current status of the systems

PSY3V3R1 and PSY2V4R1 systems have been operated at MERCATOR OCEAN since 2010 December, 15th. These systems provide the version 1 products of the MyOcean global monitoring and forecasting centre. As reminded in Table 1 (and illustrated for PSY2 in Figure 1) the atmospheric forcing is updated daily with the latest ECMWF analysis and forecast, and a new oceanic forecast is run every day for both PSY3V3R1 and PSY2V4R1. This daily update of the forcing (referred to as PSY3QV3R1 and PSY2QV4R1) is not broadcasted by MyOcean (it will be for V2).
An updated version (or release) of PSY2 called PSY2V4R2 is operated since the end of June 2011 and replaces PSY2V4R1. The PSY2QV4R2 system also replaces the PSY2QV4R1 system. The improvements of this version have been described in *QuOVaDis?* #5 and are reminded in Table 1.

The latest scientific evolutions of the systems (in red in Table 1) were described in *QuOVaDis?* #2 and #5 and will not be detailed here. The PSY3V3R1 system is started in October 2006 from a 3D climatology of temperature and salinity (World Ocean Atlas Levitus 2005) while the PSY2V4R2 is started in October 2009. After a short 3-month spin up of the model and data assimilation, the performance of PSY3V3R1 has been evaluated on the 2007-2009 period (MyOcean internal calibration report, which results are synthesised in *QuOVaDis?* #2).

System name	Domain	resolution	Model version	Assimilation software version	Assimilated observations	Inter dependencies	Status of production
PSY3V3R1	Global	¼° on the horizontal, 50 levels on the vertical	ORCA025 LIM2 EVP NEMO 3.1 3-hourly atmospheric forcing from ECMWF, bulk CORE	SAM2 (SEEK Kernel) + IAU and bias correction	RTG-SST, SLA from Jason 1, Jason 2 and Envisat, in situ profile from CORIOLIS		Weekly 14-days forecast Daily update of atmospheric forcings for daily 7-day forecast PSY3QV3
PSY4V1R3	Global	1/12° on the horizontal, 50 levels on the vertical	ORCA12 LIM2 NEMO 1.09 Daily atmospheric forcing from ECMWF, bulk CLIO	SAM2 (SEEK Kernel) + IAU	RTG-SST, SLA from Jason 1, Jason 2 and Envisat, in situ profile from CORIOLIS		Weekly 7-day forecast
PSY2V4R2	Tropical, North Atlantic and Mediterranean Sea region	1/12° on the horizontal, 50 levels on the	NATL12 LIM2 EVP NEMO 3.1 3-hourly atmospheric	SAM2 (SEEK Kernel) + IAU and bias correction +	AVHRR-AMSR Reynold ¼° SST, SLA from Jason	Open boundary conditions from PSY3V3R1	Weekly Daily update of atmospheric forcings

		vertical	forcing from ECMWF, bulk CORE	new MDT CNES/CLS09 bias corrected + more observation error near coasts	1, Jason 2 and Envisat, in situ profile from CORIOLIS		PSY2QV4
IBI36V2	North East Atlantic and West Mediterranean Sea (Iberian, Biscay and Ireland) region	1/36° on the horizontal, 50 levels on the vertical	NEATL36 NEMO 2.3 3-hourly atmospheric forcing from ECMWF, bulk CORE, tides, time-splitting, GLS vertical mixing, corrected bathymetry, river runoffs from SMHI & Prévimer	none	none	Two weeks spin up initialized with PSY2V4R1 and open boundary conditions from PSY2V4R1	Weekly spin up two weeks back in time. Daily update of atmospheric forcings for daily 5-day forecast IBI36QV1 To be broadcasted starting from June 2011.
BIOMER	Global	1° on the horizontal, 50 levels on the vertical	PISCES, NEMO 2.3, offline	none	none	Two weeks hindcast with IR global forcing degraded at 1°	1-week average two weeks back in time.

Table 1 : Synthetic description of the Mercator Ocean operational systems. In red, the major upgrades with respect to previous versions (when existing).

The PSY4V1R3 system is delivering operational products since the beginning of 2010. It does not yet benefit from the latest scientific improvements of PSY3V3R1 and PSY2V4R2. The update of PSY4 is planned for the version 3 of MyOcean 2, which will be available in April 2013. This system delivers 7-day forecast (and not 14-day like PSY3V3R1 and PSY2V4R2).

The IBI36V1 system is described in QuO Va Dis? #5 and #6 (see also Table 1 and Figure 1). The nominal MyOcean production unit for IBI is Puertos Del Estado (Spain) while Mercator Océan produces the back up products. The Mercator Océan IBI system is officially operational since June 2011. The version IBI36V2 of the system is operated since December 2011 and is very similar to IBI36V1 except it uses realistic river runoffs from SHMI and Prévimer instead of climatological runoffs.

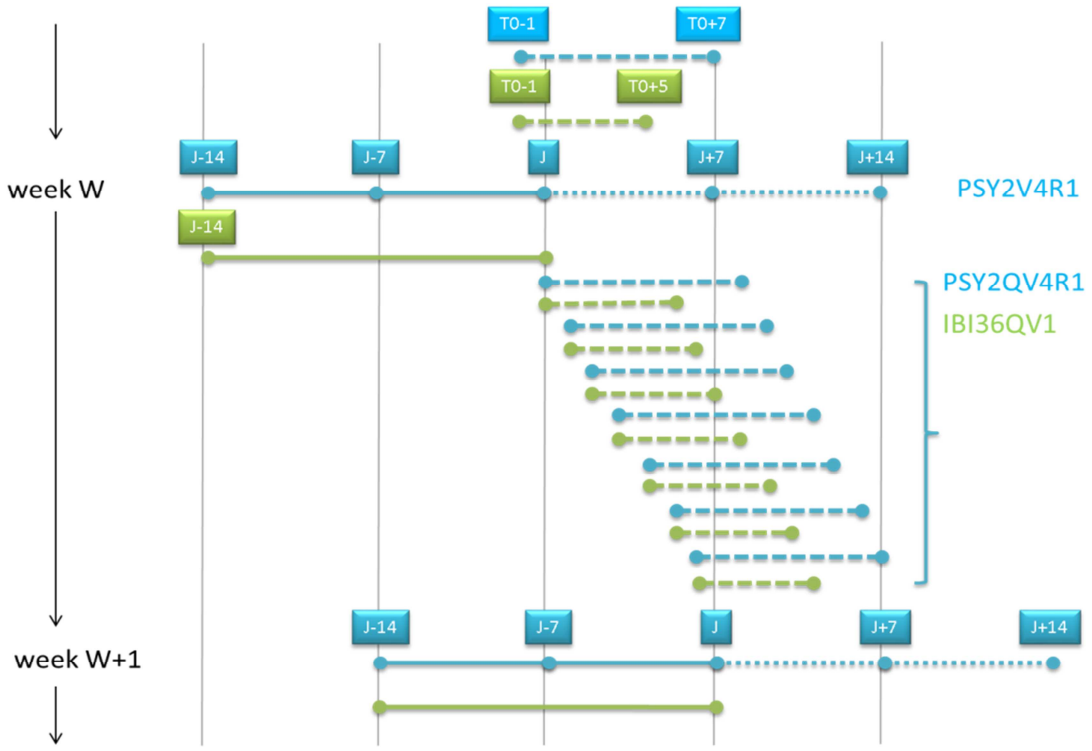

Figure 1: schematic of the operational forecast scenario for IBI36QV1 (green) and PSY2QV4R1 (blue). Solid lines are the PSY2V4R1 weekly hindcast and nowcast experiments, and the IBI36V1 spin up. Dotted lines are the weekly 14-day forecast, dashed lines are daily updates of the ocean forecast forced with the latest ECMWF atmospheric analysis and forecast. The operational scenario of PSY3V3R1 and PSY3QV3R1 is similar to PSY2's scenario. In the case of PSY4V1R3, only weekly hindcast, nowcast and 7-day forecast are performed.

The BIOMER system is described in QuO Va Dis? #6 (see also Table 1 and Figure 2). It is a global hindcast biogeochemical model forced by physical ocean fields. The biogeochemical model used is PISCES. The coupling between ocean physics and biogeochemistry is performed offline. The physical fields from PSY3V3R1 are "degraded" to 1° horizontal resolution and 7-day time resolution.

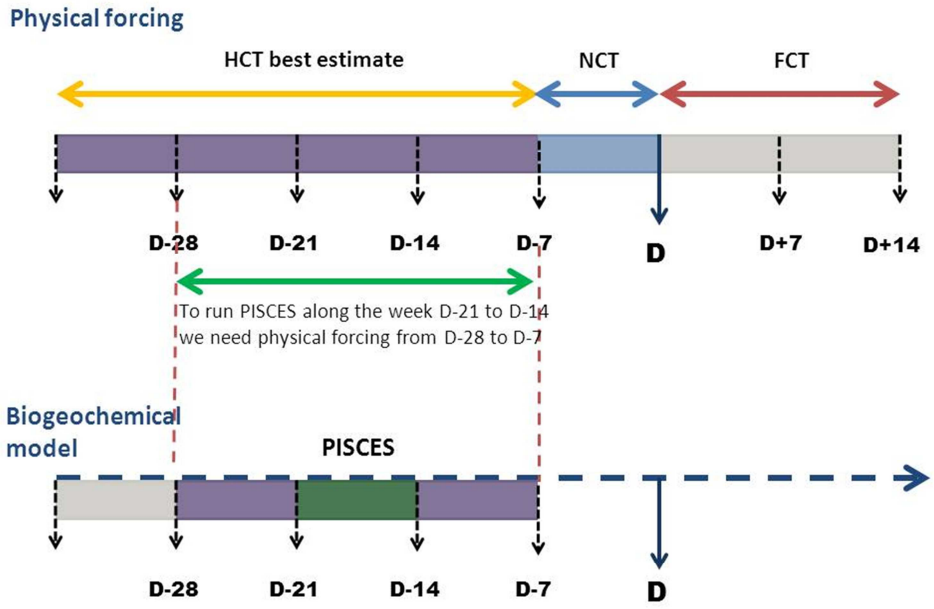

Figure 2: schematic of the operational forecast scenario for BIOMER..

An upgrade of the data assimilation systems was performed in March 2012 in order to assimilate MyOcean V2 altimetric observations and in situ observations (instead of respectively AVISO and CORIOLIS observations, corresponding to MyOcean V0 observations). In consequence, more in situ observations are assimilated in the European seas since March 2012.

II.2. Incidents in the course of JAS 2012

Two of the weekly IBI36V2 runs have been restarted due to numerical issues (the august 22nd and 29th runs). For reminder, these weekly runs are started from PSY2V4R2 initial conditions, and run two weeks in order to provide initial conditions for the IBI36V2 daily run on Thursdays. After some days of spin-up, the runs stopped due to unrealistic values of the physical parameters at one point of the model grid. This point is located in the Irish Sea, close to a cape with a steep bathymetry, an area where the model velocities can reach values of more than 3 meters per second. The two weekly runs have been restarted with an increased value of the parameter *shlat* (from 0.5 to 1) in a small region surrounding the critical point. Increasing the *shlat* parameter also increases the lateral friction of the model and consequently decreases the current velocities; the model is more stable. With this new value of *shlat*, the weekly runs have run normally. This incident already occurred with previous simulations of the IBI36 model, in the same region and during the same period of the year (summer). A steep bathymetry associated with summer specific stratification may be the cause of the model crash.

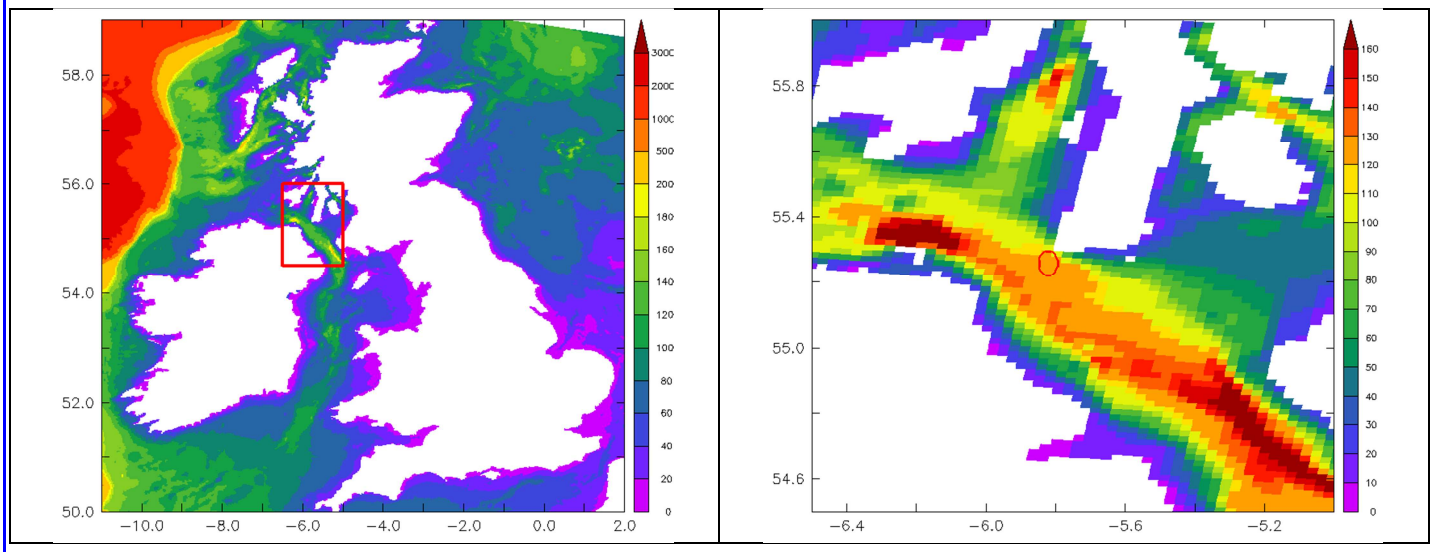

Figure 3: bathymetry (m) of IBI36V2R1. On the left : around British isles ; on the right : zoom on the red rectangle on the left figure. The red circle points out the point where the model crashes.

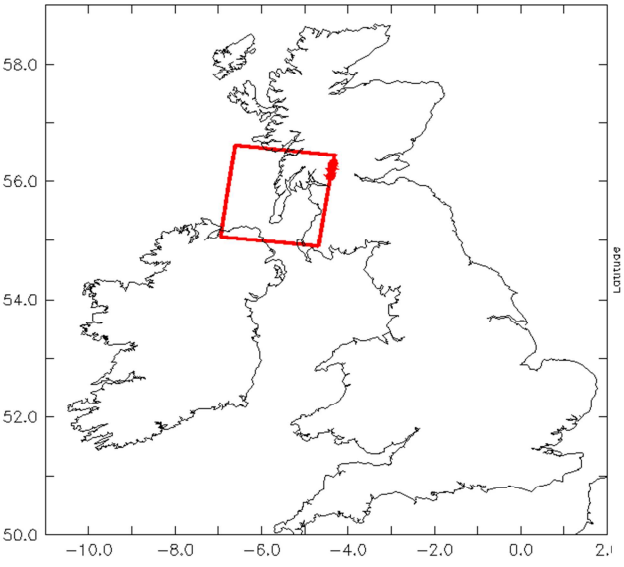

Figure 4 :the shlat parameter is changed inside the red zone

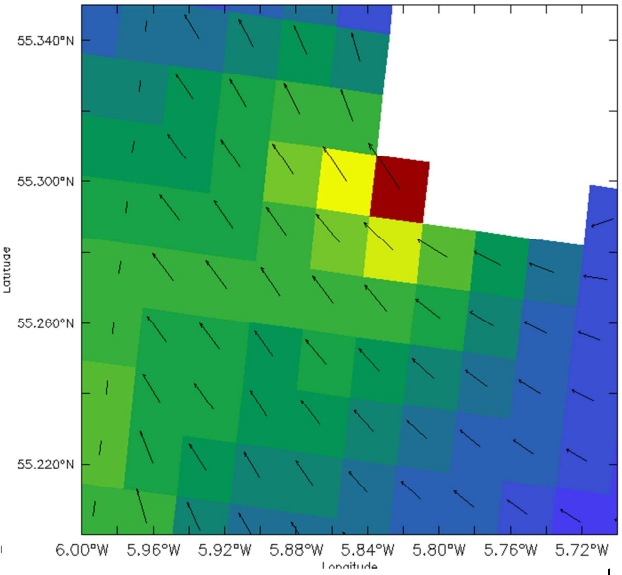

Figure 5 : surface velocities (m/s) on 29 August 2012.

III Summary of the availability and quality control of the input data

III.1. Observations available for data assimilation

III.1.1. In situ observations of T/S profiles

System	PSY3V3R1	PSY4V1R3	PSY2V4R2
Min/max number of T profiles per DA cycle	2000/3600	2000/3600	250/800

Min/max number of S profiles per DA cycle	2000/2800	2000/2800	250/400

Table 2: minimum and maximum number of observations (orders of magnitude of vertical profiles) of subsurface temperature and salinity assimilated weekly in JAS 2012 by the Mercator Ocean monitoring and forecasting systems.

As shown in Table 2 the maximum number of in situ observations is nearly similar to the previous quarter AMJ 2012 with slightly more salinity profiles (see QuO Va Dis? # 9). The number of observations higher in the second part of the quarter (Figure 6) and the maximum number of observations is reached in September.

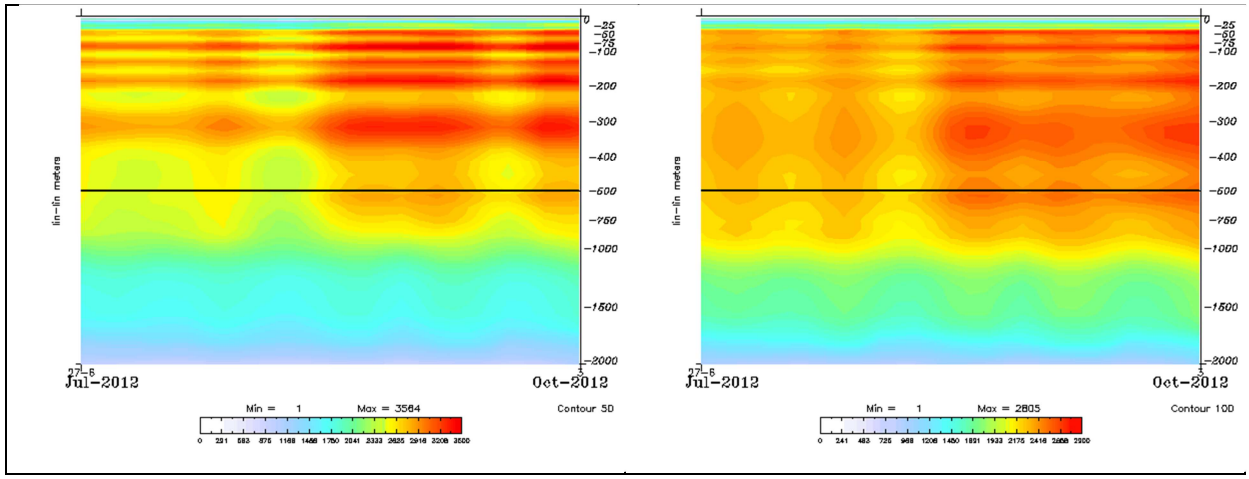

Figure 6 : Depth-time diagram of the number of observations of temperature (left column) and salinity (right column) assimilated each week in PSY3V3R1 during the JAS 2012 quarter.

III.1.2. Sea Surface Temperature

System	PSY3V3R1	PSY4V1R3	PSY2V4R2
Min/max number (in 10^3) of SST observations	174/179	176/179	26/27

Table 3: minimum and maximum number (orders of magnitude in thousands) of SST observations (from RTG-SST) assimilated weekly in JAS 2012 by the Mercator Ocean monitoring and forecasting systems.

RTG-SST is assimilated in PSY3V3R1 and PSY4V1R3, while the Reynolds ¼° "AVHRR only" product is assimilated in PSY2V4R2 in JAS 2012.

III.1.3. Sea level anomalies along track

As shown in Table 4 the data assimilated this JAS season come from Jason 1 G (for Geodetic, available since in the end of June), Jason 2 and Cryosat 2. Envisat stopped delivering data in the beginning of April, after 10 years of service.

system	PSY3V3R1	PSY4V1R3	PSY2V4R1
Min/max number (in 10^3) of Jason 2 SLA observations	83/89	83/89	15/16
Min/max number (in 10^3) of Jason 1 G SLA observations	89/94	89/94	16/18
Min/max number (in 10^3) of Cryosat 2 SLA observations	58/82	58/83	11/17

Table 4: minimum and maximum number (orders of magnitude in thousands) of SLA observations from Jason 2, Envisat and Jason 1 assimilated weekly in JAS 2012 by the Mercator Ocean monitoring and forecasting systems.

Note that depending on the satellite, the number of observations in the Antarctic circumpolar region is very different. For instance for PSY4V1R3, the median of the number of Jason 2 observations in this region is 30.10^3 while the median of Envisat observations was 22.10^3, that of Jason 1 G is 27.10^3 and that of Cryosat 2 is 20.10^3. In the Antarctic region, the number of Cryosat2 SLA observations is thus 30% lower than for contemporaneous SLA observations with other satellites (Jason 2 or Jason 1 G).

Users may witness side effects of the change of satellite cover, which is now less repetitive from one week to the other, due to the specific orbits of Jason 1G and Cryosat 2. Some discontinuities may appear locally, especially if one uses a time series of nowcast analyses.

III.2. Observations available for validation

Both observational data and statistical combinations of observations are used for the real time validation of the products. All were available in real time during the JAS 2012 season:

- T/S profiles from CORIOLIS
- OSTIA SST (with one problem on July 21st) from UKMO
- Arctic sea ice concentration and drift from CERSAT (with some delay on November 2nd)
- SURCOUF surface currents from CLS
- ARMOR-3D 3D temperature and salinity fields from CLS
- Drifters velocities from Météo-France reprocessed by CLS
- Tide gauges

Grodsky et al (GRL, May 2011) show that drifters velocities overestimate current velocities in regions and periods of strong winds due to undetected undrogued drifters. This information will be taken into account for comparisons with Mercator Ocean currents.

IV Information on the large scale climatic conditions

Mercator Ocean participates in the monthly seasonal forecast expertise at Météo France. This chapter summarizes the state of the ocean and atmosphere during the JAS 2012 season, as discussed in the “Bulletin Climatique Global” of Météo France.
This JAS 2012 season gave the first signs of an El Niño event in the Equatorial Pacific in July (not shown) but oceanic conditions finally turned back to normal in September (not shown). The equatorial Tropical Pacific Ocean was warmer than the climatology on average (Figure 7)

with positive temperature anomalies at depth in the eastern part of the basin (we show here the 0-300m layer) but negative temperature anomalies in the western part of the basin. Consistently with this cooling, a kelvin wave (upwelling) leaves the western Tropical Pacific in August and arrives in the eastern part of the basin in September (not shown). In the atmosphere the teleconnexions (especially the Pacific North American teleconnexion "PNA" in link with El Niño) are very weak.

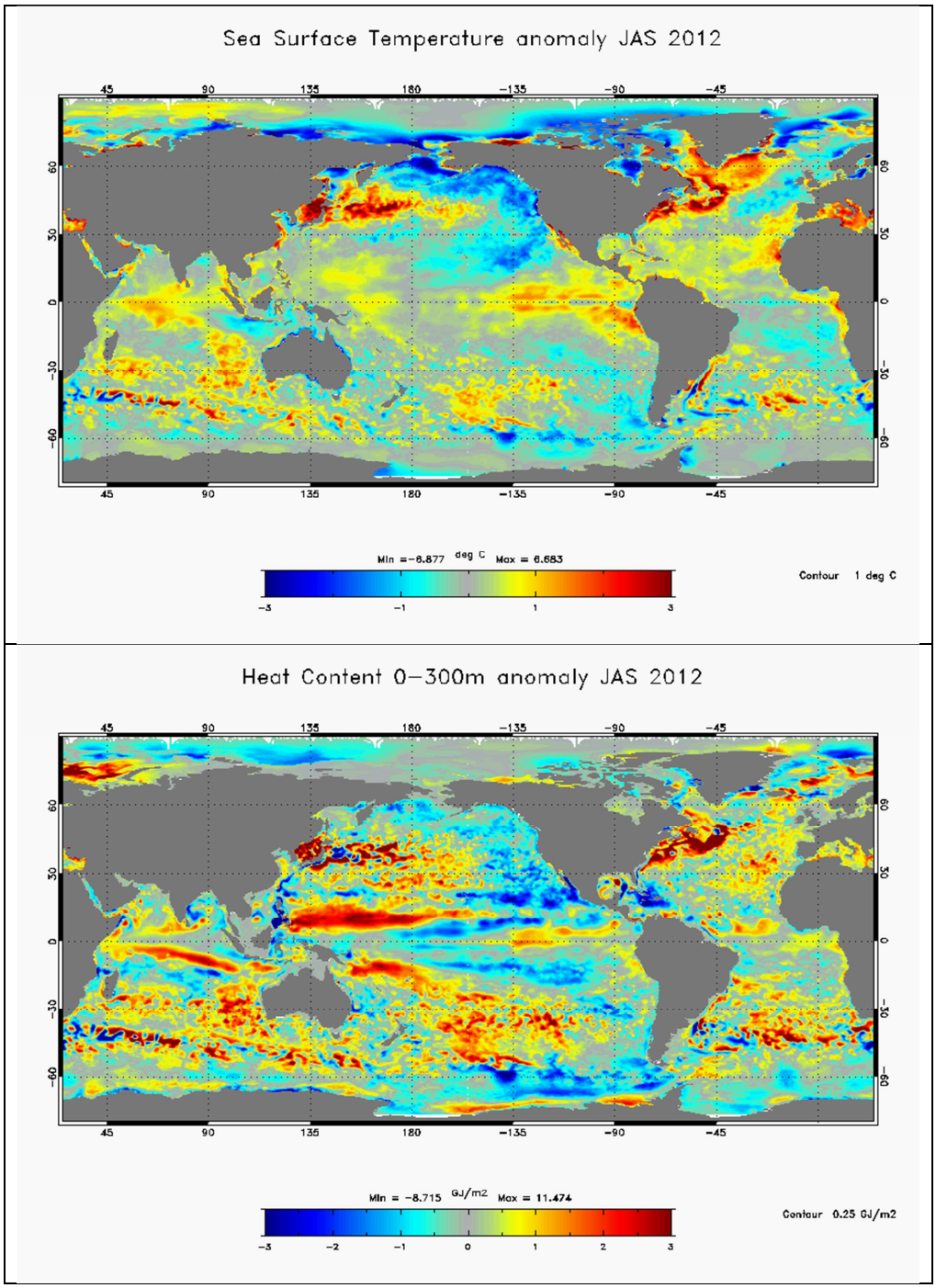

Figure 7: Seasonal JAS 2012 temperature anomalies with respect to WOA05 (World Ocean Atlas from Levitus 2005) climatology. Upper panel: SST anomaly (°C) at the global scale from the 1/4° ocean monitoring and forecasting system PSY3V3R1. Lower panel heat content anomaly ($\rho_0 C_p \Delta T$, with constant ρ_0=1020 kg/m3) from the surface to 300m.

The equator is also warmer than the climatology in the Indian Ocean. The whole basin experiences warmer than average SSTs, except the Indonesian region where atmospheric convective events slow down this season (less precipitations, not shown).

The anticyclonic atmospheric forcing on average over the Western North Atlantic (not shown) is consistent with the warmer than average Gulf Stream and subpolar gyre in the North Atlantic. Similarly, the strong warm anomalies in the Kuroshio region and surrounding cold anomalies in the eastern North Pacific are consistent with the atmospheric forcing.

In the North East Atlantic, colder than normal conditions are observed at the surface, while in subsurface the heat content anomaly is positive over most of the North Atlantic. SSTs are warmer than normal in the Mediterranean and along the Moroccan coasts this summer season.

South of 40°S in the southern ocean the SST conditions are close to the climatology this austral winter (no strong large scale signal) except for warm anomalies in the center of the South Pacific, South Atlantic and in the South Eastern Indian basin near 30°S-40°S.

As can be seen in Figure 8, the sea ice extent in the Arctic Ocean reaches a new historical minimum in September 2012. The sea ice extent is far less (one million square km) than in 2007, the previous historical minimum.

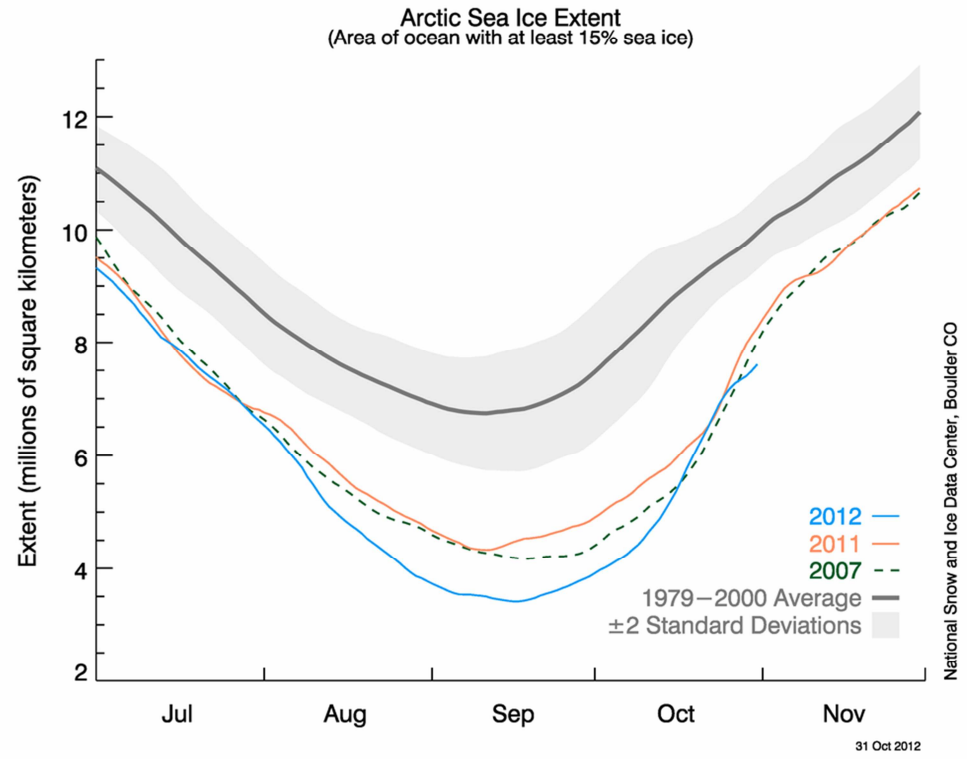

Figure 8: Arctic sea ice extent from the NSIDC: http://nsidc.org/arcticseaicenews/files/2000/11/Figure2.png

V Accuracy of the products

V.1. Data assimilation performance

V.1.1. Sea surface height

V.1.1.1. North Atlantic Ocean and Mediterranean Sea

The Tropical and North Atlantic Ocean SLA assimilation scores for all systems in JAS 2012 are displayed in Figure 9. The different systems (PSY4V1R3, PSY3V3R1, and PSY2V4R2) reach identical levels of performance on average. The biases are generally small (less than 2 cm) during this summer season. PSY2V4R2 exhibits positive biases (PSY2V4R2 is lower than SLA observations) in most regions. Note that prescribed errors are different in PSY2V4R2 and PSY4V1R3 which can explain different behaviours in spite of identical resolution. PSY2V4R2 assimilated fewer observations near the coasts, like in the Florida Strait region. Part of the biases can be attributed to local errors in the current mean dynamical topography (MDT). The RMS errors are almost identical in all systems, and stay below 10 cm in most regions, except regions of high mesoscale variability.

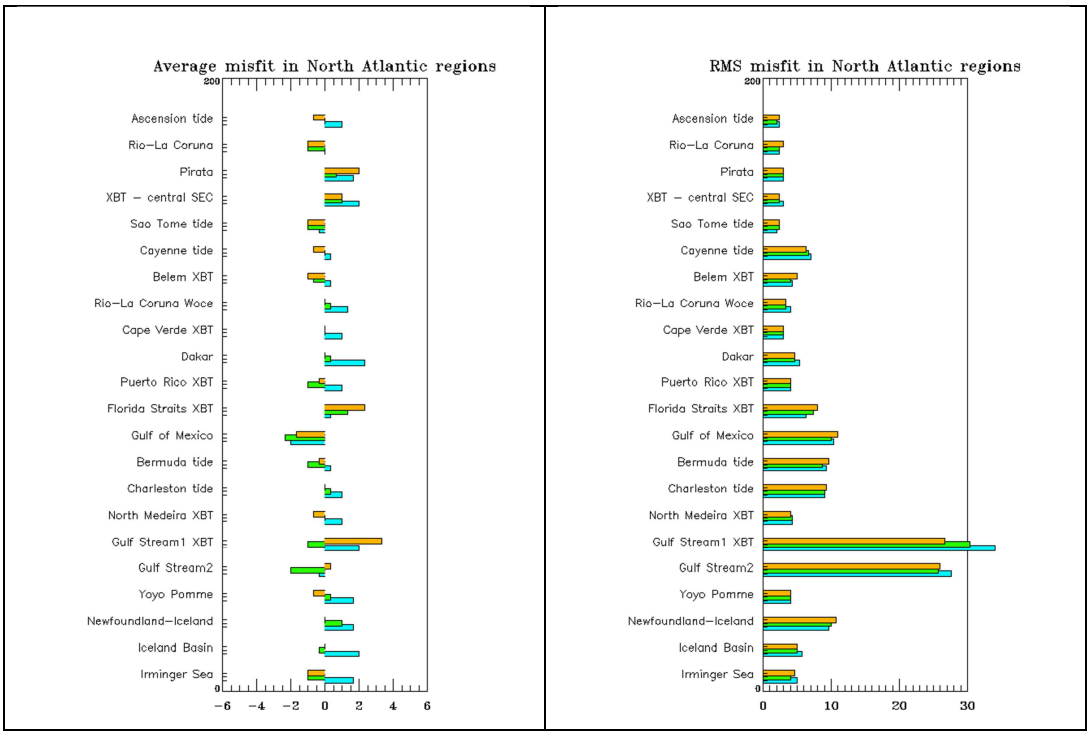

Figure 9: Comparison of SLA data assimilation scores (left: average misfit in cm, right: RMS misfit in cm) in JAS 2012 and between all available Mercator Ocean systems in the Tropical and North Atlantic. The scores are averaged for all available satellite along track data (Jason 1 G, Jason 2, Cryosat 2 and Envisat). For each region the bars refer respectively to PSY2V4R2 (cyan), PSY3V3R1 (green), PSY4V1R3 (orange). The geographical location of regions is displayed in annex A.

In the Mediterranean Sea biases of more than 6 cm are present in PSY2V4R2 in the Adriatic and Aegean Seas, while it is less than 4 cm in other regions, as can be seen in Figure 10. This bias is generally higher in summer and autumn seasons (from 6 to 8 cm). These regions are

circled by coasts, and consequently few observations are assimilated. The RMS of the innovation (misfit) of PSY2V4R2 is generally less than 10 cm. The western Mediterranean exhibits slightly better performance than the eastern Mediterranean. However in the eastern part of the basin, most of the RMS error is linked with the bias, and thus the variability is well represented.
The system still shows overall good performance as the RMS of the innovation is generally lower than the intrinsic variability of the observations in the North Atlantic and Mediterranean (not shown).

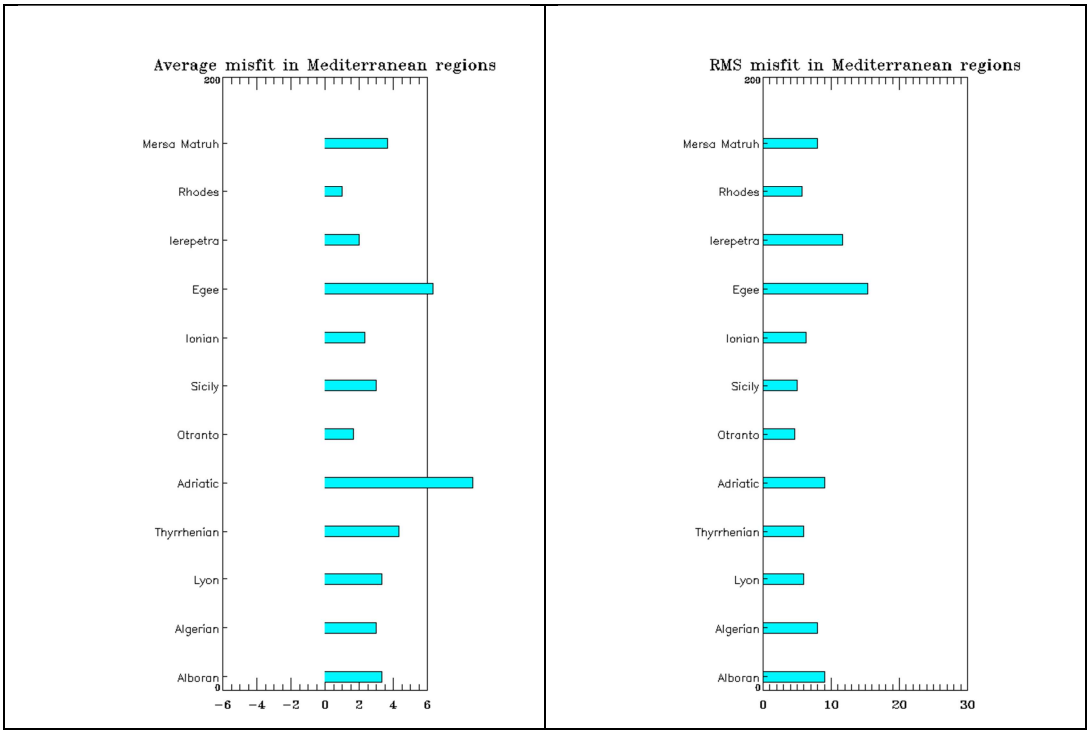

Figure 10: Comparison of SLA data assimilation scores (left: average misfit in cm, right: RMS misfit in cm) in JAS 2012 for PSY2V4R2. The scores are averaged for all available satellite along track data (Jason 1 G, Jason 2, Cryosat 2 and Envisat). See annex B for geographical location of regions.

V.1.1.2. Performance at global scale in PSY3 (1/4°) and PSY4 (1/12°)

As can be seen in Figure 11 the performance of intermediate resolution global PSY3V3R1 and the performance of high resolution global PSY4V1R3 in terms of SLA assimilation are of the same order of magnitude. The bias is small except in the “Nino 5” box centred on the Banda Sea in Indonesia which corresponds to a MDT problem. These problems disappear when using the MDT updated with GOCE and bias correction (tests made by E. Greiner, B. Tranchant, O. Le Galloudec, this MDT is used in the PSY2V4R2 release in the Atlantic and Mediterranean). The RMS error reaches its highest values in the Agulhas and Falkland Currents where the variability is high.

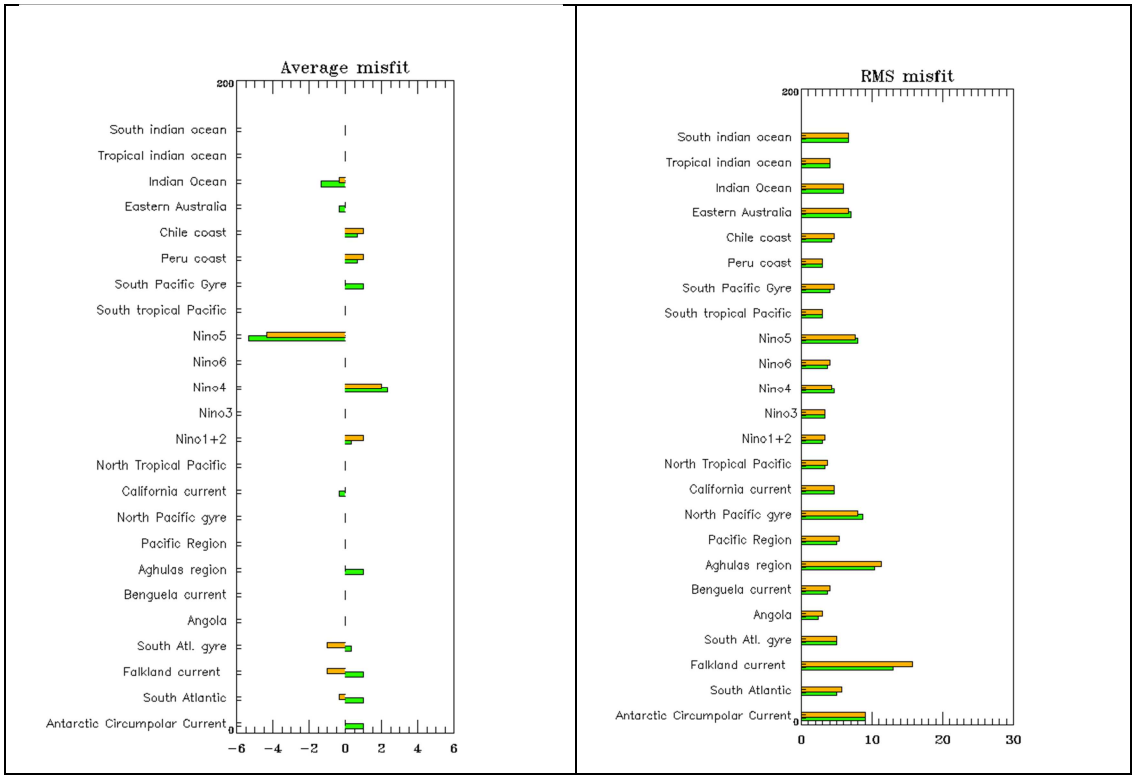

Figure 11: Comparison of SLA data assimilation scores (left: average misfit in cm, right: RMS misfit in cm) in JAS 2012 and between all available global Mercator Ocean systems in all basins but the Atlantic and Mediterranean: PSY3V3R1 (green) and PSY4V1R3 (orange). The scores are averaged for all available satellite along track data (Jason 1 G, Jason 2, Cryosat 2 and Envisat). The geographical location of regions is displayed in annex B.

V.1.2. Sea surface temperature

V.1.2.1. North and Tropical Atlantic Ocean and Mediterranean Sea in all systems

In the Atlantic the three systems display different regional behaviours in terms of SST bias as illustrated in Figure 12. A cold bias of around 0.1°C is usually diagnosed in most regions of high resolution global PSY4V1R3. This season the PSY4V1R3 bias reaches higher values (around 0.2 °C) in the tropical regions with respect to mid and high latitude regions. The bias is reduced in PSY3V3R1 with respect to PSY4V1R3 in the tropics but it is far higher this season than in PSY2V4R2 and PSY4V1R3 in the mid latitude regions. The cold bias in PSY3V3R1 is a seasonal bias appearing in summer, which reaches 1°C and is linked with mixing problems in the model and the inability of the data assimilation to correct this surface bias. We also recall that PSY3V3R1 assimilates RTG SST products that are known to be of lower quality in the northern most regions than the Reynolds AVHRR product which is assimilated in PSY2V4R2.

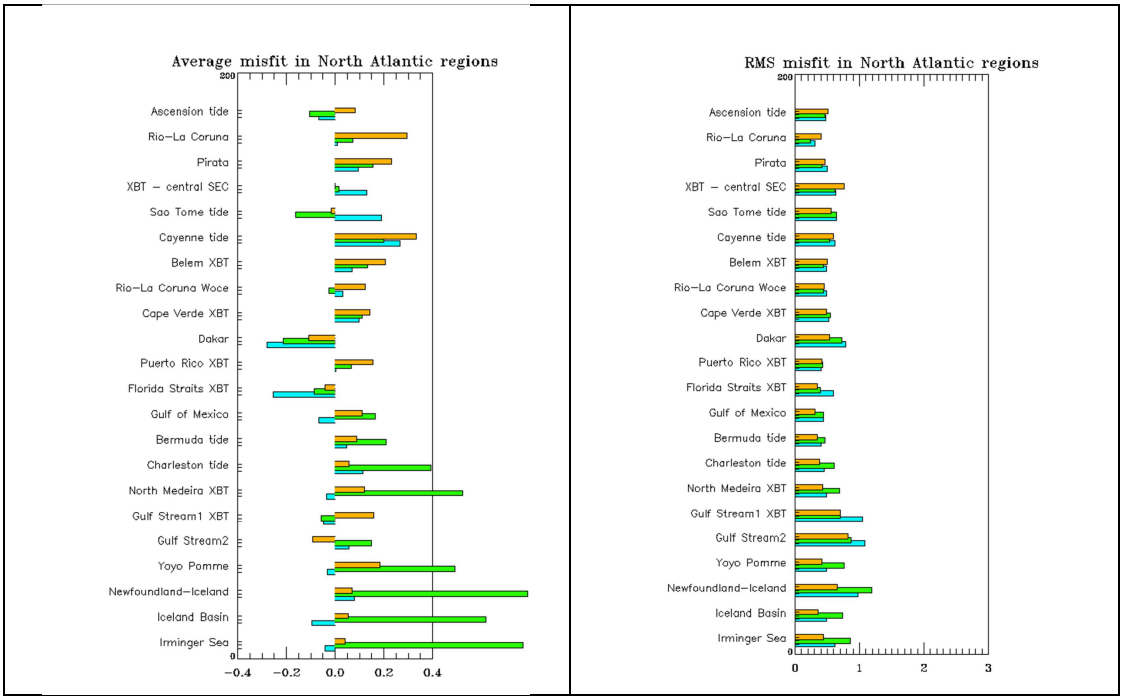

Figure 12: Comparison of RTG-SST data assimilation scores (left: average misfit in °C, right: RMS misfit in °C) in JAS 2012 and between all available Mercator Ocean systems in the Tropical and North Atlantic: PSY4V1R3 (orange), PSY3V3R1 (green). In cyan: Reynolds ¼°AVHRR-AMSR-E data assimilation scores for PSY2V4R2. The geographical location of regions is displayed in annex B.

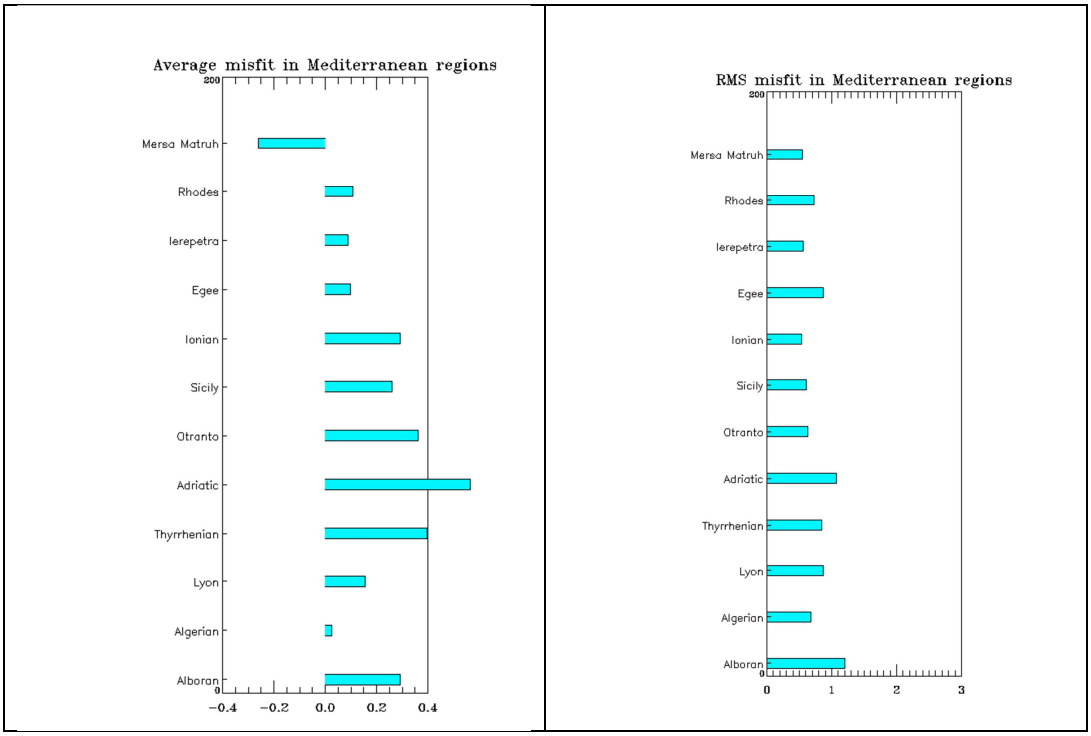

Figure 13: Comparison of SST data assimilation scores (left: average misfit in °C, right: RMS misfit in °C) in JAS 2012 for each region for PSY2V4R2 (comparison with Reynolds ¼° AVHRR-AMSR). The geographical location of regions is displayed in annex B.

The Mediterranean regions display a cold bias of 0.3°C on average (Figure 13). The RMS error is generally lower than 1 °C. As in SLA, the performance of PSY2V4R2 is lower in the Adriatic Sea where a 1°C bias appears, explaining most of the RMS error.

V.1.2.2. Performance at global scale in PSY3 (1/4°) and PSY4 (1/12°)

PSY4V1R3 exhibits a cold bias at the global scale this JAS season of about 0.1°C to 0.4°C. In general PSY3V3R1 performs better than PSY4V1R3 (Figure 14). Nevertheless PSY4V1R3 performs better than this summer in the North Pacific due to the seasonal cold bias appearing in the Northern hemisphere mid-latitudes. The RMS error is of the same order of magnitude for both systems. It is higher in PSY3V3R1 than in PSY4V1R3 in the Pacific region, consistently with the apparition of the strong biases.

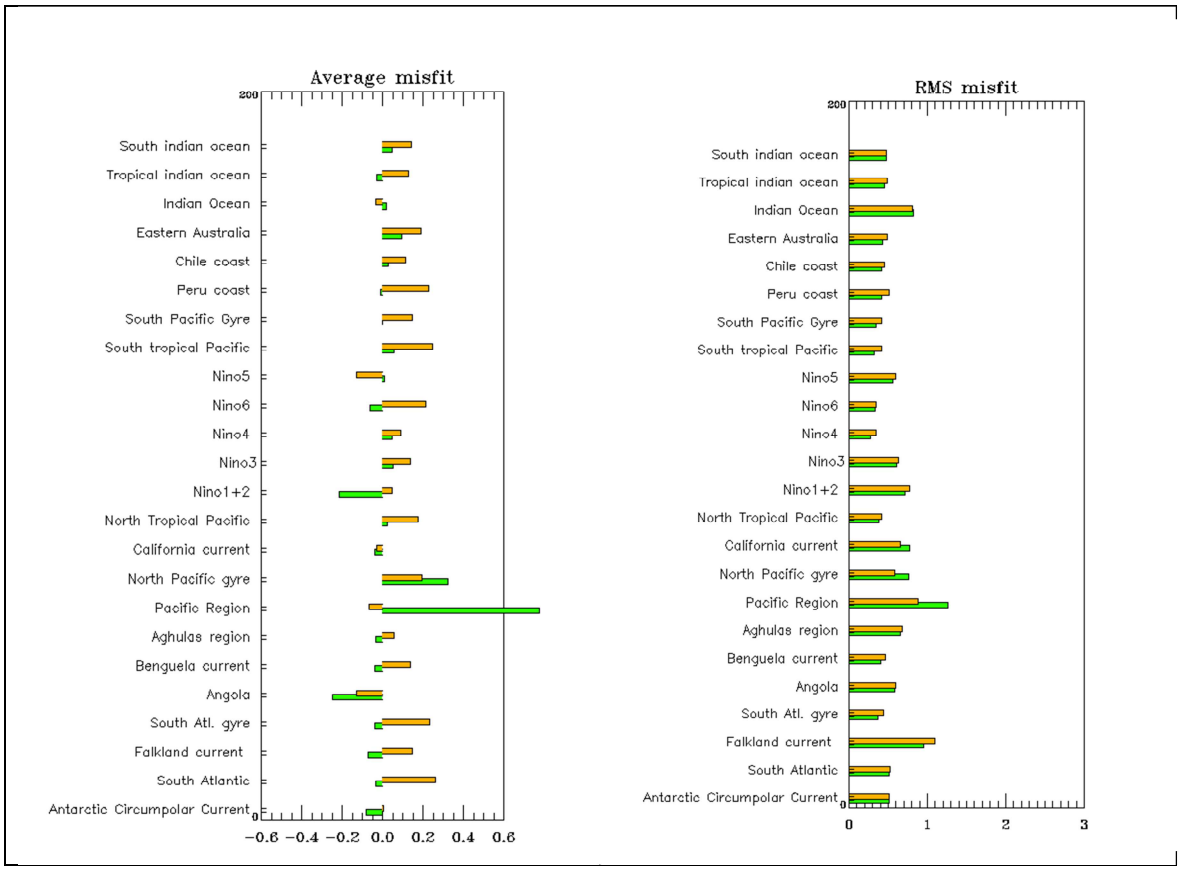

Figure 14: Comparison of RTG-SST data assimilation scores (left: average misfit in °C, right: RMS misfit in °C) in JAS 2012 and between all available global Mercator Ocean systems in all basins but the Atlantic and Mediterranean: PSY3V3R1 (green) and PSY4V1R3 (orange). See annex B for geographical location of regions.

V.1.3. Temperature and salinity profiles

V.1.3.1. Methodology

All systems innovation (**observation – model first guess**) profiles are systematically intercompared in all regions given in annex B. In the following, intercomparison results are shown on the main regions of interest for Mercator Ocean users in JAS 2012. Some more regions are shown when interesting differences take place, or when the regional statistics illustrate the large scale behaviour of the systems.

V.1.3.1.1. North Pacific gyre (global systems)

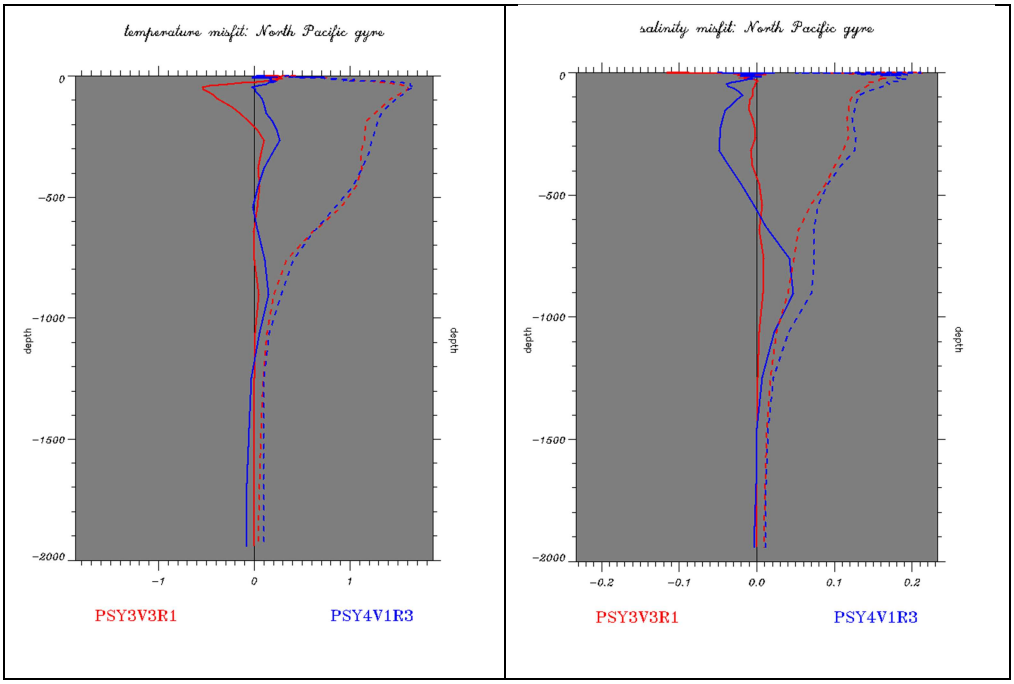

Figure 15: Profiles of JAS 2012 innovations of temperature (°C, left panel) and salinity (psu, right panel), mean (solid line) and RMS (dotted line) for PSY3V3R1 in red and PSY4V1R3 in blue in North Pacific gyre region. The geographical location of regions is displayed in annex B.

As can be seen in Figure 15, the ¼° global PSY3V3R1 benefits from bias correction but it is too warm near 100 m (up to 0.5 °C this JAS season, twice the bias observed in AMJ). This bias due to mixing problems is known to be maximum in summer. PSY4V1R3 is too cold between 0 and 500 m and near 900 m. It is too salty between 0 m and 600 m (0.05 psu) while it is fresher than observations between 600 m and 1200 m. This salinity bias of unprecedented amplitude appears in JFM 2012 (see *QuO Va Dis?* #8 for a special focus on this bias).

V.1.3.1.2. South Atlantic Gyre (global systems)

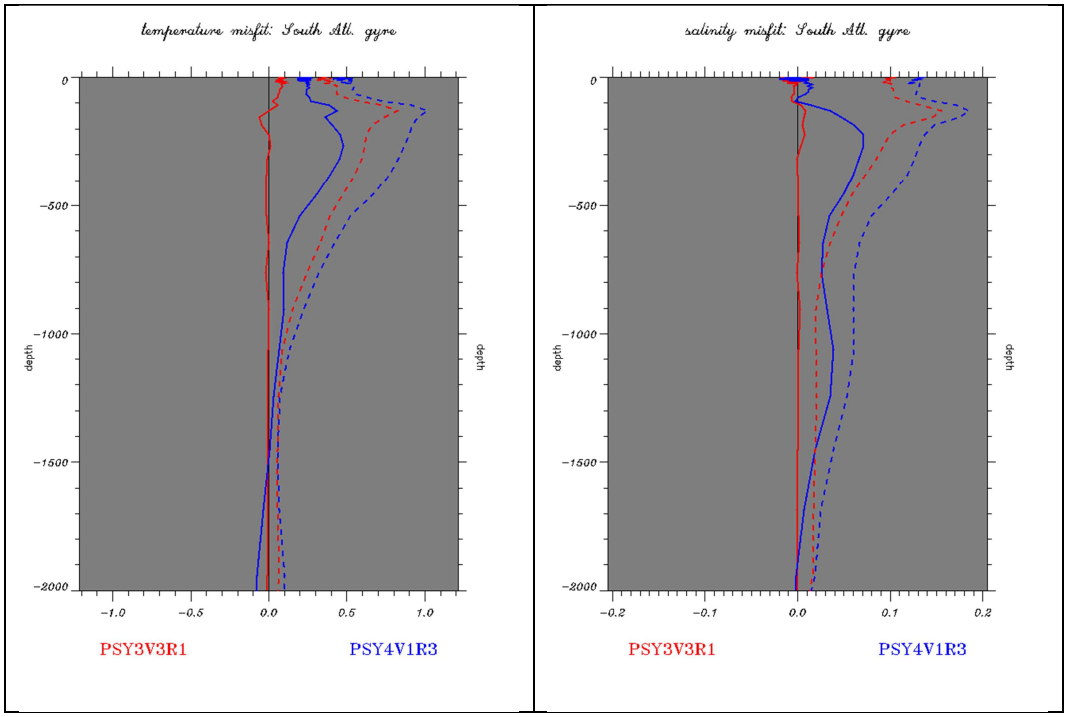

Figure 16: Profiles of JAS 2012 innovations of temperature (°C, left panel) and salinity (psu, right panel), mean (solid line) and RMS (dotted line) for PSY3V3R1 in red and PSY4V1R3 in blue in South Atlantic gyre region. The geographical location of regions is displayed in annex B.

In this region a large cold bias (up to 0.4 °C) is present in PSY4V1R3 between 0 and 800 m, while PSY3V3R1 experiments a small cold bias (0.1 °C) at the surface and a warm bias of similar amplitude near 150 m. PSY4V1R3 experiments a fresh bias on average which reaches a maximum of 0.07 psu near 300 m. This region illustrates well that PSY3V3R1 is closer to subsurface in situ observations than PSY4V1R3 thanks to bias correction.

V.1.3.1.3. Indian Ocean (global systems)

In the Indian Ocean under 800 m, PSY3V3R1 is clearly closer to the observations than PSY4V1R3 in Figure 17. This is again due to the application of a bias correction in PSY3V3R1. From 0 to 800 m PSY3V3R1 is less biased than PSY4V1R3, but it is nevertheless fresher (0.1 psu) and colder (0.1°C) than the observations at the surface. The most significant biases appear for both systems between 50 and 150 m (PSY3V3R1 is too warm and salty and PSY4V1R3 is too cold and salty), and near 700 m where both systems are too warm and salty (0.2°C and 0.05 psu in PSY4V1R3 where the bias is stronger than in PSY3V3R1).

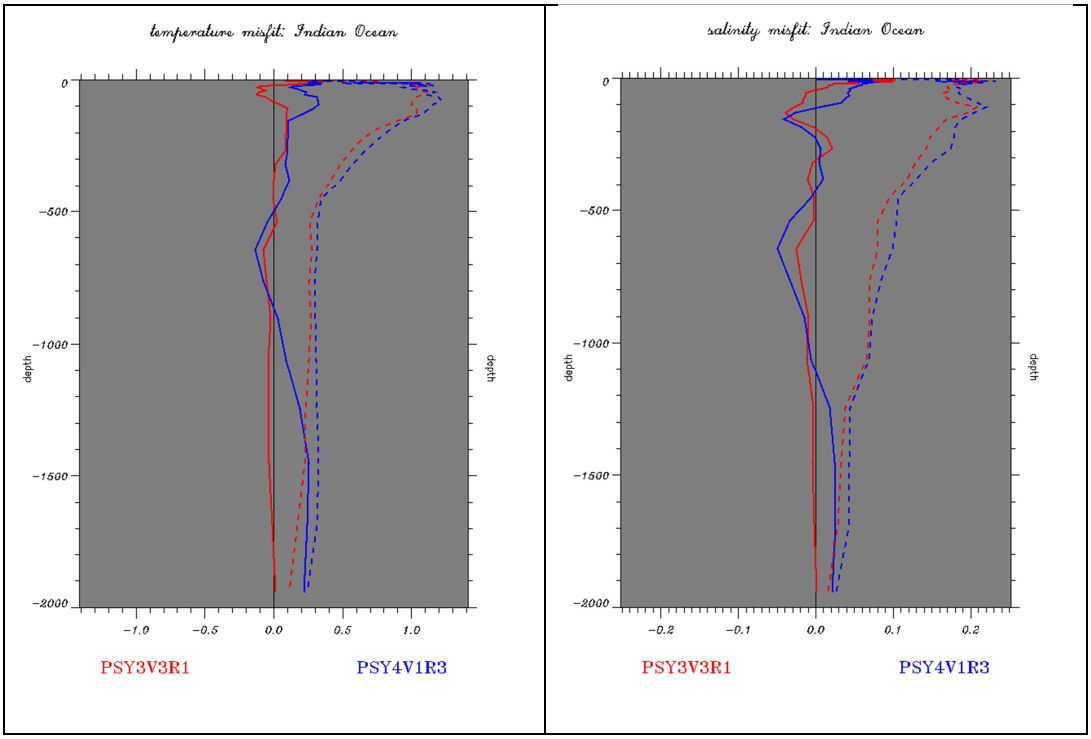

Figure 17: Profiles of JAS 2012 innovations of temperature (°C, left panel) and salinity (psu, right panel), mean (solid line) and RMS (dotted line) for PSY3V3R1 (in red) and PSY4V1R3 (in blue) in the Indian Ocean region. The geographical location of regions is displayed in annex B.

V.1.3.2. Tropical and North Atlantic Ocean (all systems)

The regional high resolution system (PSY2V4R2) and the global 1/4° PSY3V3R1 have a better average performance than the global 1/12° PSY4V1R3 in the North Atlantic in JAS 2012, again due to uncorrected biases in the PSY4V1R3 system. It is the case for the temperature and salinity in the North Madeira region as illustrated in Figure 18. Strong biases are present in PSY4V1R3 between 1000m and 1500m, at the location of the Mediterranean outflow. The bias correction improves the results of PSY3V3R1 and PSY2V4R2 between 800 m and 2000 m with respect to PSY4V1R3. Mediterranean waters are too warm and salty near 800 m in PSY2V4R2. We note that PSY2V4R2 is warmer and saltier than PSY3V3R1 on most of the water column. PSY3V3R1 appears to be slightly less biased than PSY2V4R2 while PSY2V4R2 RMS error in the 0-500 m layer is slightly lower than PSY3V3R1's.

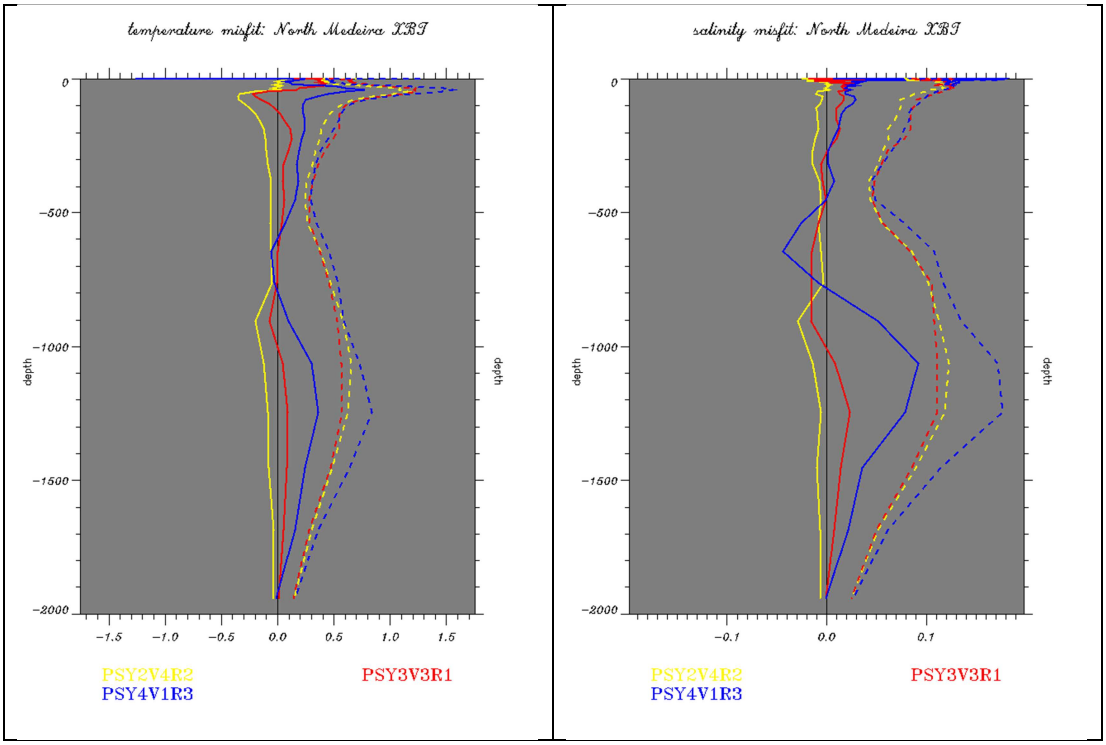

Figure 18: Profiles of JAS 2012 innovations of temperature (°C, left panel) and salinity (psu, right panel), mean (solid line) and RMS (dotted line) for PSY4V1R3 in blue, PSY3V3R1 in red, and PSY2V4R2 in yellow in North Madeira region. The geographical location of regions is displayed in annex B.

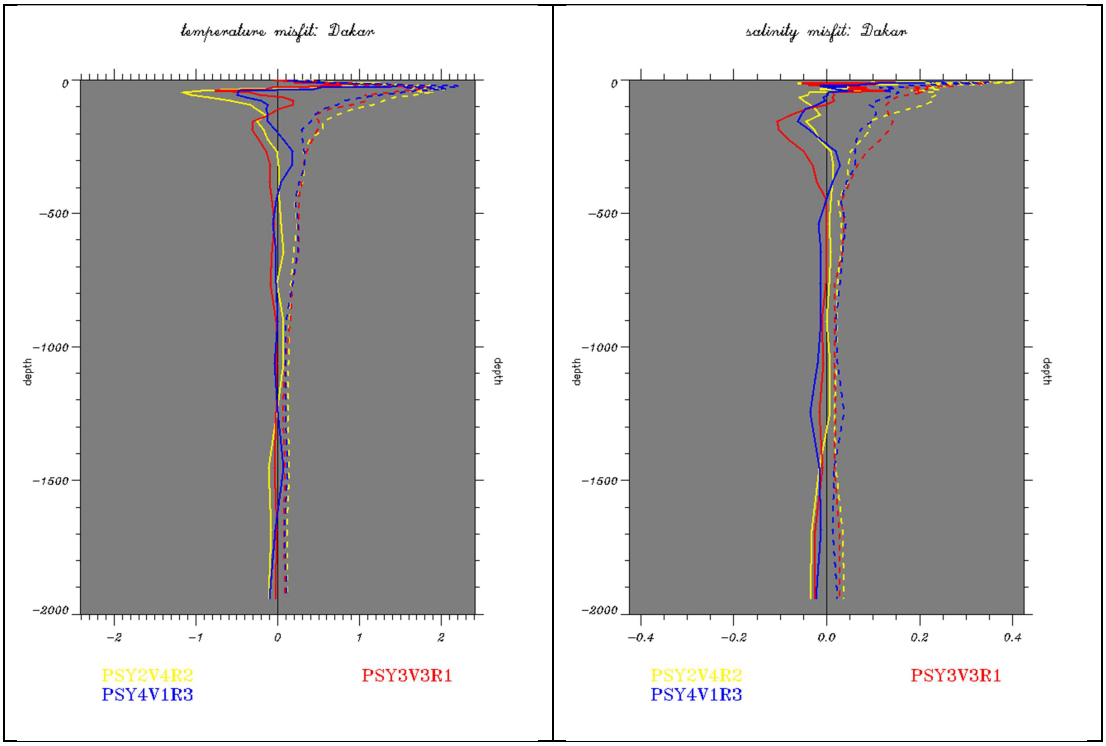

Figure 19: Profiles of JAS 2012 innovations of temperature (°C, left panel) and salinity (psu, right panel), mean (solid line) and RMS (dotted line) for PSY4V1R3 in blue, PSY3V3R1 in red, and PSY2V4R2 in yellow in Dakar region. The geographical location of regions is displayed in annex B.

The upwelling is not well represented by any of the systems In the Dakar region (Figure 19): it is too generally weak resulting in a warm (1°C) and salty (0.1 psu) bias between 50 m and 150 m this JAS season. One can notice a salty bias at depth (0.05 psu, under 1200m) in both PSY4V1R3 and PSY3V3R1 in JAS 2012, that was present in PSY2V4R2 and not in PSY4V1R3 in AMJ 2012.

In the Gulf Stream region (Figure 20) all systems display similar levels of salinity RMS error. This season PSY3V3R1 is less biased than the other systems in temperature. We note that the departures from observations are large in this region compared to other regions because of the high spatial and temporal variability of temperature and salinity due to eddy activity. Despite the bias correction, PSY3V3R1 and PSY2V4R2 are too warm and salty between 200 m and 1200 m. PSY4V1R3 which is usually too cold is consequently less biased in temperature than the other systems under 200m this season. It is still too warm from the surface to 200m and under 500m, too cold under 1000m, and too salty under 50m.

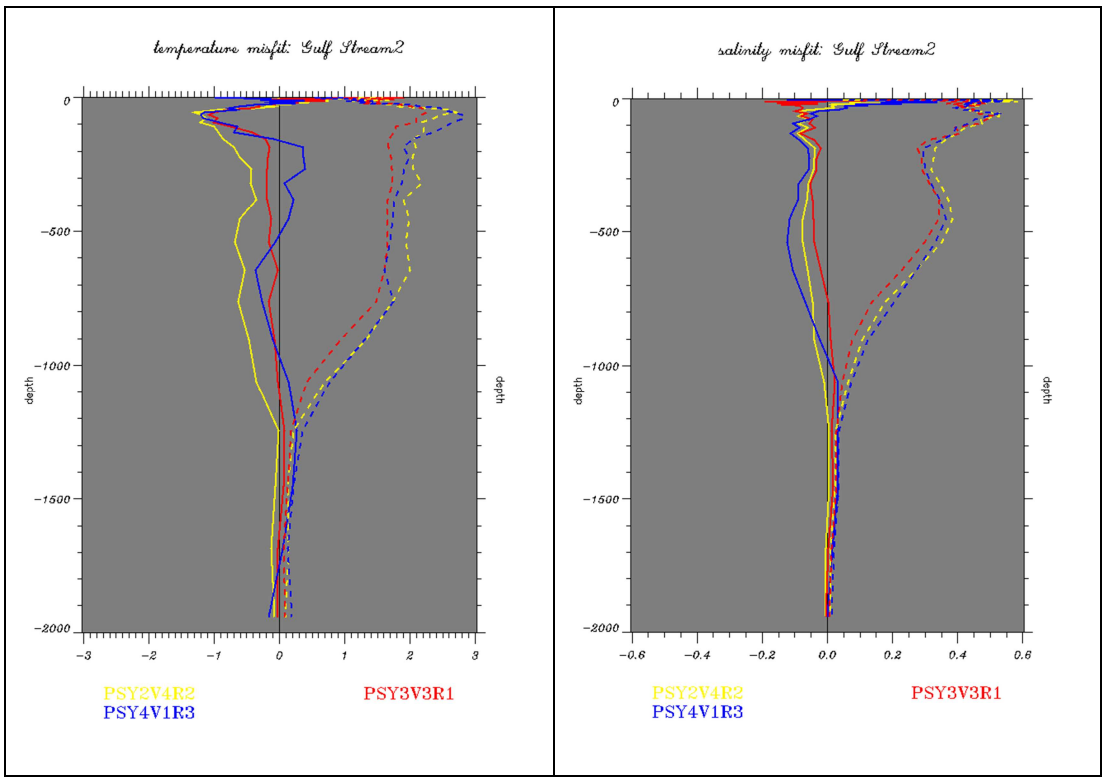

Figure 20: Profiles of JAS 2012 innovations of temperature (°C, left panel) and salinity (psu, right panel), mean (solid line) and RMS (dotted line) for PSY4V1R3 in blue, PSY3V3R1 in red, and PSY2V4R2 in yellow in Gulf Stream 2 region. The geographical location of regions is displayed in annex B.

The Cape Verde region is characteristic of the subtropical gyre in the North Atlantic where all systems stay on average close to the temperature and salinity profiles as can be seen in Figure 21. The highest errors are located near the thermocline and halocline. A fresh bias (0.1 psu) is diagnosed in PSY2V4R2 at the surface. As in many regions, the global high resolution system with no bias correction PSY4V1R3 is too cold from the surface to 700m.

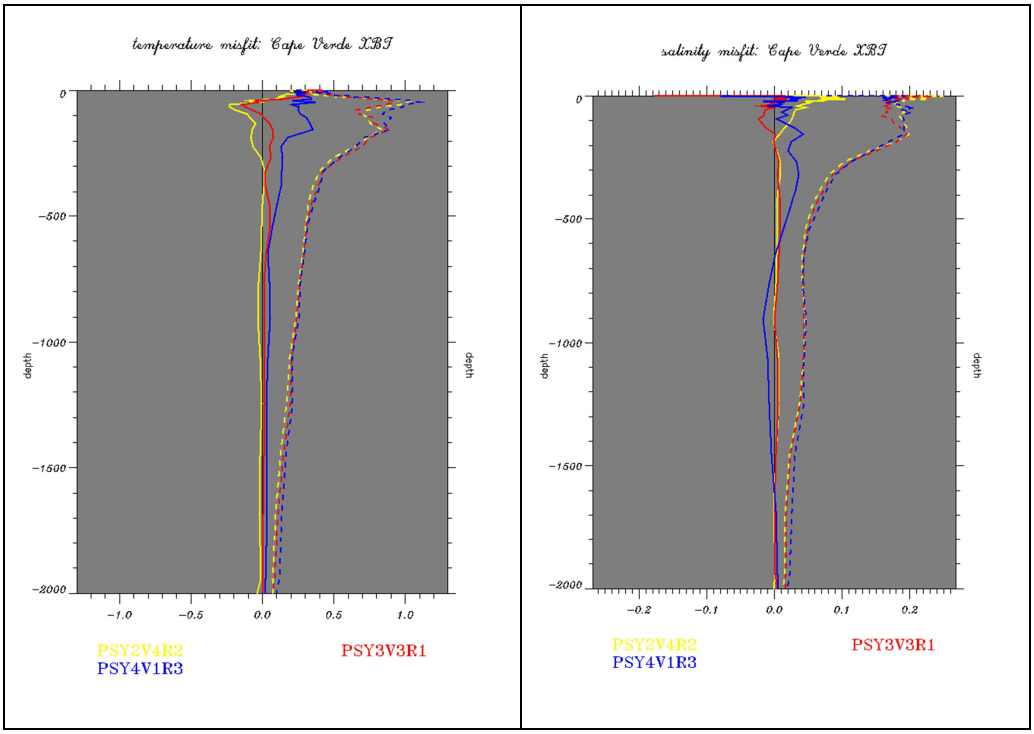

Figure 21: Profiles of JAS 2012 innovations of temperature (°C, left panel) and salinity (psu, right panel), mean (solid line) and RMS (dotted line) for PSY4V1R3 in blue, PSY3V3R1 in red, and PSY2V4R2 in yellow in Cape Verde region. The geographical location of regions is displayed in annex B.

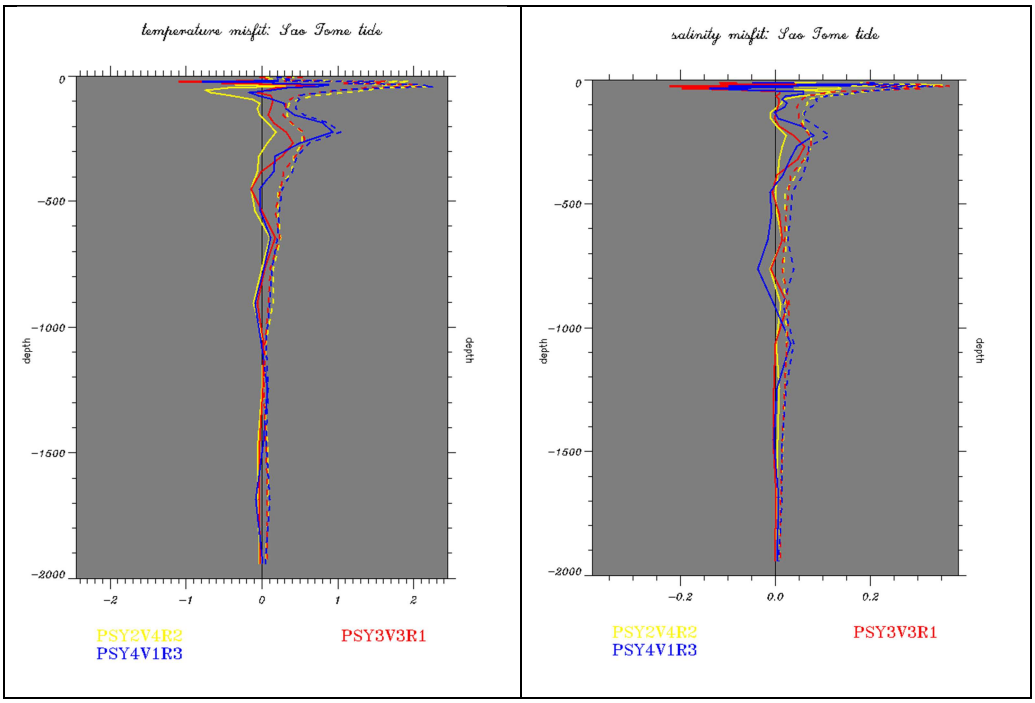

Figure 22: Profiles of JAS 2012 innovations of temperature (°C, left panel) and salinity (psu, right panel), mean (solid line) and RMS (dotted line) for PSY4V1R3 in blue, PSY3V3R1 in red, and PSY2V4R2 in yellow in Sao Tome region. The geographical location of regions is displayed in annex B.

Around 20 profiles were sampled in the beginning of May in the small area of the Sao Tome tide region where usually not more than 4 profiles are assimilated per week. As can be seen in Figure 22 the systems have difficulties in reproducing the undercurrents in this region as a small number of profiles are available to constrain the water masses. The bias correction partly solves this problem in PSY2V4R2 and PSY3V3R1.

V.1.3.1. Mediterranean Sea (high resolution regional systems at 1/12°)

In the Mediterranean Sea the high resolution is mandatory to obtain good level of performance. Only PSY2V4R2 with bias correction is displayed as it has the best level of performance on this zone. We note in Figure 23 that the system displays a cold bias near the surface and then a warm bias with a peak at around 0.7 °C between 50 m and 100 m in the Algerian region. This bias reaches its strongest values this JAS season and is present in most Mediterranean regions in summer and autumn. In most regions a fresh bias can be detected between 0 and 200 m. It reaches 0.2 psu in the Algerian region. The bias is consistent with a general underestimation of the stratification in the systems, and with errors in the positioning of the separation between the Atlantic Inflow and the Levantine intermediate waters. Biases with similar feature but with smaller amplitudes can be observed in the Gulf of Lion (Figure 24).

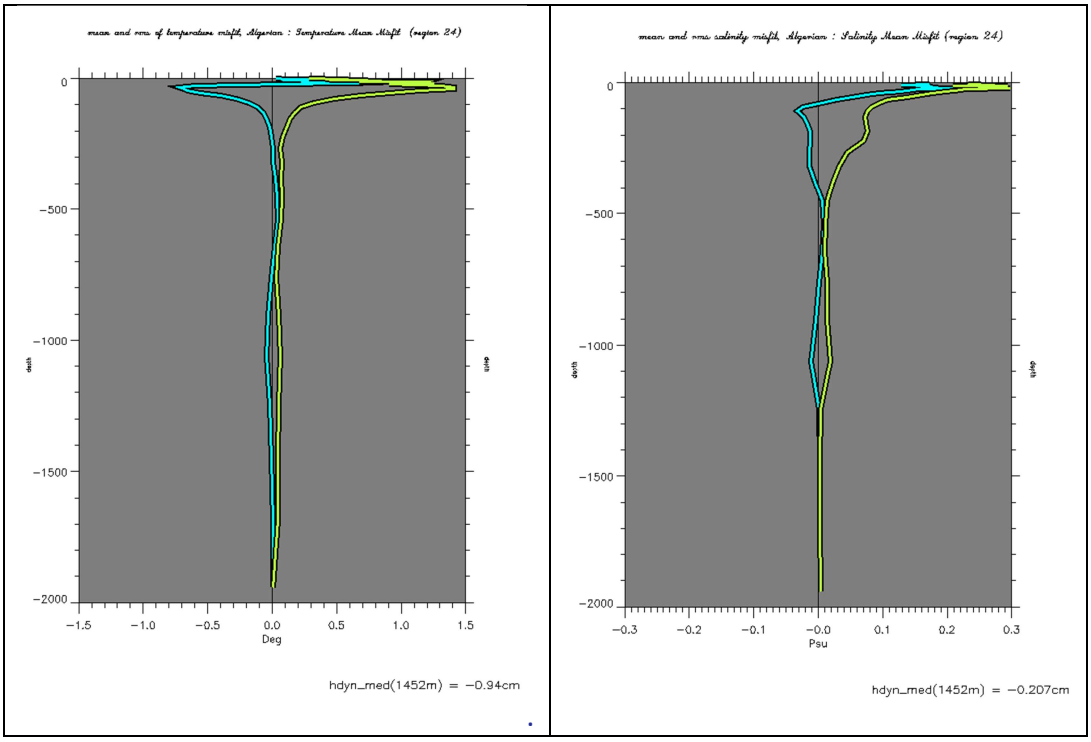

Figure 23: Profiles of JAS 2012 mean (cyan) and RMS (yellow) innovations of temperature (°C, left panel) and salinity (psu, right panel) in the Algerian region. The geographical location of regions is displayed in annex B.

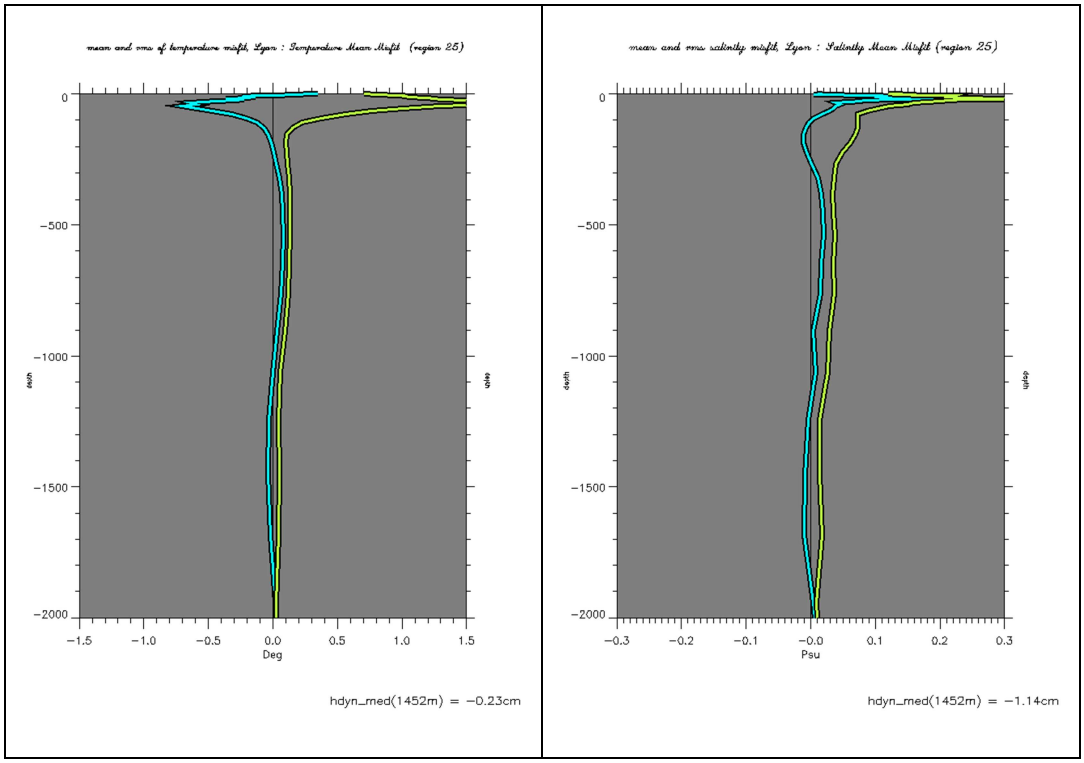

Figure 24: Profiles of JAS 2012 mean (cyan) and RMS (yellow) innovations of temperature (°C, left panel) and salinity (psu, right panel) in the Gulf of Lion region. The geographical location of regions is displayed in annex B.

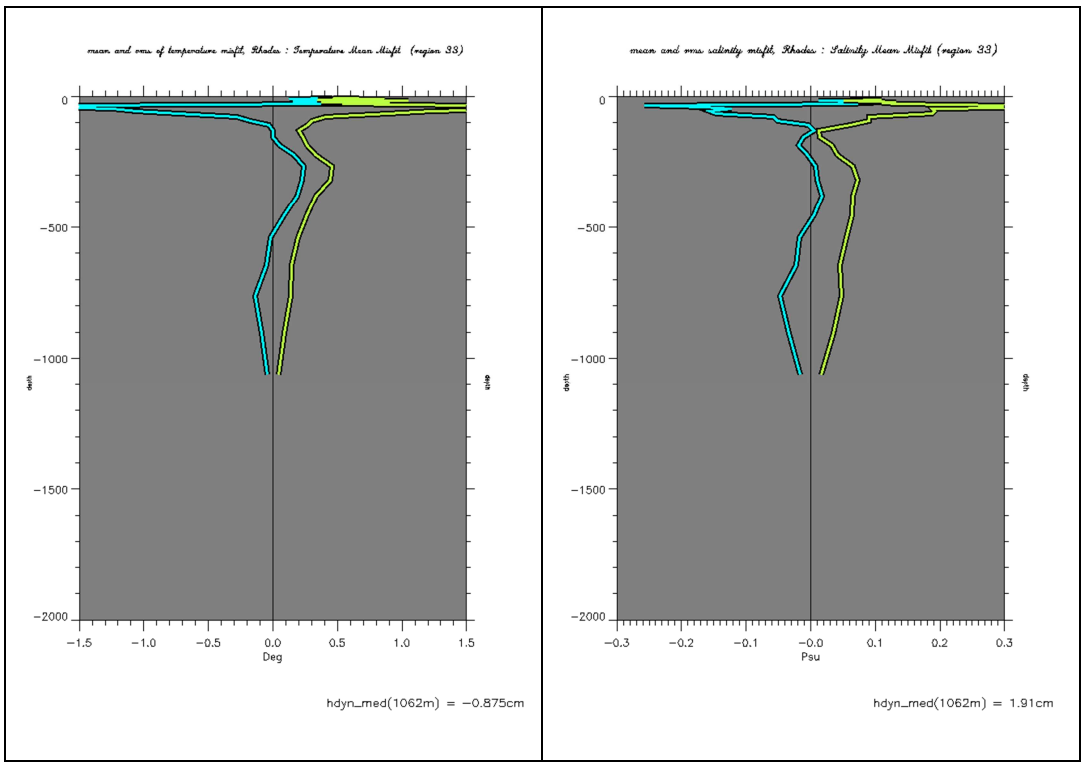

Figure 25: Profiles of JAS 2012 mean (cyan) and RMS (yellow) innovations of temperature (°C, left panel) and salinity (psu, rightpanel) in the Rhodes region. The geographical location of regions is displayed in annex B.

In the Rhodes region (Eastern Mediterranean basin) a strong cold (1.5°C) and fresh (0.25 psu) bias appears on the 50-100 m layer, while a warm and salty bias of smaller amplitude can be diagnosed between 600 and 2000 m.

Summary: While most of the deep biases disappear in the systems including bias correction, seasonal biases remain. One of the hypotheses is that the SST assimilation is not as efficient as it used to be. The Incremental Analysis Update together with the bulk formulation rejects part of the increment. There is too much mixing in the surface layer inducing a cold (and salty) bias in surface and warm (and fresh) bias in subsurface. The bias is intensifying with the summer stratification and the winter mixing episodes reduce the bias. In the northern hemisphere in JAS this bias reaches a maximum as can be seen in the North Pacific. The bias correction is not as efficient on reducing seasonal biases as it is on reducing long term systematic biases. A correction of air-sea fluxes depending on the SST increment is considered for future versions of the system. The use of Reynolds ¼° L4 SST product (AVHRR AMSR-E) for data assimilation reduces part of the surface bias in the North Atlantic and changes the signal in the Mediterranean. The use of Reynolds ¼° AVHRR analyses will be extended to the other Mercator Ocean systems in 2012. The PSY2V4R2 system is different from the other systems:

- Update of the MDT with GOCE and bias correction
- Assimilation of Reynolds ¼° AVHRR-AMSRE SST observations instead of ½° RTG-SST
- Increase of observation error for the assimilation of SLA near the coast and on the shelves, and for the assimilation of SST near the coast
- Modification of the correlation/influence radii for the analysis specifically near the European coast.
- Restart from October 2009 from WOA05 climatology

In PSY2V4R2:

- The products are less constrained by altimetry near the coast and on the shelves but are generally closer to in situ observations and climatologies in these regions
- The quality is slightly degraded in the Eastern Mediterranean and in the Caribbean region

In PSY4V1R3:
A strong salinity bias (PSY4V1R3 is too salty near 100 m) is present in the North Pacific (Alaska Gyre) and alters the global statistics.

V.2.Accuracy of the daily average products with respect to observations

V.2.1. T/S profiles observations

V.2.1.1. Global statistics for JAS 2012

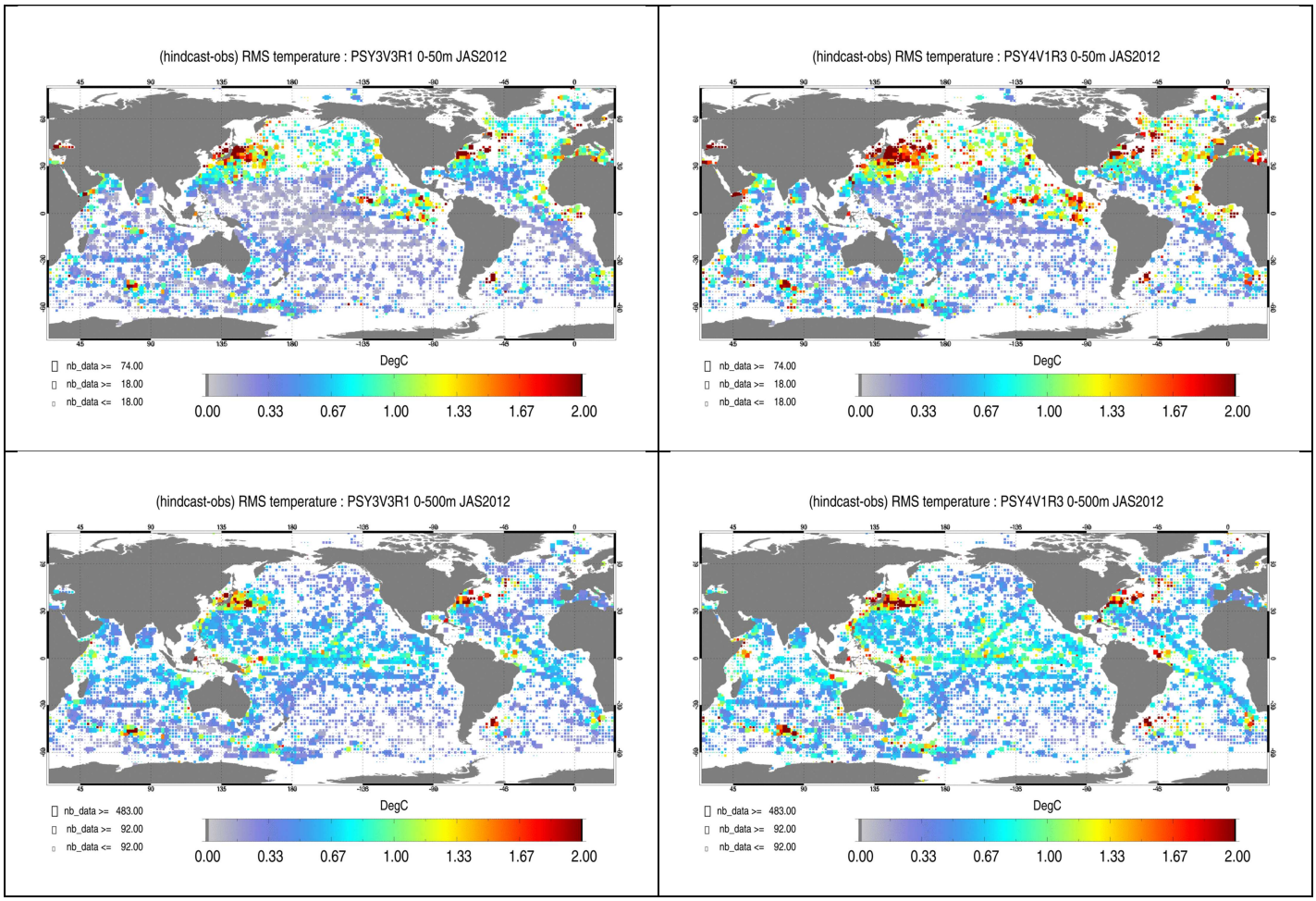

Figure 26: RMS temperature (°C) difference (model-observation) in JAS 2012 between all available T/S observations from the Coriolis database and the daily average hindcast PSY3V3R1 products on the left and hindcast PSY4V1R3 on the right column colocalised with the observations. Averages are performed in the 0-50m layer (upper panel) and in the 0-500m layer (lower panel). The size of the pixel is proportional to the number of observations used to compute the RMS in 2°x2° boxes.

As can be seen in Figure 26, in both PSY3V3R1 and PSY4V1R3 temperature errors in the 0-500m layer stand between 0.5 and 1°C in most regions of the globe. Regions of high mesoscale activity (Kuroshio, Gulf Stream, Agulhas current) and regions of upwelling in the tropical Atlantic and Tropical Pacific display higher errors (up to 3°C). PSY4V1R3 has higher variability and no bias correction and thus departures from the observations are higher than in PSY3V3R1 on average in these regions. PSY3V3R1 seems to perform better than PSY4V1R3 in the tropical Pacific but both systems have a strong temperature (cold) biases in the Eastern part of the Pacific basin at the surface (in the 0-50m layer) and in the western part of the Pacific basin in the 0-500m layer (warm pool). This is mainly due to the transition

towards El Niño conditions. The RMS error is higher in the Northern Pacific and Northern Atlantic than in the previous season (AMJ 2012), due to the seasonal bias, consistently with Figure 12 and Figure 14.

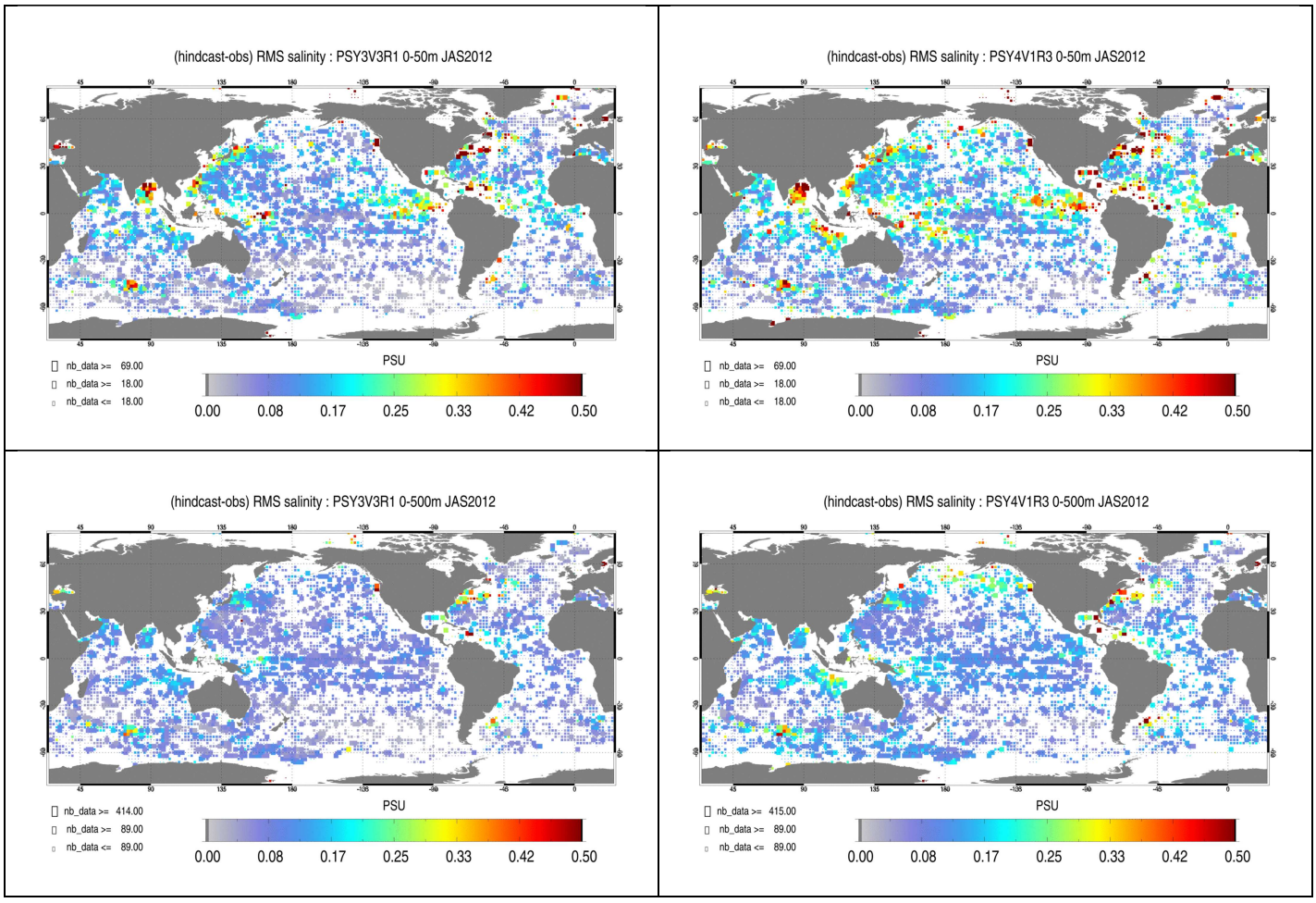

Figure 27: RMS salinity (psu) difference (model-observation) in JAS 2012 between all available T/S observations from the Coriolis database and the daily average hindcast PSY3V3R1 products on the left and hindcast PSY4V1R3 on the right column, colocalised with the observations. Averages are performed in the 0-50m layer (upper panel) and in the 0-500m layer (lower panel). The size of the pixel is proportional to the number of observations used to compute the RMS in 2°x2° boxes.

The salinity RMS errors (Figure 27) are usually less than 0.2 psu but can reach higher values in regions of high runoff (Amazon, Sea Ice limit) or precipitations (ITCZ, SPCZ, Gulf of Bengal), and in regions of high mesoscale variability. The salinity error is generally less in PSY3V3R1 than in PSY4V1R3 for instance here in the North Pacific gyre (where a salty bias develops as already mentioned), the Indian Ocean, the South Atlantic Ocean or the Western Pacific Ocean. Precipitations are overestimated in the tropical band, leading to a fresh bias in this region.

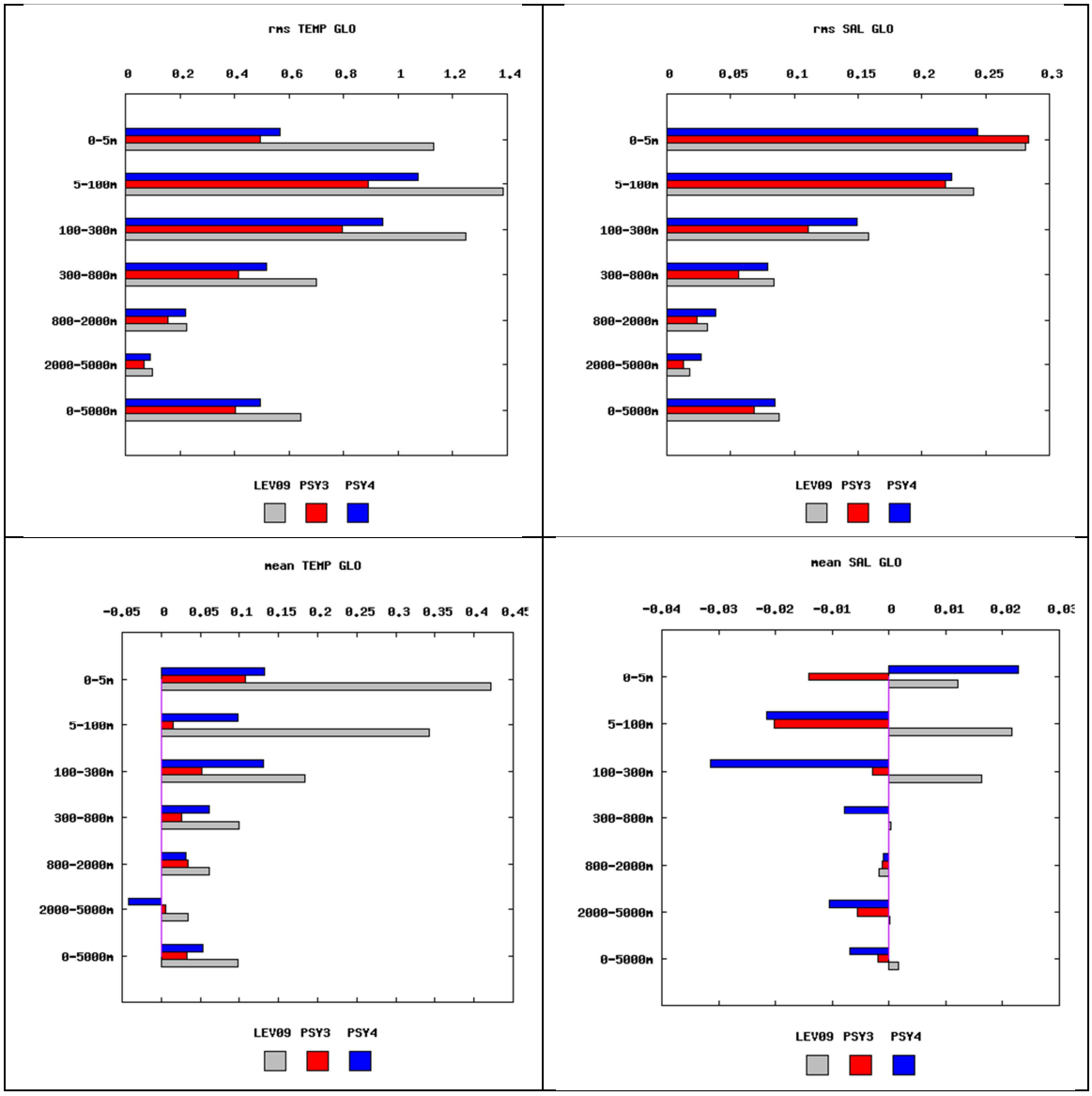

Figure 28 : JAS 2012 global statistics of temperature (°C, left column) and salinity (psu, right column) averaged in 6 consecutive layers from 0 to 5000m. RMS difference (upper panel) and mean difference (observation-model, lower panel) between all available T/S observations from the Coriolis database and the daily average hindcast PSY3V3R1 products (green) , hindcast PSY4V1R3 (red) and WOA09 climatology (blue) colocalised with the observations. NB: average on model levels is performed as an intermediate step which reduces the artefacts of inhomogeneous density of observations on the vertical.

For the global region in Figure 28, the intermediate resolution model (PSY3V3R1) is more accurate than the high resolution model (PSY4V1R3) in terms of RMS and mean difference for both temperature and salinity mainly thanks to the bias correction which is applied in PSY3V3R1 and not yet in PSY4V1R3. The effects of this correction are on the whole water column for temperature and salinity. Both global systems are too cold on the whole water column, PSY3V3R1 being significantly closer to the observations than PSY4V1R3. A warm bias seems to appear under 2000m but cannot be confirmed because only few observations are available at these depths. PSY4V1R3 and PSY3V3R1 are globally too salty in the 5-800 m layer and 5-300 m layer respectively. At the surface PSY3V3R1 exhibits a salty bias while PSY4V1R3 is too fresh on average. In PSY3V3R1 the salty surface bias is very small as the departures from the observations are centred around zero (not shown). This explains why

the RMS difference is finally slightly higher in PSY3V3R1 at the surface than in PSY4V1R3. In PSY4V1R3 the fresh bias mostly comes from the tropical belt (not shown).The two systems are more accurate than the WOA09 climatology (Levitus 2009) over the whole water column in temperature. In salinity, PSY3V3R1 is performing better than PSY4V1R3.

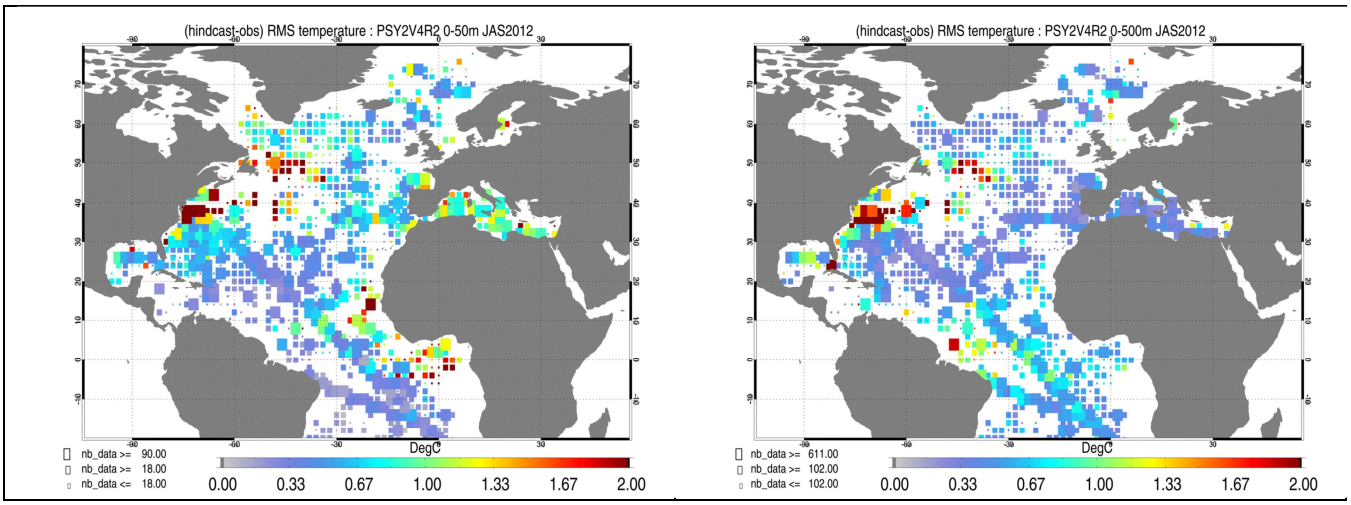

Figure 29: Upper panel: RMS difference (model-observation) of temperature (°C) in JAS 2012 between all available T/S observations from the Coriolis database and the daily average PSY2V4R2 hindcast products colocalised with the observations in the 0-50m layer (left column) and 0-500m layer (right column).

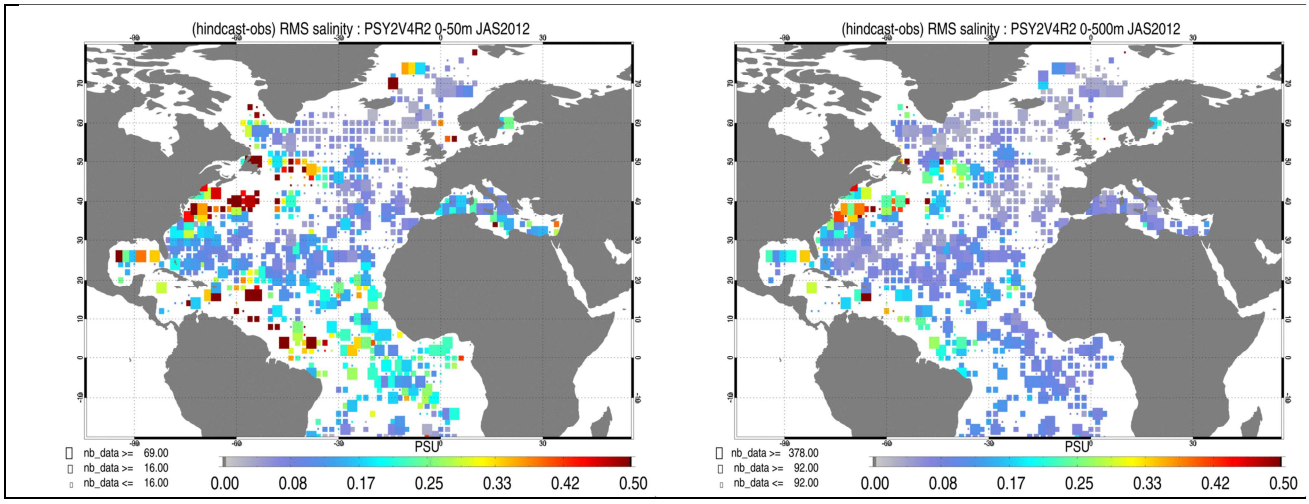

Figure 30: Upper panel: RMS difference (model-observation) of salinity (psu) in the 0-50m layer in JAS 2012 between all available T/S observations from the Coriolis database and the daily average PSY2V4R2 hindcast products colocalised with the observations in the 0-50m layer (left column) and 0-500m layer (right column).

The general performance of PSY2V4R2 (departures from observations in the 0-500m layer) is less than 0.3°C and 0.05 psu in many regions of the Atlantic and Mediterranean (Figure 29 and Figure 30). The strongest departures from temperature and salinity observations are always observed in the Gulf Stream and the tropical Atlantic. Near surface salinity biases appear in the Algerian Sea, the Gulf of Guinea, the Caribbean Sea, the Labrador Sea, the Baltic Sea and the Gulf of Mexico. In the eastern tropical Atlantic biases concentrate in the 0-50m layer (cold and fresh bias), while in the Western tropical Atlantic the whole 0-500m layer is biased (not shown).

V.2.1.2. Water masses diagnostics

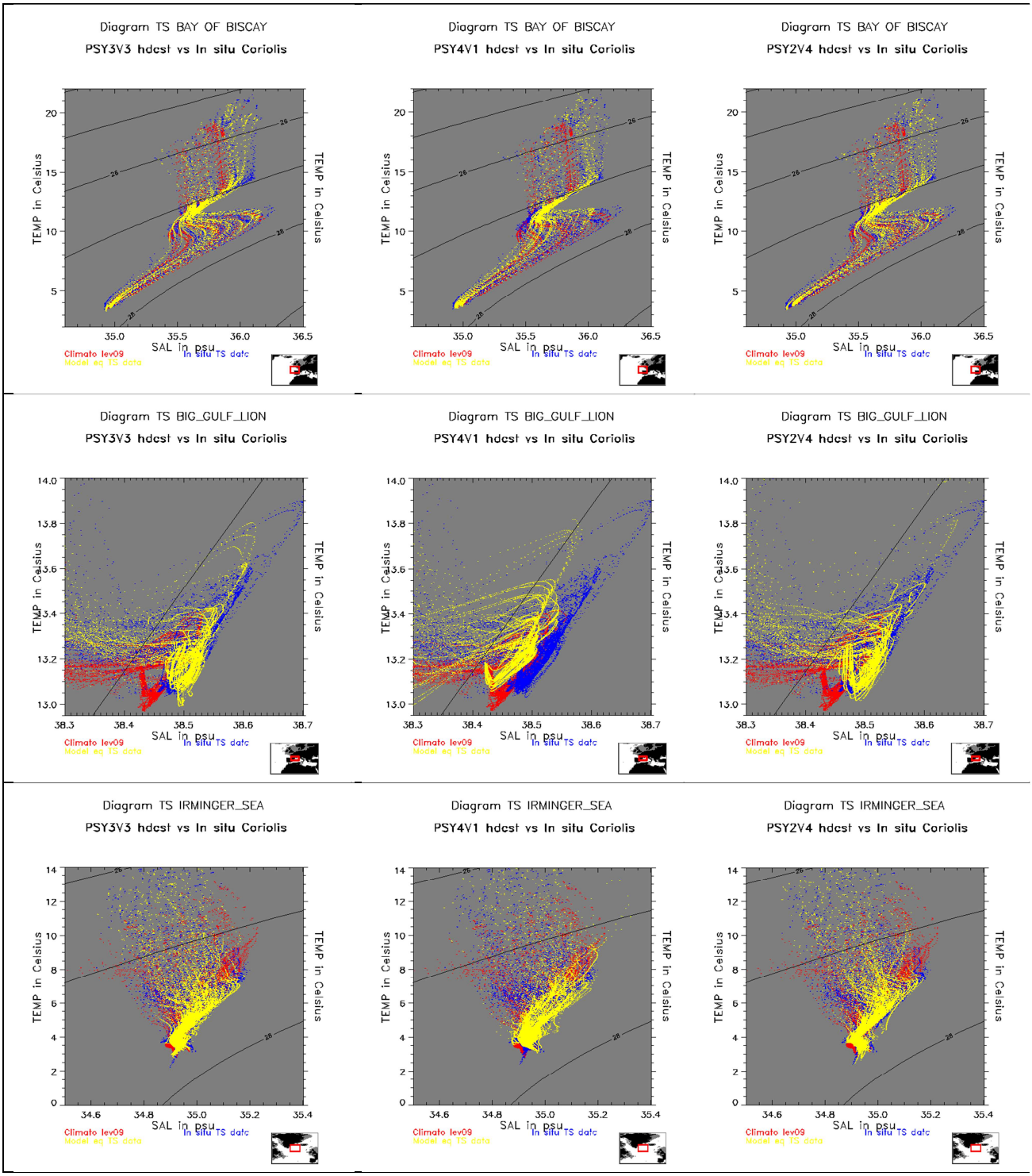

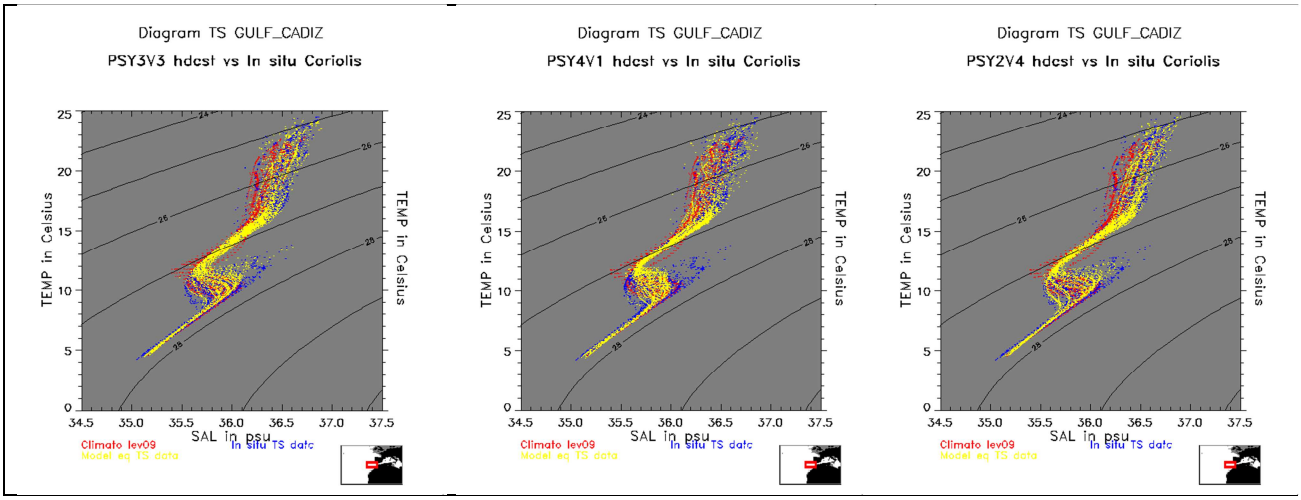

Figure 31: Water masses (Theta, S) diagrams in the Bay of Biscay (upper panel), Gulf of Lion (second panel) and Irminger Sea (third panel) and Baltic Sea (upper panel), comparison between PSY3V3R1 (left column) and PSY4V1R3 (middle column) and PSY2V4R2 (right column) in JAS 2012. PSY2, PSY3 and PSY4: yellow dots; Levitus WOA09 climatology: red dots; in situ observations: blue dots.

We use here the daily products (analyses) collocated with the T/S profiles to draw "T, S" diagrams.

In the Bay of Biscay (Figure 31) we have the main influence of the Eastern North Atlantic Central Water, Mediterranean and Labrador Sea Water.

- Between 11°C and 20°C, 35.5 and 36.5 psu, warm and relatively salty Eastern North Atlantic Central Water gets mixed with the shelf water masses. PSY3V3R1 and PSY2V4R2 with bias correction both capture the spread of the freshest waters (35.5 psu, 11 °C)
- The "bias corrected" systems PSY3V3R1 and PSY2V4R2 better represent the Mediterranean Water characterized by high salinities (Salinities near 36psu) and relatively high temperatures (Temperatures near 10°C).
- Between 4°C and 7°C, 35.0 and 35.5 psu the fresher waters of the Labrador Sea are slightly better represented in PSY2V4R2 than in PSY3V3R1 and PSY4V1R3.

In the Gulf of Lion:

- The Levantine Intermediate Water (salinity maximum near 38.6 psu and 13.6°C) is too fresh in all systems this JAS season. PSY4V1R3 intermediate waters are the freshest of all systems. This JAS 2012 season, PSY2V4R2 gives the most realistic water masses characteristics in this region

In the Irminger Sea:

- The North Atlantic Water (T > 7°C and S > 35.1 psu) is well represented by the three systems.
- The Irminger Sea Water (≈ 4°C and 35 psu) is too salty and warm in the three systems but PSY2V4R2 and PSY3V3R1 seems to be better than the global 1/12° PSY4V1R3.
- Waters colder than 3°C and ≈ 34.9 psu (Iceland Scotland Overflow waters) are not represented by PSY3V3R1 and PSY4V1R3 and slightly too salty in PSY2V4R2.

In the Gulf of Cadiz:

- The Mediterranean waters (T around 10°C) are quite well represented by the three systems but PSY4V1R3 misses the saltiest waters. PSY2V4R2 better reproduces the

spread. Near the surface, PSY3V3R1 seems to better reproduce the spread of the values.

In the western tropical Atlantic and in the Gulf of Guinea the water masses are well represented by all systems. PSY2V4R2 does not represent well the subsurface salinity maximum between the isopycn 24 and 26 (South Atlantic Subtropical waters) that both global systems capture. Some observations in the Gulf of Guinea (around 5°C) seem erroneous and has been rejected by the assimilation system.

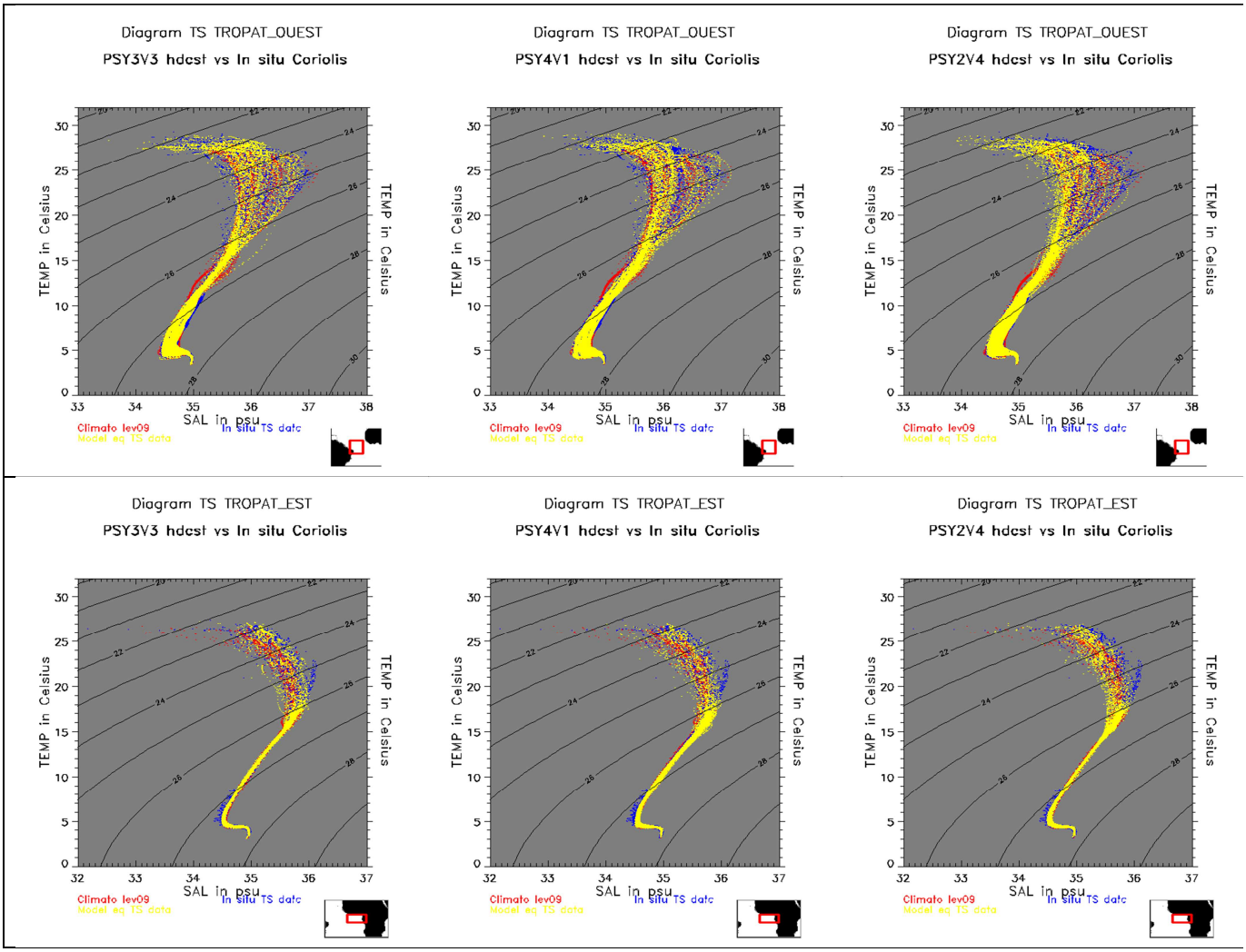

Figure 32 : Water masses (T, S) diagrams in the Western Tropical Atlantic (upper panel) and in the Eastern Tropical Atlantic (lower panel): for PSY3V3R1 (left); PSY4V1R3 (middle); and PSY2V4R2 (right) in JAS 2012. PSY2, PSY3 and PSY4: yellow dots; Levitus WOA09 climatology; red dots, in situ observations: blue dots.

In the Agulhas current and Kuroshio Current (Figure 33) PSY3V3R1 and PSY4V1R3 give a realistic description of water masses. In general, the water masses characteristics display a wider spread in the high resolution 1/12° than in the ¼°, which is more consistent with T and S observations. This is especially true at the surface in the highly energetic regions of the Agulhas and of the Gulf Stream.

In the Gulf Stream region, models are too salty from the '27' to the '28' isopycn, where they miss the cold and fresh waters of the Labrador current.

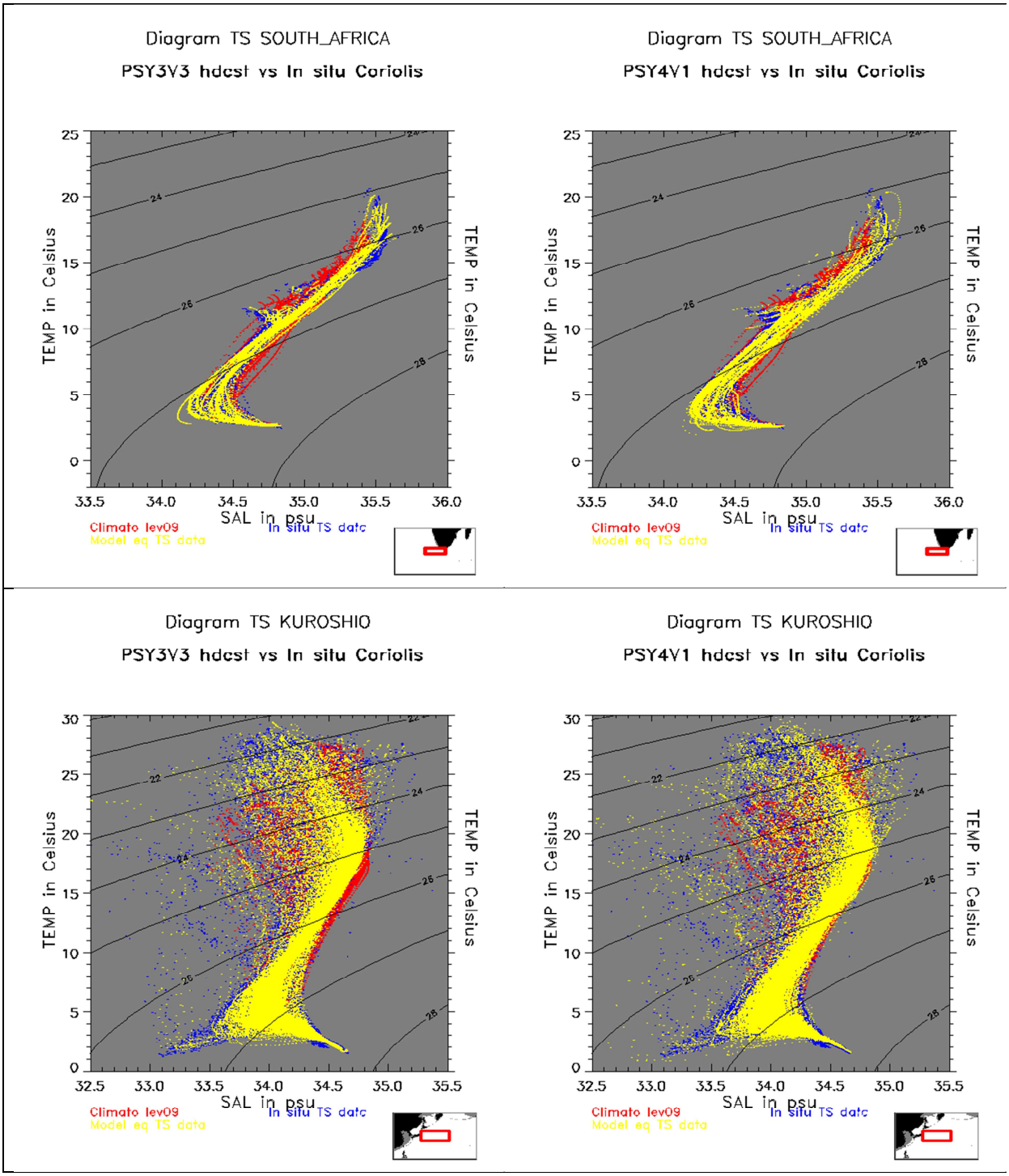

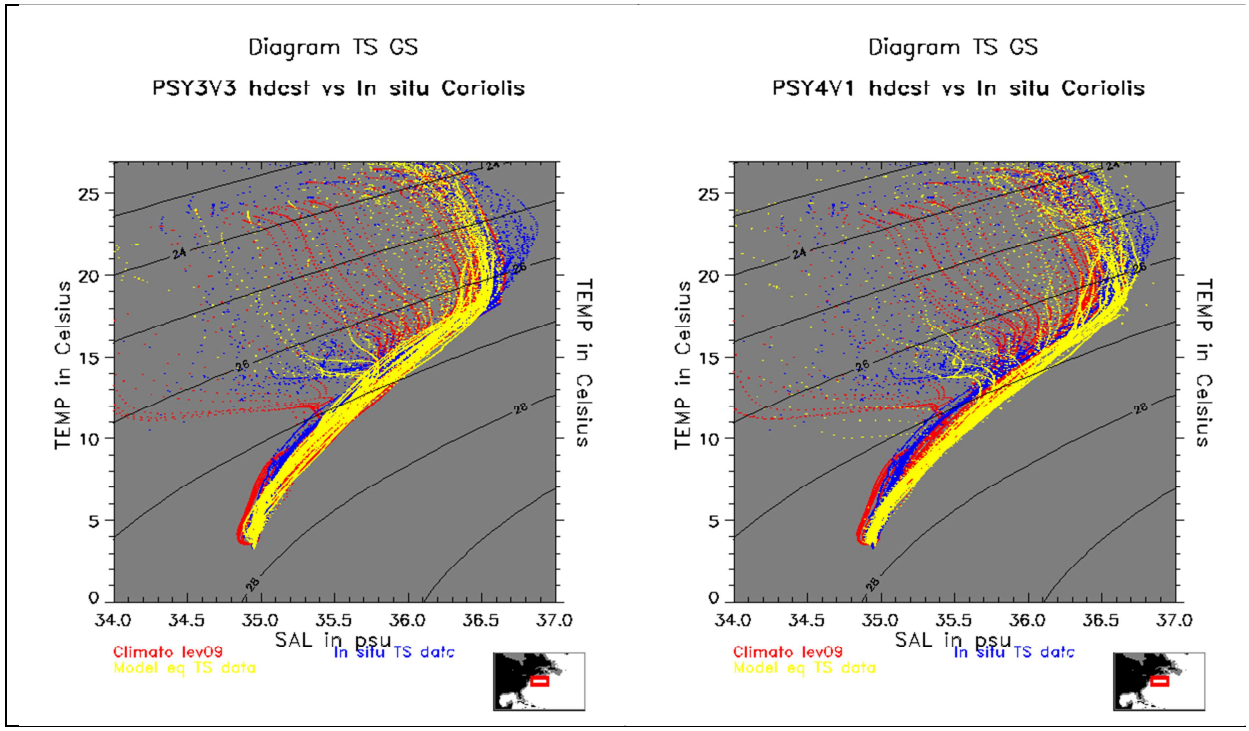

Figure 33: Water masses (T, S) diagrams in South Africa, Kuroshio, and Gulf Stream region (respectively from top to bottom): for PSY3V3R1 (left); PSY4V1R3 (right) in JAS 2012. PSY3 and PSY4: yellow dots; Levitus WOA09 climatology: red dots; in situ observations: blue dots.

V.2.2. SST Comparisons

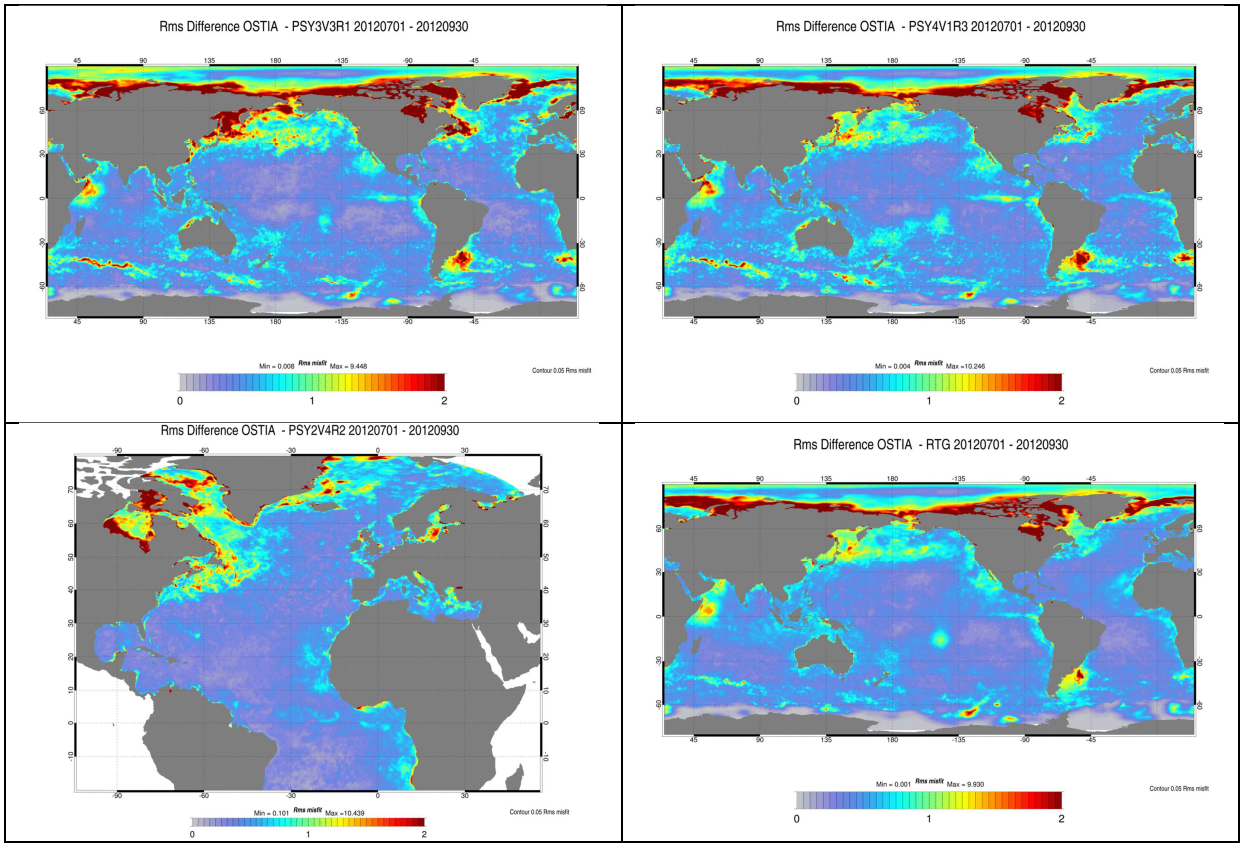

Figure 34 : RMS temperature (°C) differences between OSTIA daily analyses and PSY3V3R1 daily analyses (upper left); between OSTIA and PSY4V1R3 (upper right), between OSTIA and PSY2V4R2 (lower left), and between OSTIA and RTG daily analyses (lower right). The Mercator Océan analyses are colocalised with the satellite observations analyses.

Quarterly average SST differences with OSTIA analyses show that in the subtropical gyres the SST is very close to OSTIA, with difference values staying below the observation error of 0.5 °C on average. High RMS difference values are encountered in high spatio-temporal variability regions such as the Gulf Stream or the Kuroshio. The stronger is the intrinsic variability of the model (the higher the resolution), the stronger is the RMS difference with OSTIA. Strong regional biases are diagnosed in summer in the PSY3V3R1 global system in the North Pacific (like every summer, see *QuO Va Dis?*#6), with cold biases of around 1°C in the Northern Hemisphere (Figure 35). Strong differences can be detected near the sea ice limit in the Arctic in all the systems particularly in the Labrador Sea and in the Barents Sea for the global systems. There are also differences in the Bering Sea where ice cover remained unusually extensive. Part of this disagreement with the OSTIA analysis can be attributed to the assimilation of RTG SST in PSY3V3R1 and PSY4V1R3, while Reynolds ¼° AVHRR only is assimilated in PSY2V4R2. These products display better performance than RTG SST especially in the high latitudes[1]

[1] Guinehut, S.: Validation of different SST products using Argo dataset, CLS, Toulouse, Report CLS-DOS-NT-10-264, 42 pp., 2010.

The difference between PSY3 and OSTIA in the South Pacific near 20°S and 140°W is due to a warm SST core in this region that is present in OSTIA and not in the other products (either RTG or AVHRR, Figure 35).

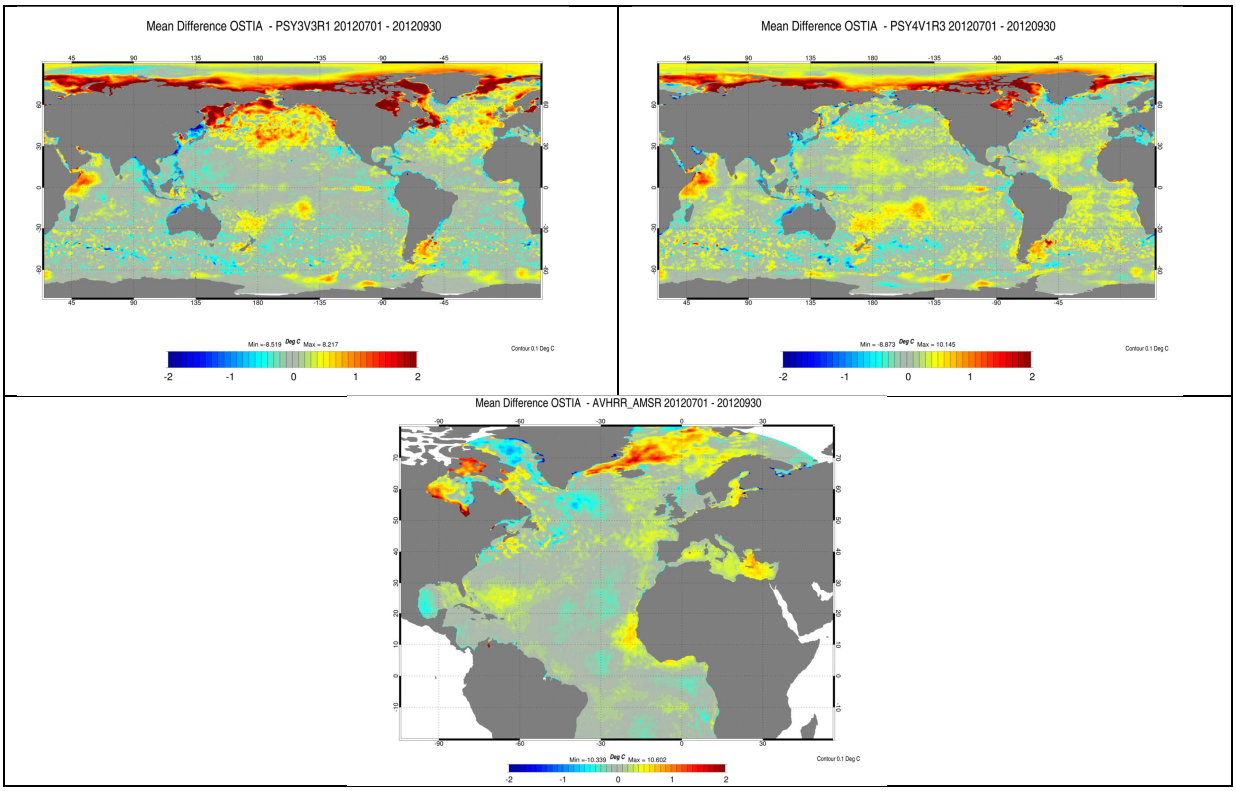

Figure 35: Mean SST (°C) daily differences between OSTIA daily analyses and PSY3V3R1 daily analyses (upper left), between OSTIA and RTG daily analyses (upper right) and between OSTIA and Reynolds ¼° AVHRR daily analyses (lower left).

V.2.3. Drifting buoys velocity measurements

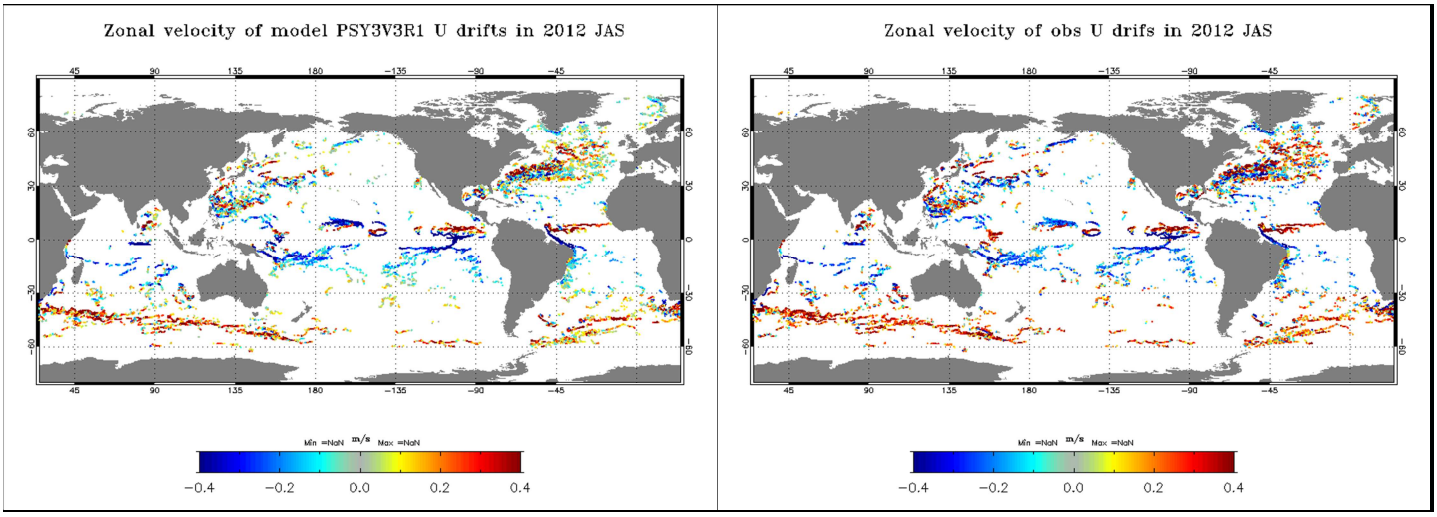

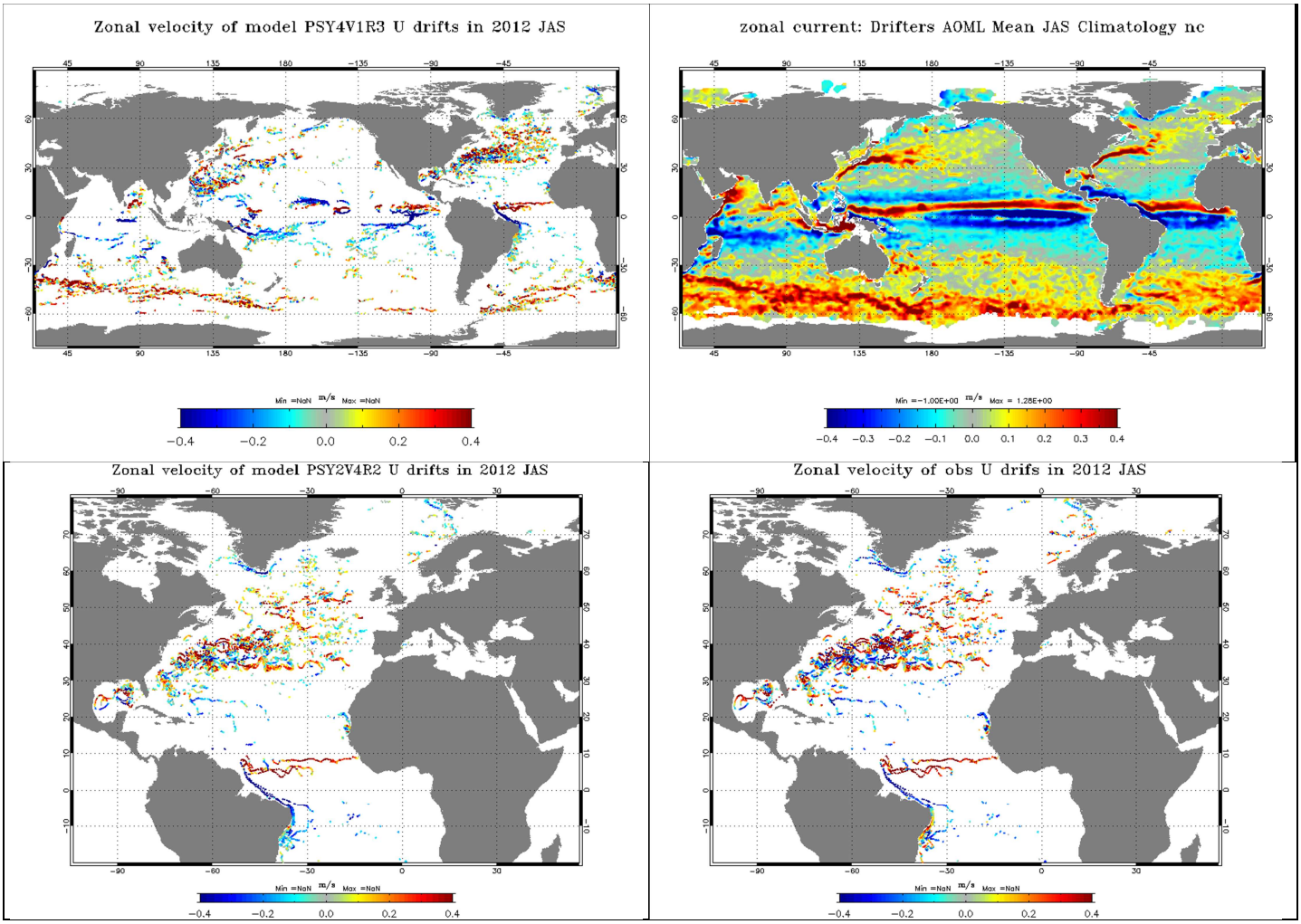

Figure 36: Comparison between modelled zonal current (left panel) and zonal current from drifters (right panel) in m/s. In the left column: velocities collocated with drifter positions in JAS 2012 for PSY3V3R1 (upper panel), PSY4V1R3 (middle panel) and PSY2V4R2 (bottom panel). In the right column, zonal current from drifters in JAS 2012 (upper panel) at global scale, AOML drifter climatology for JAS with new drogue correction from Lumpkin & al, in preparation (middle) and zonal current in JAS 2012 from drifters (lower panel) at regional scale.

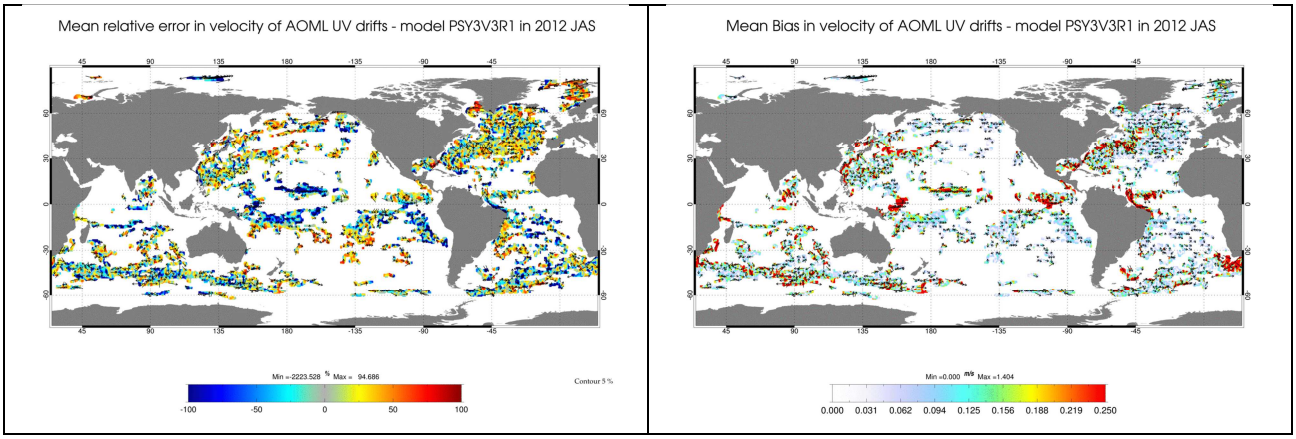

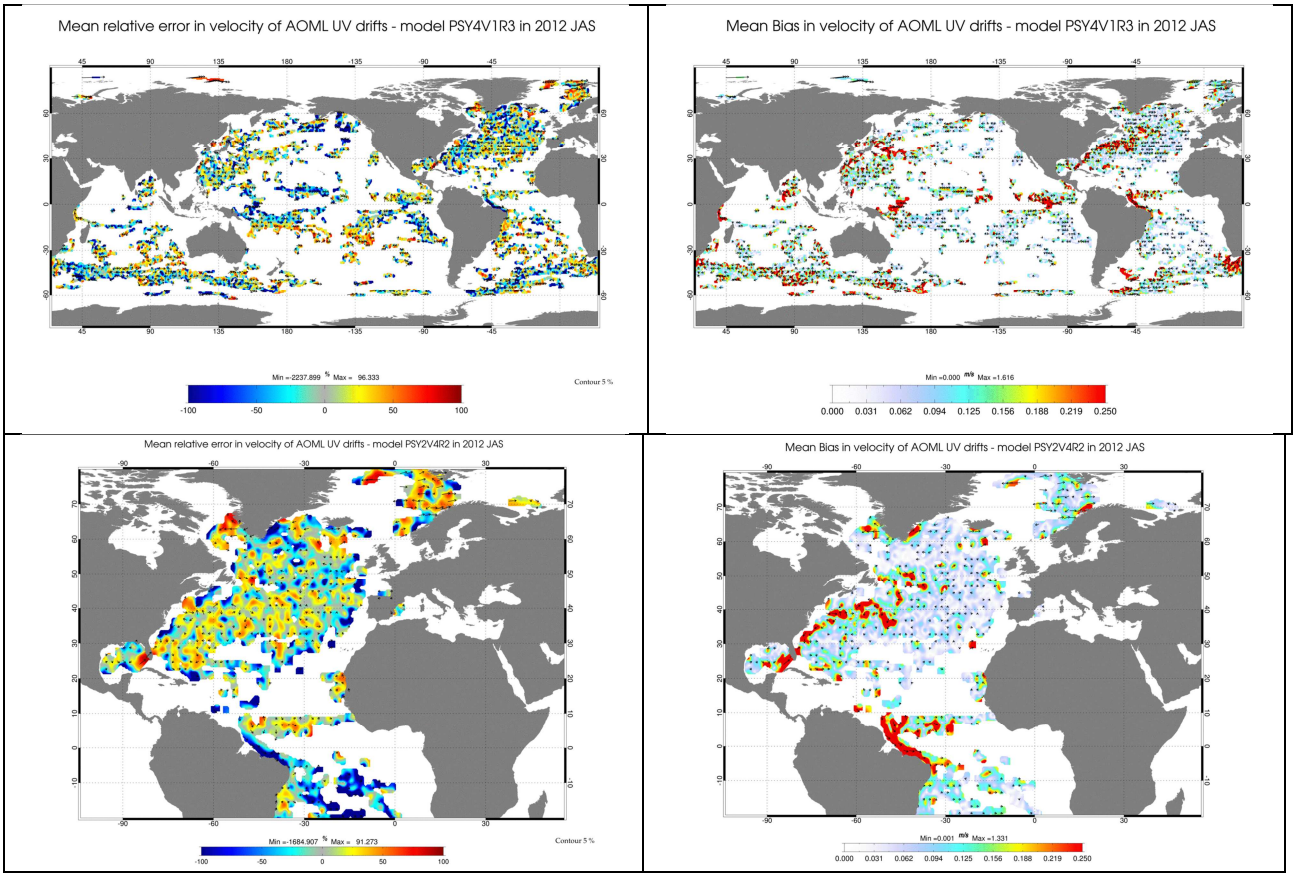

Figure 37 : In JAS 2012, comparison of the mean relative velocity error between in situ AOML drifters and model data on the left side and mean zonal velocity bias between in situ AOML drifters with Mercator Océan correction (see text) and model data on the right side. Upper panel: PSY3V3R1, middle panel: PSY4V1R3, bottom panel : PSY2V4R2. NB: zoom at 500% to see the arrows

Since *QuO Va Dis?* #5 we have been taking into account the fact that velocities estimated by the drifters happen to be biased towards high velocities.
As in *QuO Va Dis?* #5 we compute comparisons with slippage and windage corrections (cf *QuO Va Dis?* #5 and Annex C) . Once this "Mercator Océan" correction is applied to the drifter observations, the zonal velocity of the model (Figure 37) at 15 m depth and the meridional velocity (not shown) seem to be more consistent with the observations for the JAS 2012 period.

The main differences between the systems appear in the North Atlantic and North Pacific Oceans where PSY3V3R1 underestimate on average the eastward currents, which is less pronounced in the high resolution systems PSY4V1R3 and PSY2V4R2. This season especially in the northern hemisphere, and in the Equatorial Indian Ocean, PSY4V1R3 is closer to observed velocities than PSY3V3R1.

On average over longer periods, the usual behaviour compared to drifters' velocities is that PSY4V1R3 and PSY3V3R1 underestimate the surface velocity in the mid latitudes. All systems overestimate the Equatorial currents and southern part of the North Brazil Current (NBC).
For all systems the largest direction errors are local (not shown) and generally correspond to ill positioned strong current structures in high variability regions (Gulf Stream, Kurioshio,

North Brazil Current, Zapiola eddy, Agulhas current, Florida current, East African Coast current, Equatorial Pacific Countercurrent).

V.2.4. Sea ice concentration

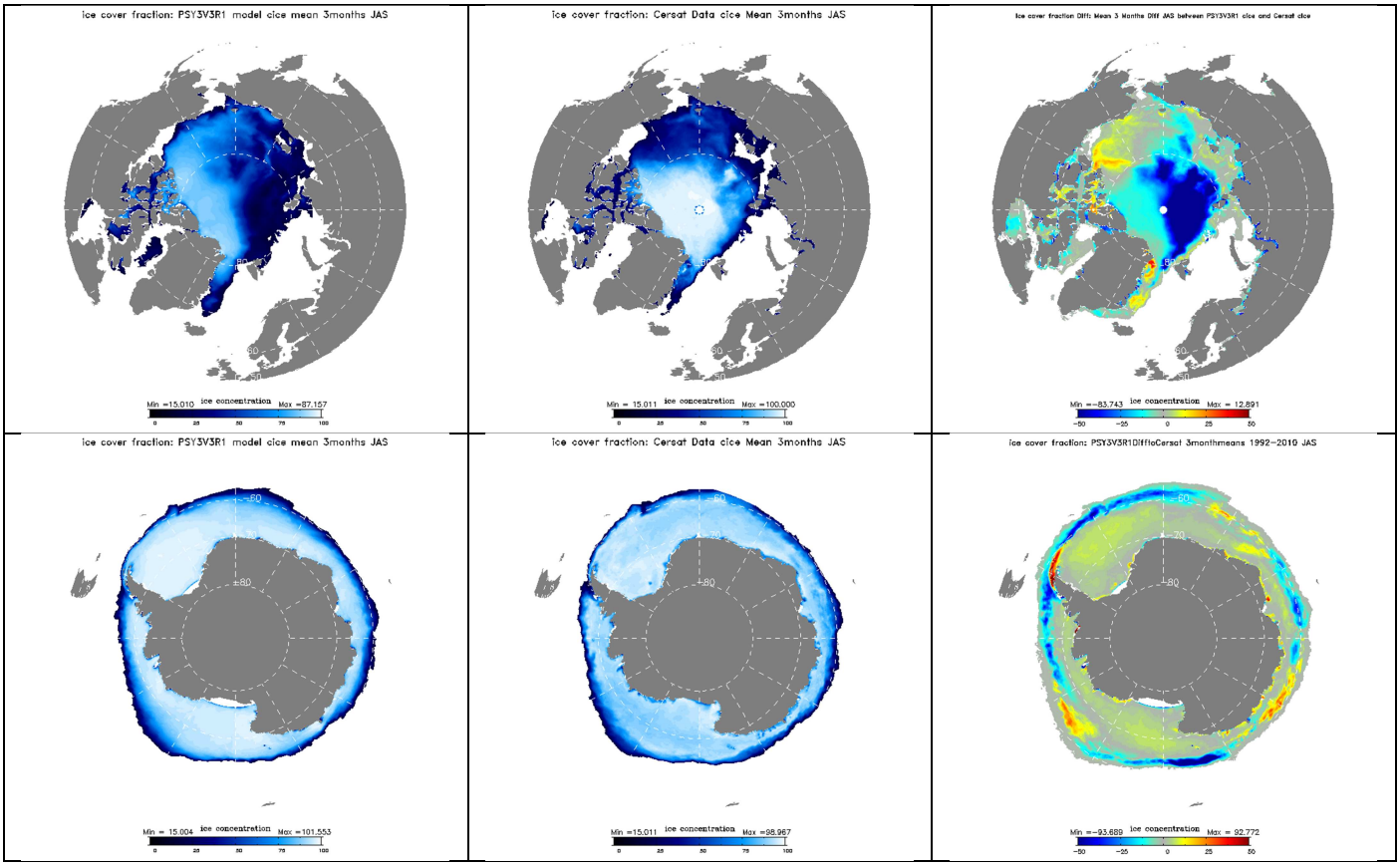

Figure 38: Comparison of the sea ice cover fraction mean for JAS 2012 for PSY3V3R1 in the Arctic (upper panel) and in the Antarctic (lower panel), for each panel the model is on the left, the mean of Cersat dataset in the middle and the difference on the right.

In JAS 2012 the PSY3V3R1 Arctic sea ice fraction is in agreement with the observations on average. The relatively small discrepancies inside the sea ice pack will not be considered as significant as the sea ice concentration observations over 95% are not reliable. Strong discrepancies with observed concentration remain in the marginal seas mainly in the North Atlantic Ocean side of the Arctic, especially in the Fram strait and the Barents Sea this JAS 2012 season (Figure 38).

Model studies show that the overestimation in the Canadian Archipelago is first due to badly resolved sea ice circulation (should be improved with higher horizontal resolution). The overestimation in the eastern part of the Labrador Sea is due to a weak extent of the West Greenland Current; similar behaviour in the East Greenland Current.

The calibration on years 2007 to 2009 has shown that the PSY3V3R1 system tends to melt too much ice during the summer, while the winter sea ice covers are much more realistic in PSY3V3R1 than in previous versions of PSY3. See Figure 60 for monthly averages time series over the last 12 months. On the contrary PSY4V1R3 sea ice cover is unrealistic

(overestimation throughout the year) due to the use of a previous version of LIM2 and daily atmospheric forcings.

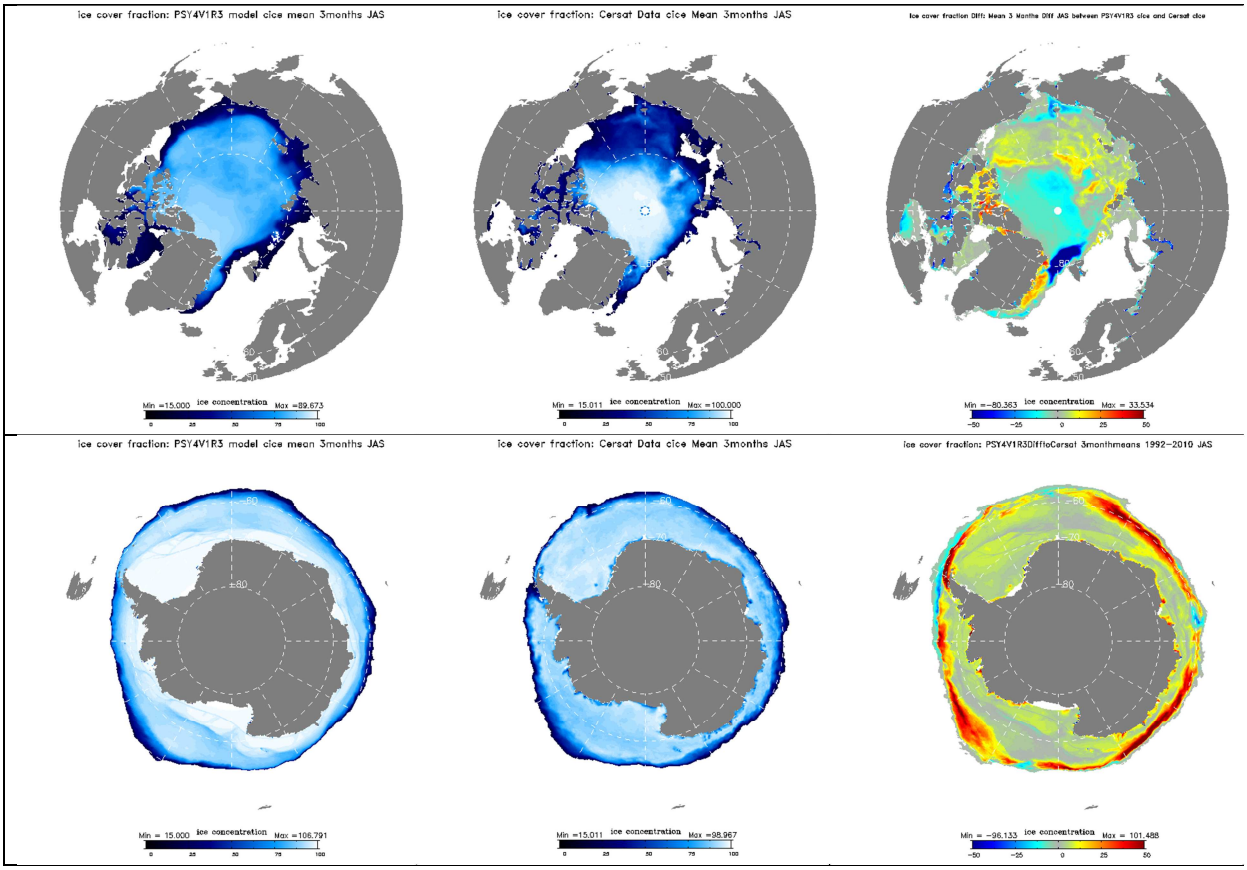

Figure 39: Comparison of the sea ice cover fraction mean for JAS 2012 for PSY4V1R3 in the Arctic (upper panel) and in the Antarctic (lower panel), for each panel the model is on the left, the mean of Cersat dataset in the middle and the difference on the right.

As expected in the Antarctic during the austral winter the sea ice concentration is underestimated in the model PSY3V3R1 and overestimated in PSY4V1R3, especially at the south of the Ross Sea, in the Weddel Sea, Bellinghausen and Admundsen Seas and along the Eastern coast.

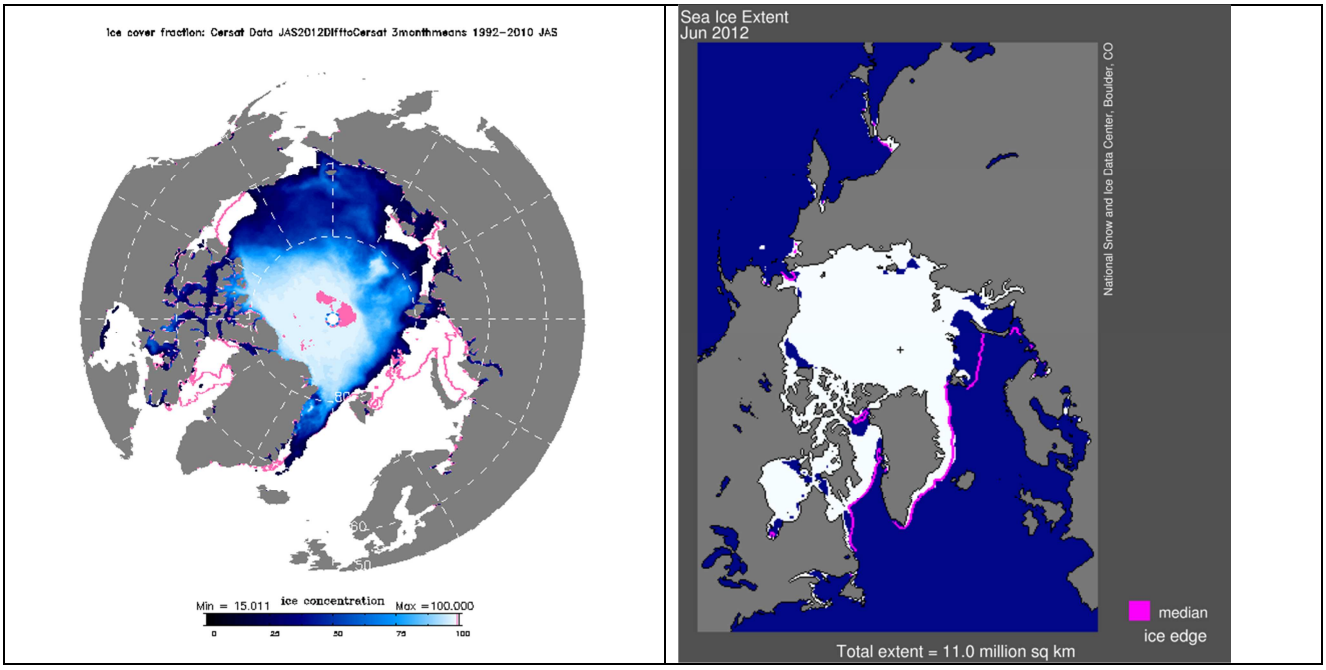

Figure 40: JAS 2012 Arctic sea ice extent in PSY3V3R1 with overimposed climatological JAS 1992-2010 sea ice fraction (magenta line, > 15% ice concentration) (left) and NSIDC map of the sea ice extent in the Arctic for June 2012 in comparison with a 1979-2000 median extend (right).

Figure 40 illustrates the fact that sea ice cover in JAS 2012 is less than the past years climatology, especially in the Barents Sea, even with a slight underestimation in PSY3V3R1 in this region in JAS 2012. In the Antarctic the model bias prevents us from commenting the climate signal (not shown).

V.2.5. Closer to the coast with the IBI36V2 system: multiple comparisons

V.2.5.1. Comparisons with SST from CMS

Figure 41 displays bias, RMS error and correlation calculated from comparisons with SST measured by satellite in JAS 2012 (Météo-France CMS high resolution SST at 0.02°). The cold bias already noticed in the North Sea in AMJ 2012 is still present and extends to the Channel (except around the western part of Britanny) and the Irish and Celtic Seas. A warm bias is present along the Maroccan coast and western Iberian coast, where upwellings occur, and in the gulf of Lion. In the English Channel and Celtic Sea, the biases are linked to tidal mixing. In the Mediterranean Sea, biases are associated to the Alboran gyre and the Algerian current. Away from the shelf, the bias is near zero and the RMS error is small (less than 0.5°C). The lower correlation is between 45 and 50°N and in the northern part of the domain; but these areas have the smallest number of observations. The biases are higher in shelf areas this summer JAS 2012 season with respect to the previous spring season, especially in upwellings regions.

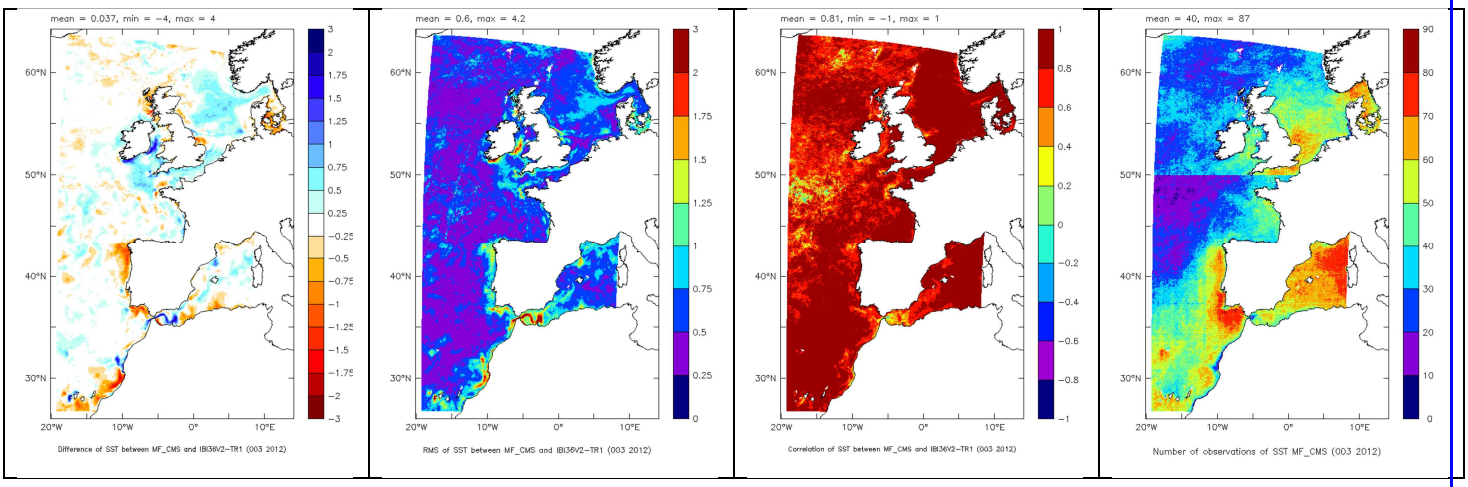

Figure 41 : Comparisons (observation-model) between IBI36V2 and analysed SST from MF_CMS for the JAS 2012 period. From the left to the right: mean bias, RMS error, correlation, number of observations

V.2.5.2. Comparisons with in situ data from EN3/ENSEMBLE for JAS 2012

Averaged temperature profiles (Figure 42) show that the strongest mean bias and RMS error (more than 2°C) are observed between 20 and 80 m depth, in the thermocline, and also near 1200m, at the average depth of the Mediterranean outflow. Apart from the thermocline, the model is close to the observations on the whole water column. Below the thermocline, the mean bias is almost zero, and the strongest RMS is found at the Mediterranean Sea Water level. In the Bay of Biscay, the bias and RMS error are reduced compared to the global average (maximum bias of 0.5°C and maximum RMS error of 0.9°C); the Mediterranean waters are significantly too warm. As shown by the mean temperature profiles, PSY2V4R2 is closer to the temperature observations than IBI36V2 on the whole water column thanks to data assimilation. It is also the case when we compare RMS errors (not shown). However, IBI36V2 tends to display at least as good results as PSY2V4R2 in the Bay of Biscay.

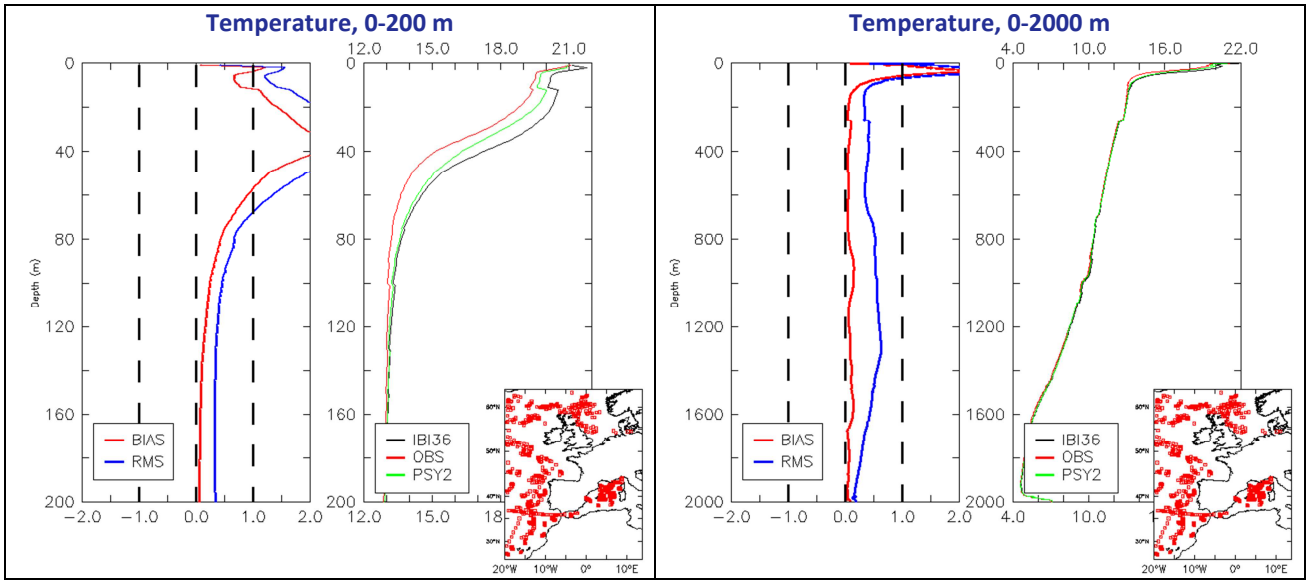

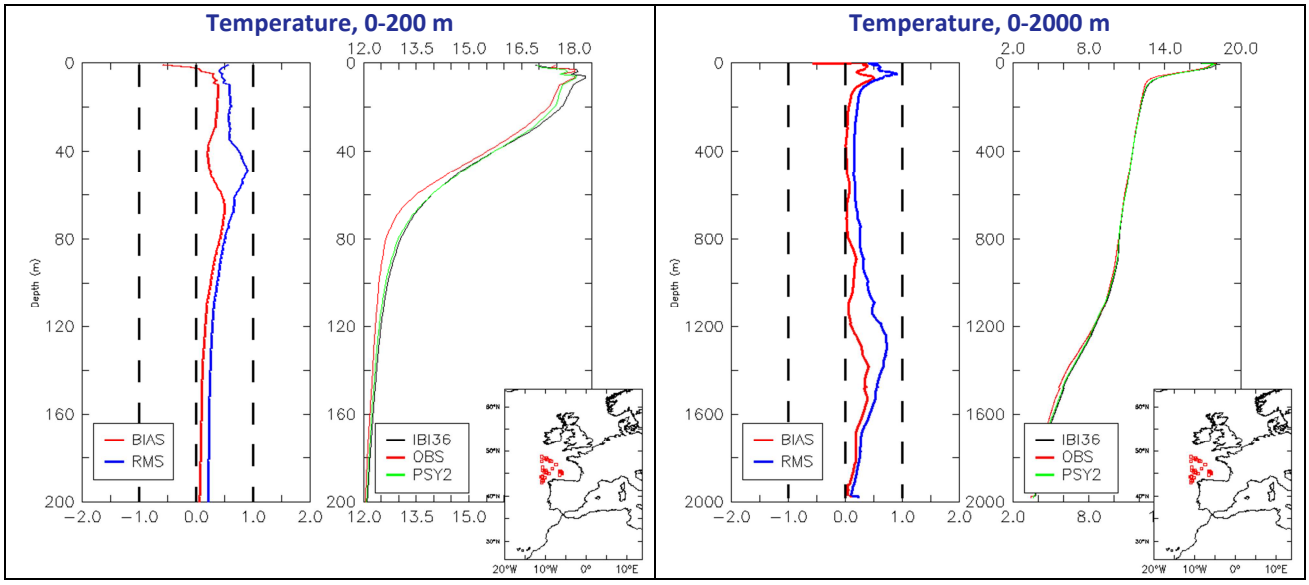

Figure 42 : For IBI36V2: On the left: mean "model - observation" temperature(°C) bias (red curve) and RMS error (blue curve) in JAS 2012, On the right: mean profile of the model (black curve), of the observations (red curve), and of the PSY2V4R2 model (green curve) in JAS 2012. In the lower right corner: position of the profiles. Top panel: the whole domain; bottom panel: the Bay of Biscay region.

The maximum salinity bias and RMS error (Figure 43) occur near the surface. The model is too fresh between the surface and 50 m depth, and too salty between 100 and 300 m depth. The RMS error is strong at the Mediterranean Sea Water level (as for temperature). In the Bay of Biscay the Mediterranean waters are too salty.
Note: averaged profiles are discontinuous because the number of observations varies with depth.

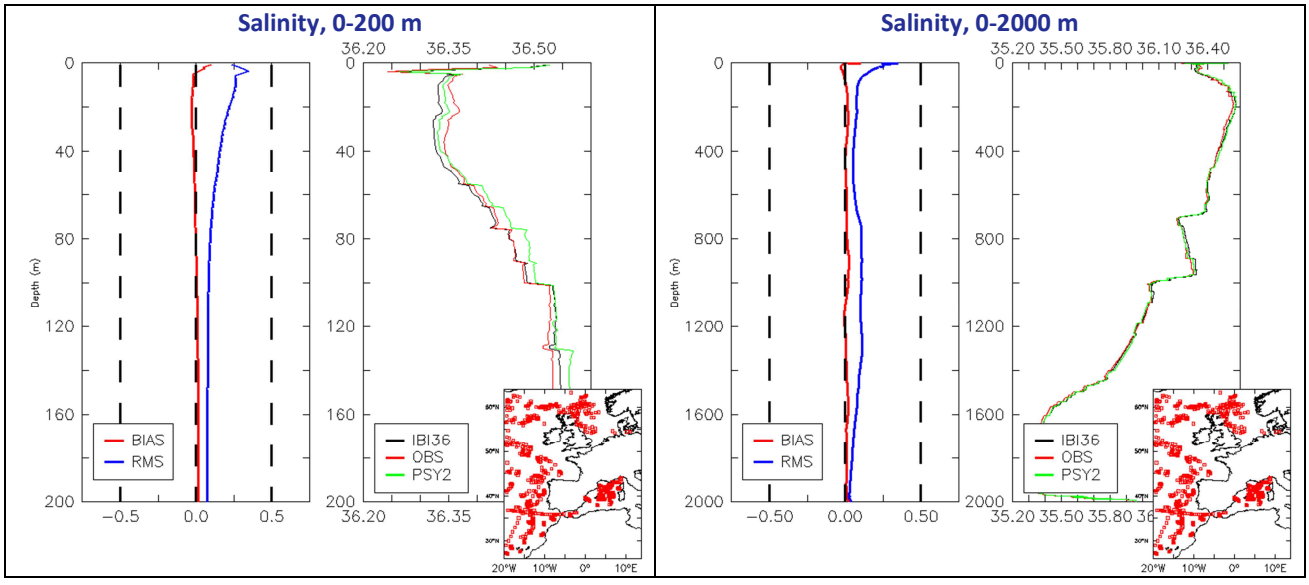

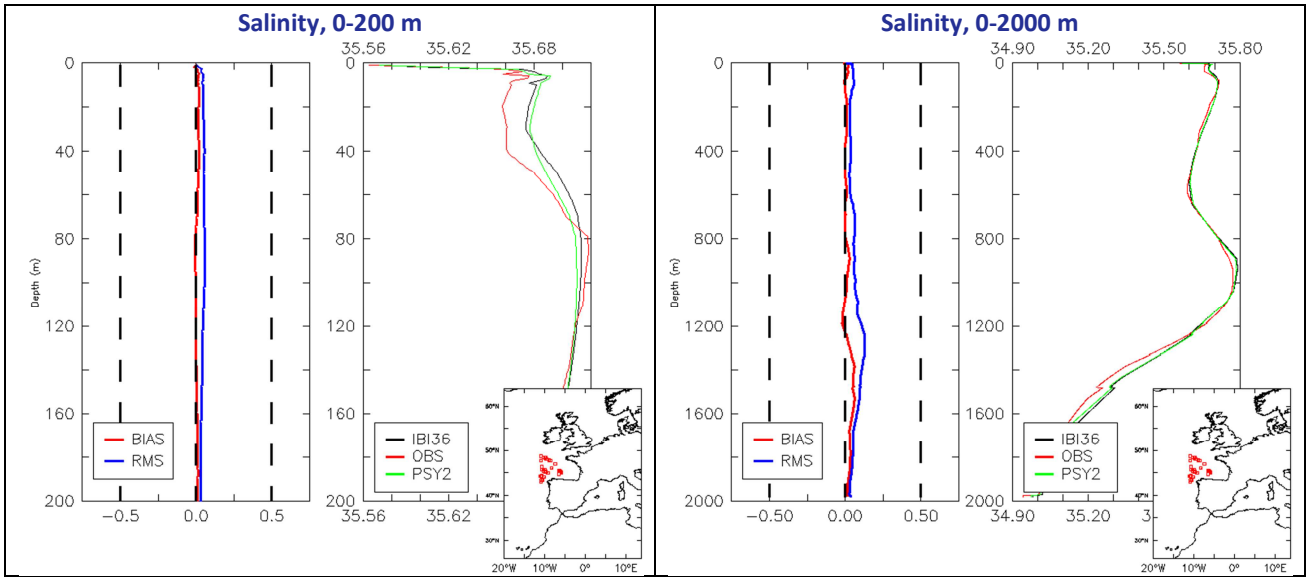

Figure 43: For IBI36V2: On the left: mean "model - observation" salinity (psu) bias (red curve) and RMS error (blue curve) in JAS 2012, On the right: mean profile of the model (black curve), of the observations (red curve), and of the PSY2V4R2 model (green curve) in JAS 2012. In the lower right corner: position of the profiles. Top panel: the whole domain; bottom panel: the Bay of Biscay region.

V.2.5.3. MLD Comparisons with in situ data

Figure 44 shows that the distribution of modeled mixed layer depths among the available profiles is close to the observed distribution. Values of the mixed layer depth between 10 m and 15 m, and between 20 and 30 m occur too often in the model compared with the observations. On the contrary, values between 15 and 20 m are under-estimated by the model. IBI36V2 and PSY2V4R2 have closed results. In the Bay of Biscay they differ slightly: IBI36V2 under-estimates values of the MLD between 20 and 25 m depth, while PSY2V4R2 over-estimates them.

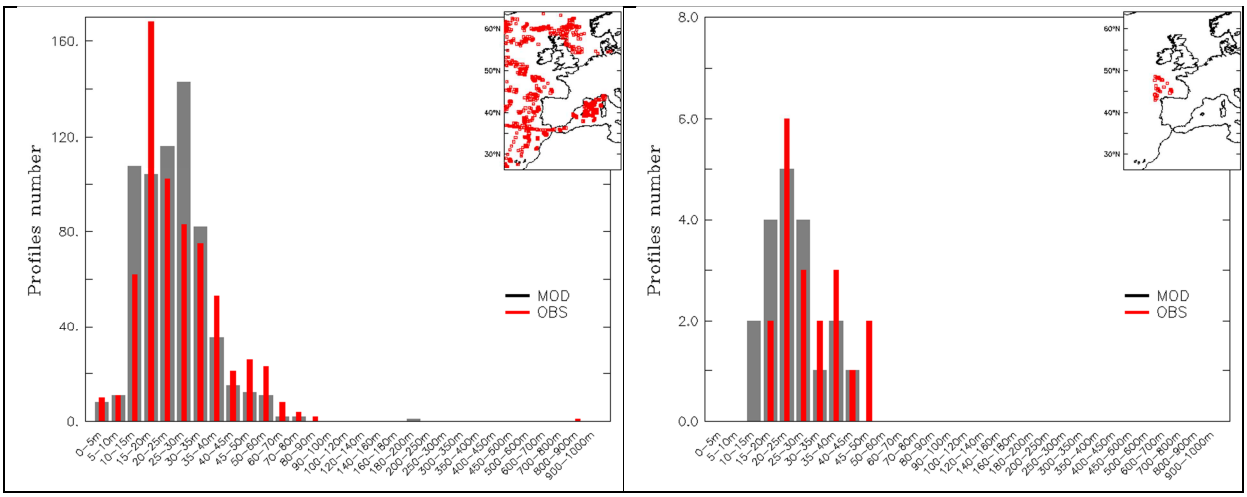

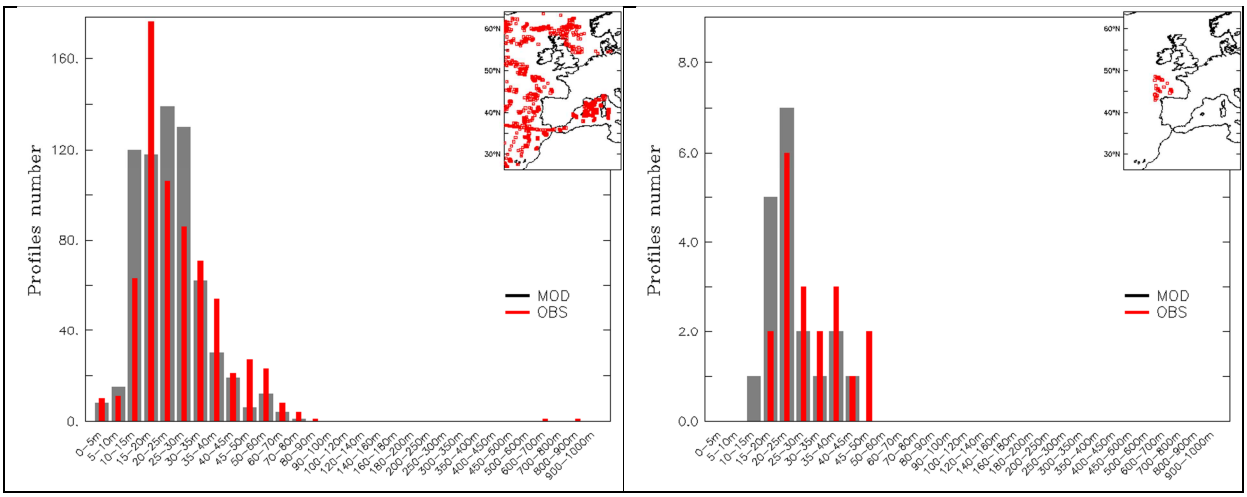

Figure 44 : For IBI36V2 (top panels): Mixed Layer Depth distribution in JAS 2012 calculated from profiles with the temperature criteria (difference of 0.2°C with the surface); the model is in grey, the observations in red. Left panel: whole domain; right panel: Bay of Biscay. Bottom panel: the same for PSY2V4R2.

V.2.5.4. Comparisons with moorings and tide gauges

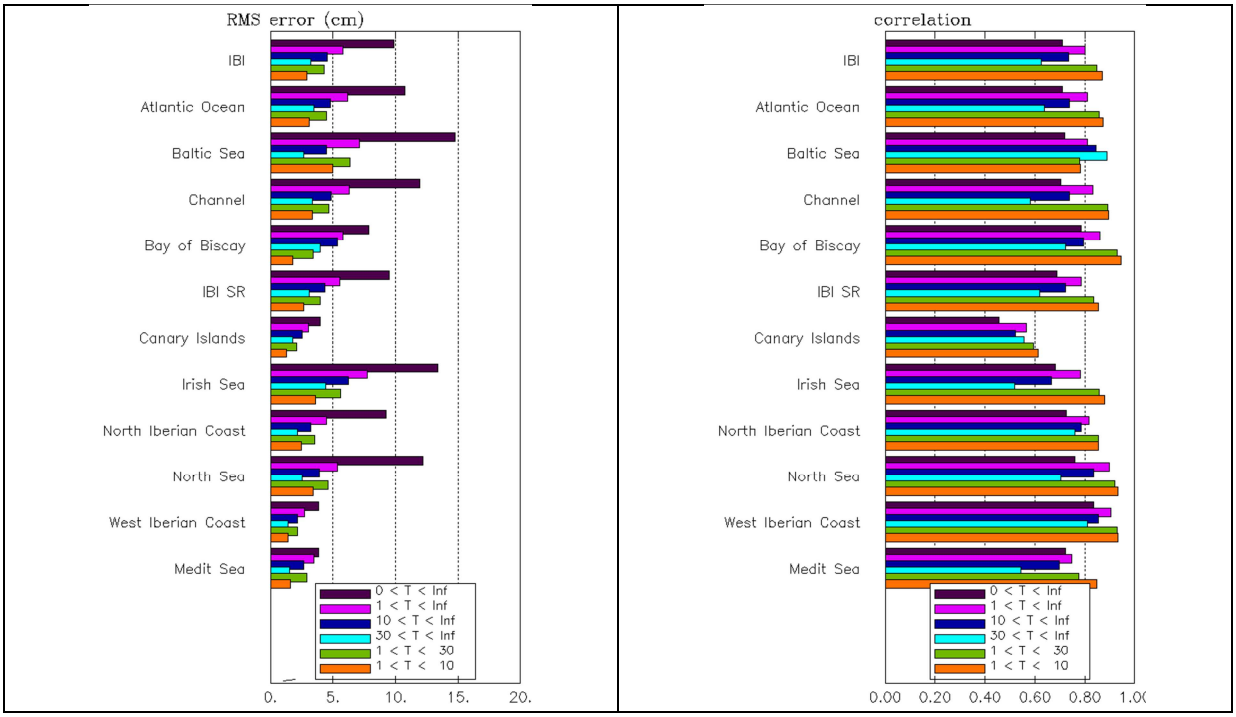

Figure 45 : For IBI36V2: RMS error (cm) and correlation for the non-tidal Sea Surface Elevation at tide gauges in JAS 2012, for different regions and frequencies.

The RMS error of the residual elevation of sea surface (Figure 45) computed with a harmonic decomposition method (Foreman 1977) and a Loess low-pass filtering, is comprised between 5 and 15 cm. It is close to 5 cm in the Canary Islands and in the Mediterranean Sea. The RMS decreases for some frequency bands, and the smallest values occur in the 1-10-day band. The correlation is significant at all frequencies, and reaches high values for periods lower than 30 days (at high frequencies).

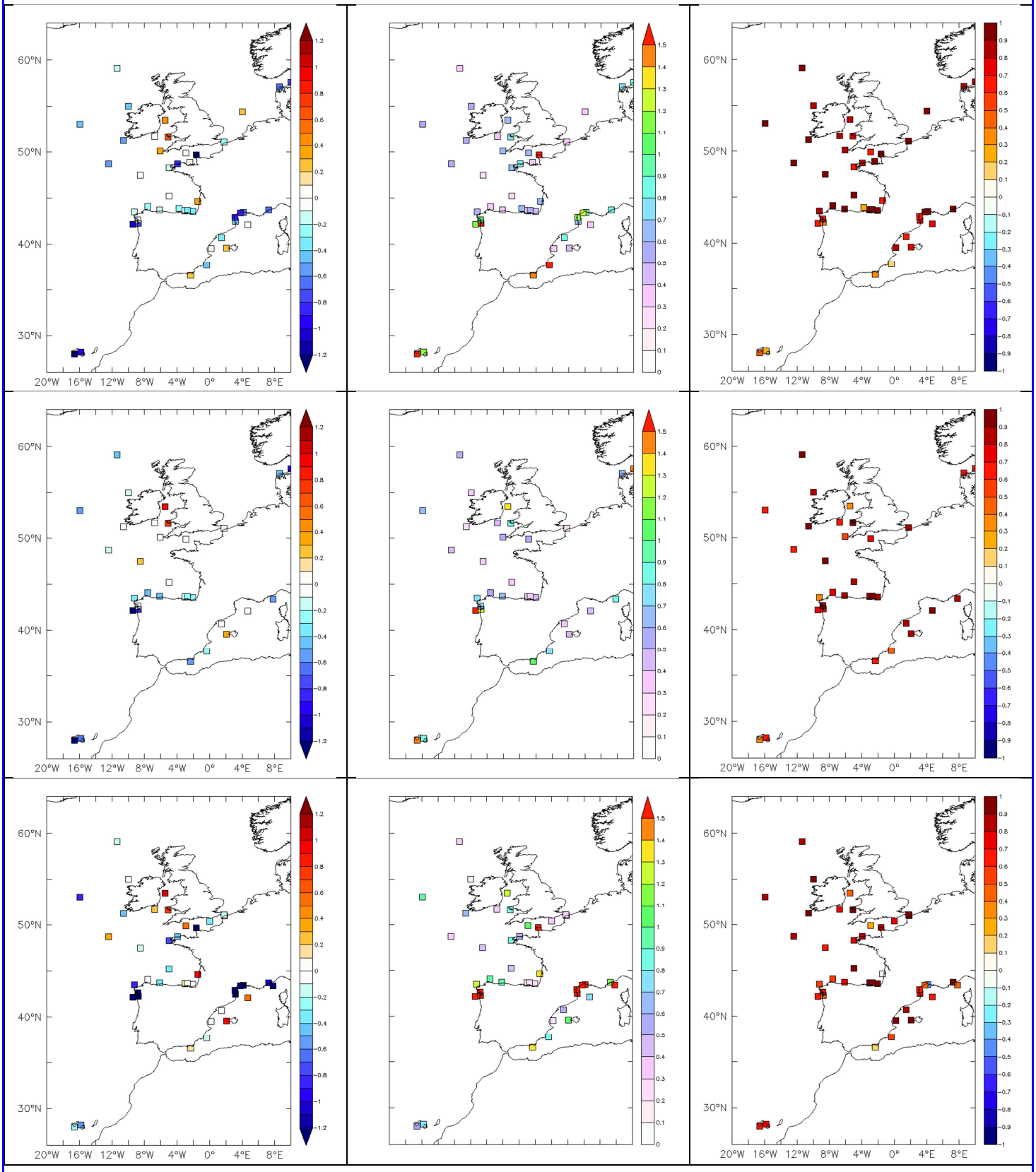

Figure 46 : For IBI36V2: Bias (observation-model), RMS error (°C) and correlation of the Sea Surface Temperature between IBI model and moorings measurements in July (upper panel), August (middle panel) and September 2012 (lower panel).

In Figure 46 we can see that the SST correlations between the coastal moorings and the IBI model are generally good for the three months in nearly the whole domain. The maximum biases and RMS errors are located in shelf areas (especially near Cherbourg, along the Iberian west coast and in the gulf of Lion); maximum values are reached in September. The model temperature is generally higher than the observations, except in the Irish Sea, consistently with the L3 SST biases of Figure 41.

V.2.6. Biogeochemistry validation: ocean colour maps

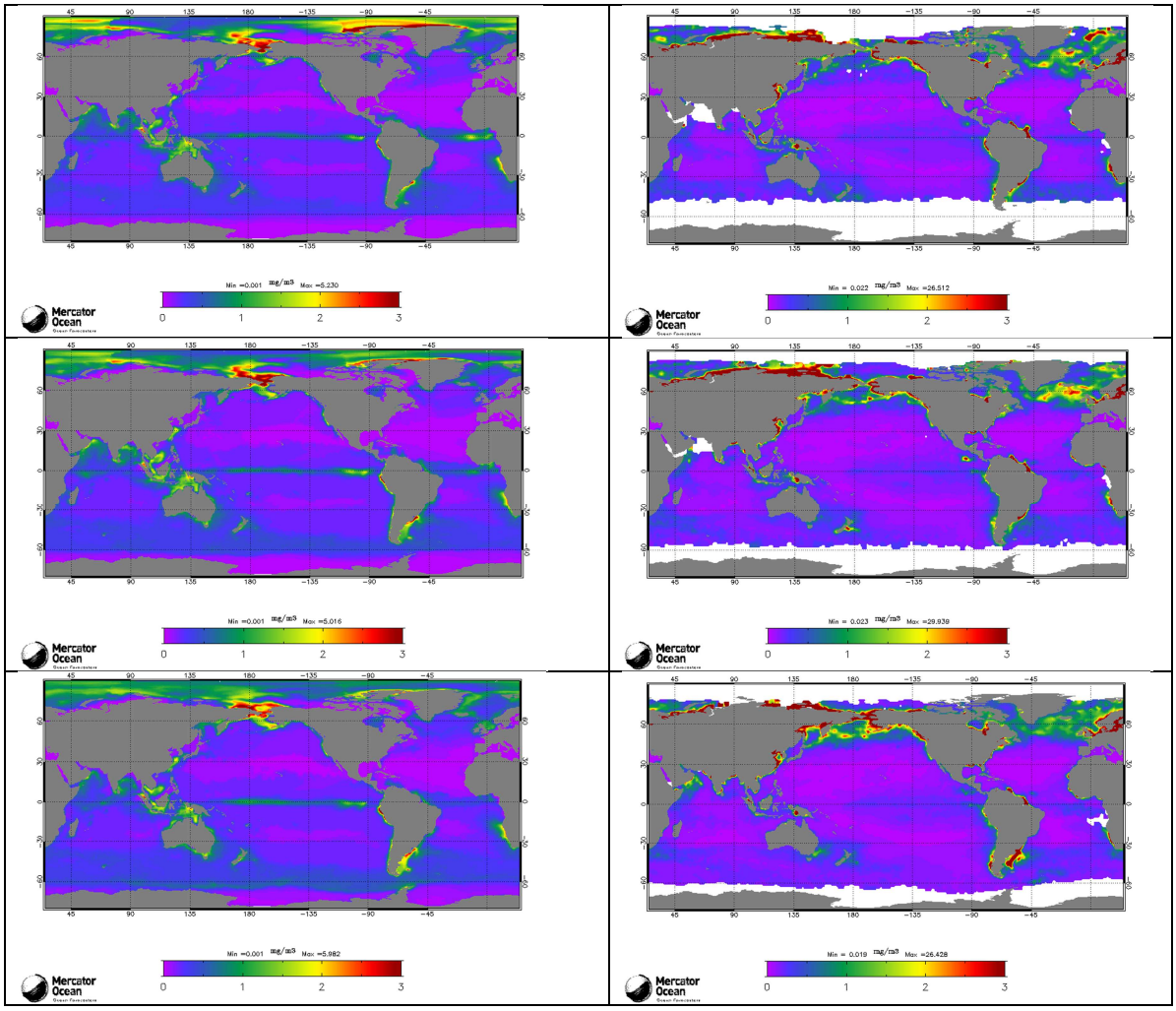

Figure 47 : Chlorophyll-a concentration (mg/m^3) for the Mercator system BIOMER (left panels) and Chlorophyll-a concentration from Globcolour (right panels). The upper panel is for July, the medium panel is for August and the bottom panel is for September 2012.

As can be seen on Figure 47 the surface chlorophyll-a concentration is overestimated by BIOMER on average over the globe. The production is especially overestimated in the Pacific and Atlantic equatorial upwellings. On the contrary near the coast BIOMER displays significantly lower chlorophyll concentrations than Globcolour ocean colour maps. In North Atlantic, the spring bloom in Globcolour data persists over July, August and September north of 45°N whereas it is over in BIOMER. Figure 48 shows the PDF of the Chl-a bias in North Atlantic. The shift towards the positive values reflects the time lag between the bloom in observations and in BIOMER (too early in the model).

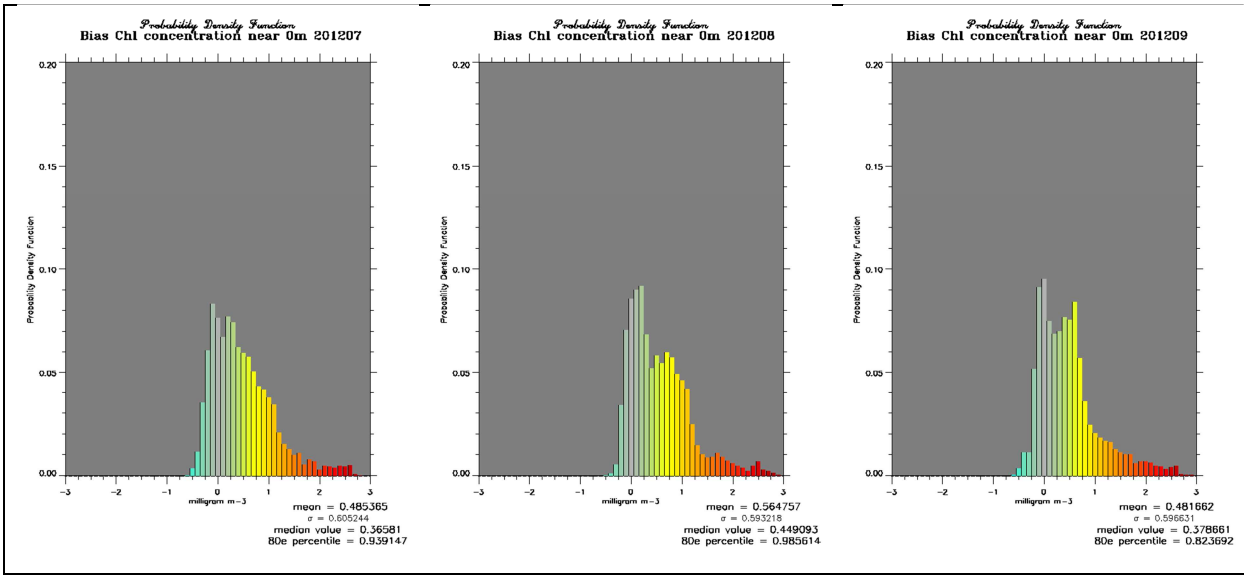

Figure 48 : Probability Density Function (PDF) of Chl-a bias in log scale (log10(obs)-log10(model)) in North Atlantic (30-70N; 80W:20E)

The discrepancies at global scale appear in the RMS differences for the mean JAS season (Figure 49).

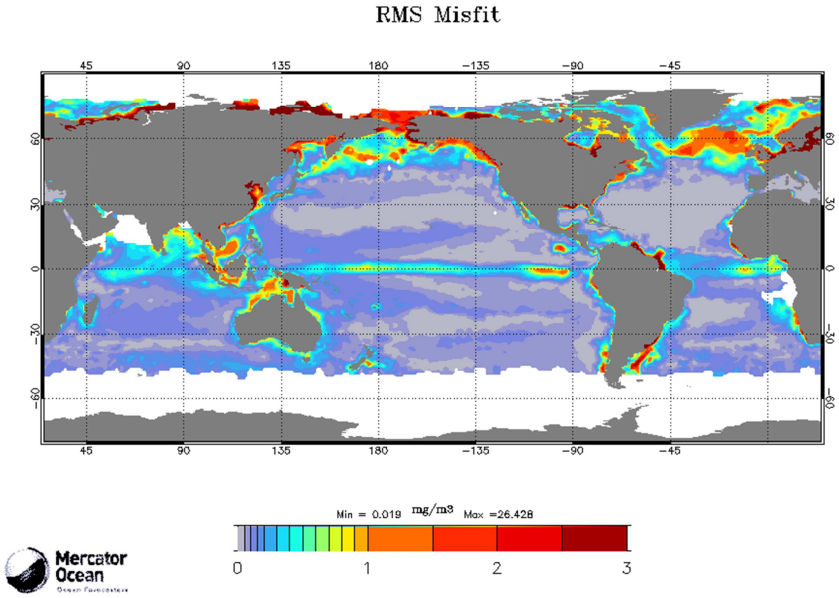

Figure 49 : RMS difference between BIOMER and Globcolour Chl-a concentrations (mg/m^3) in JAS 2012.

VI Forecast error statistics

VI.1. General considerations

The daily forecasts (with updated atmospheric forcings) are validated in collaboration with SHOM/CFUD. This collaboration has been leading us to observe the actual degradation of the forecast quality depending on the forecast range. When the forecast range increases the quality of the ocean forecast decreases as the initialization errors propagate and the quality of the atmospheric forcing decreases. Additionally the atmospheric forcing frequency also changes (see Figure 50). The 5-day forecast quality is optimal; starting from the 6th day a drop in quality can be observed which is linked with the use of 6-hourly atmospheric fields instead of 3-hourly; and starting from the 10th day the quality is strongly degraded due to the use of persisting atmospheric forcings (but not constant from the 10th to the 14th day as they are relaxed towards a 10-day running mean).

Figure 50: Schematic of the change in atmospheric forcings applied along the 14-day ocean forecast.

VI.2. Forecast accuracy: comparisons with observations when and where available

VI.2.1. North Atlantic region

As can be seen in Figure 51 the PSY2V4R2 products have a better accuracy than the climatology in the North Atlantic region in JAS 2012, except for temperature at depth (but in the 2000-5000m layer, the statistics are performed on a very small sample of observations, and thus are not really representative of the region or layer). In general the analysis is more accurate than the 3-day and 6-day forecast for both temperature and salinity. The RMS error thus increases with the forecast range (shown for NAT region Figure 51 and MED region Figure 52). The biases in temperature and salinity are generally small (of the order of 0.1 °C and 0.02 psu) compared to the climatology's biases (of the order of 0.4 °C and 0.05 psu).
In the North Atlantic, the PSY2V4R2 system is too salty on the whole water column, too cold at the surface and too warm below.

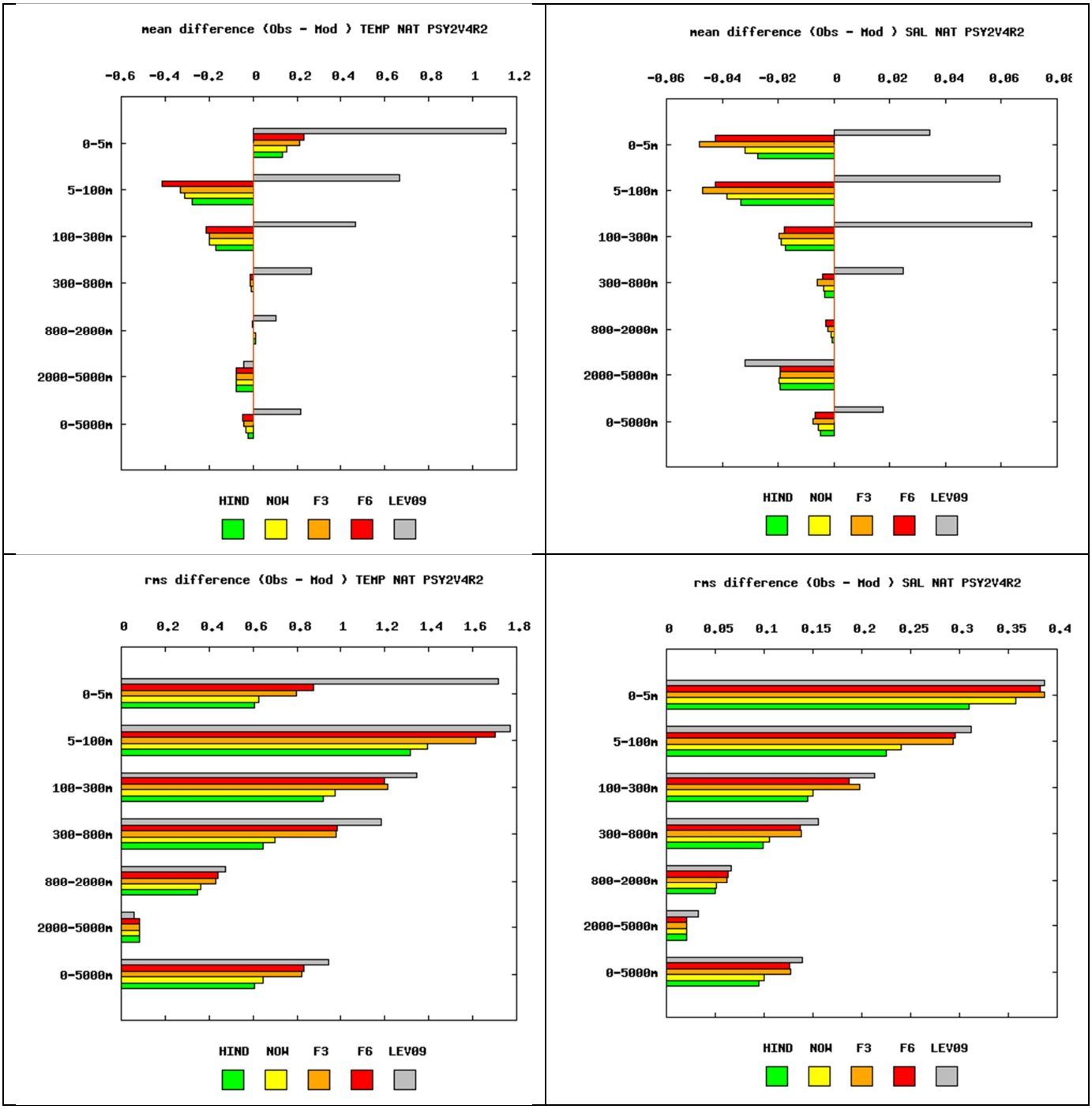

Figure 51: Accuracy intercomparison in the North Atlantic region for PSY2V4R2 in temperature (left panel) and salinity (right panel) between hindcast, nowcast, 3-day and 6-day forecast and WO09 climatology. Accuracy is measured by a mean difference (upper panel) and by a rms difference (lower panel) of temperature and salinity with respect to all available observations from the CORIOLIS database averaged in 6 consecutive layers from 0 to 5000m. All statistics are performed for the JAS 2012 period. NB: average on model levels is performed as an intermediate step which reduces the artefacts of inhomogeneous density of observations on the vertical.

VI.2.2. Mediterranean Sea

In the Mediterranean Sea in JAS 2012 (Figure 52) the PSY2V4R2 products are more accurate than the climatology on average. PSY2V4R2 is biased at the surface (fresh and cold bias). Between 5 and 100m the system is generally too warm and fresh.

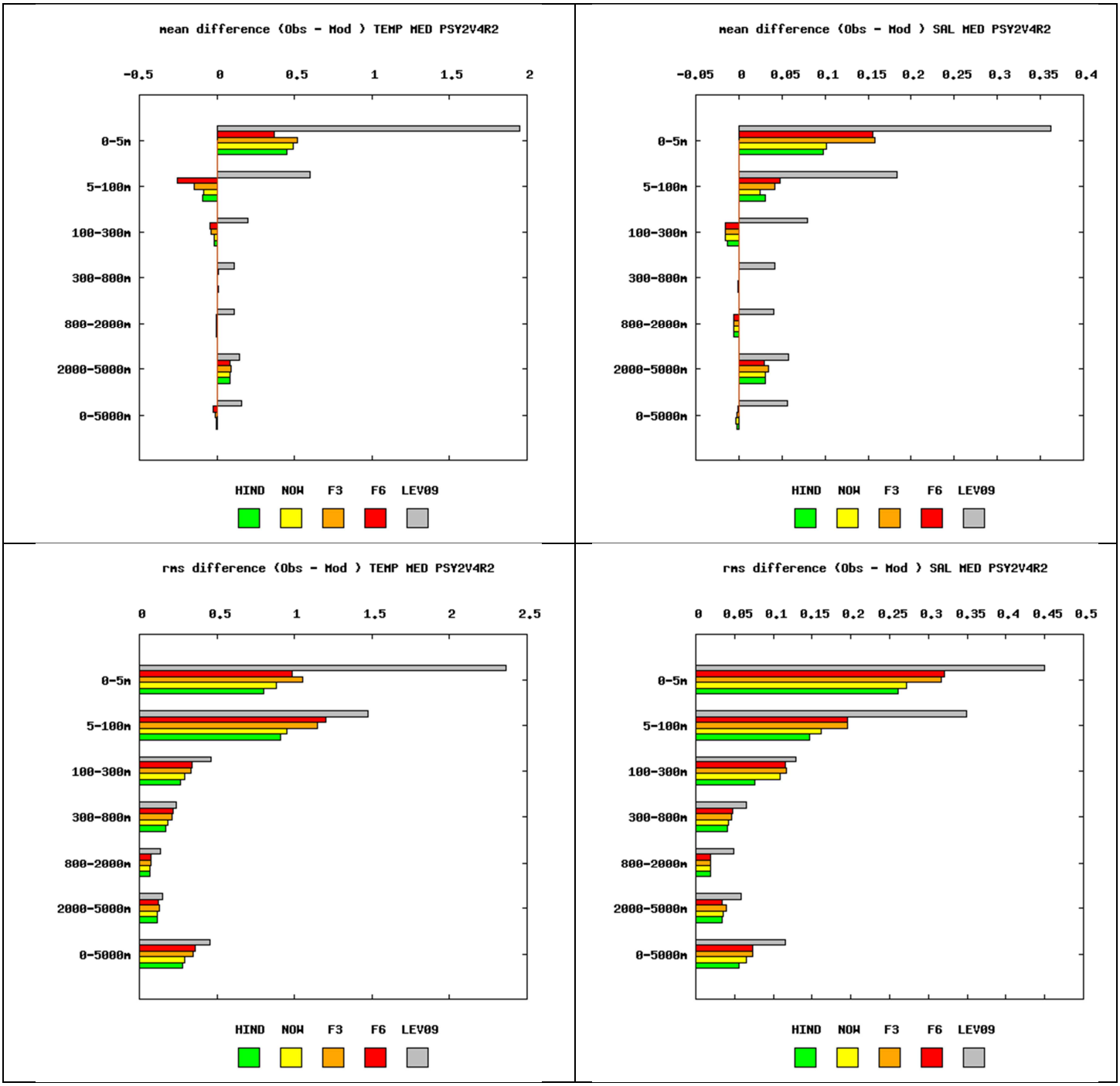

Figure 52: Accuracy intercomparison in the Mediterranean Sea region for PSY2V4R2 in temperature (°C, left column) and salinity (psu, right column) between hindcast, nowcast, 3-day and 6-day forecast and WO09 climatology. Accuracy is measured by a rms difference (lower panel) and by a mean difference (upper panel) with respect to all available observations from the CORIOLIS database averaged in 6 consecutive layers from 0 to 5000m. All statistics are performed for the JAS 2012 period. NB: average on model levels is performed as an intermediate step which reduces the artefacts of inhomogeneous density of observations on the vertical.

VI.2.3. Tropical Oceans, Indian, Global: what system do we choose in JAS 2012?

The best performing system in JAS 2012 in terms of water masses is PSY3V3R1 (with similar performances with PSY2V4R2 in the Tropical Atlantic) as can be seen in Figure 53. This is not surprising when we take into account that PSY4V1R3 has no bias correction for the moment. Nevertheless, the high resolution global PSY4V1R3 beats the climatology and is very promising in many regions, for instance in the Atlantic, the Indian ocean or the North Pacific. PSY4V1R3 surface currents may also be preferred to PSY3V3R1's currents, as mentioned in V.2.3.

We also note that at all depth in all regions the PSY3V3R1 RMS error increases with forecast range, as could be expected, and that the 6-day forecast still beats the climatology. Some exceptions are noted under 2000 m in the tropical Atlantic and Indian oceans, probably corresponding to sampling problems (very few observations are available at these depths).

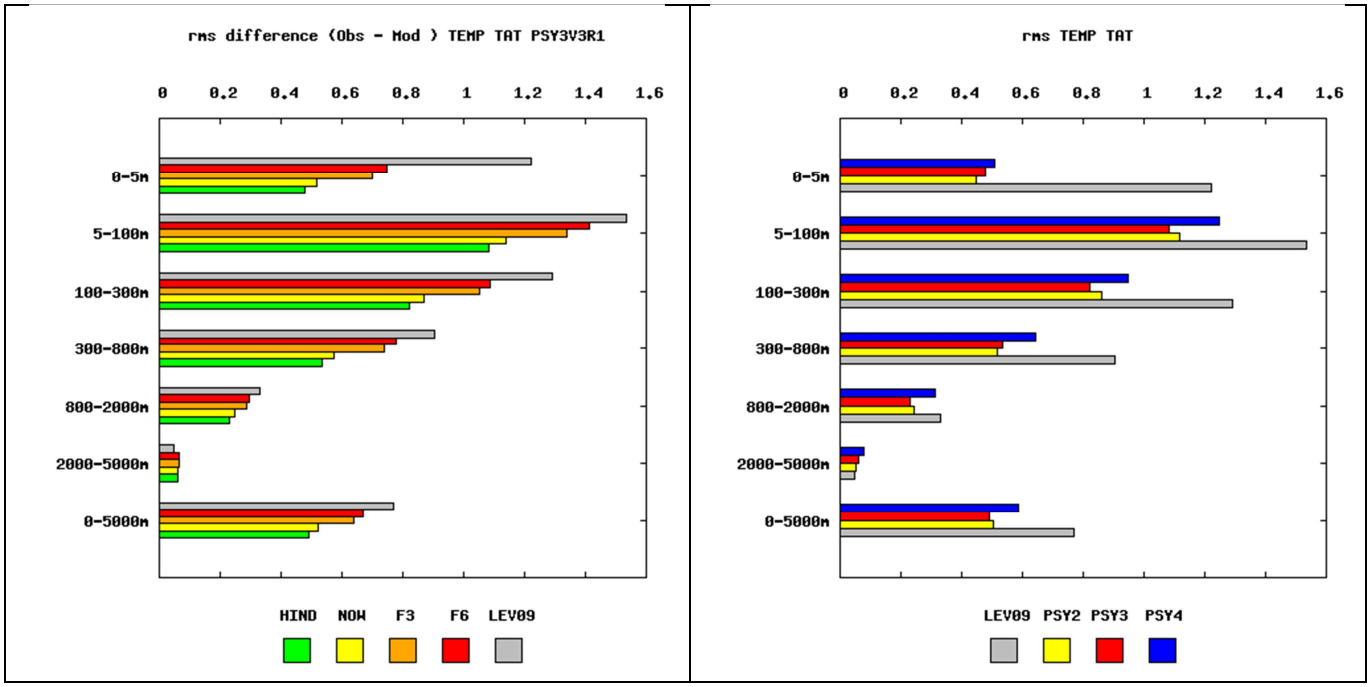

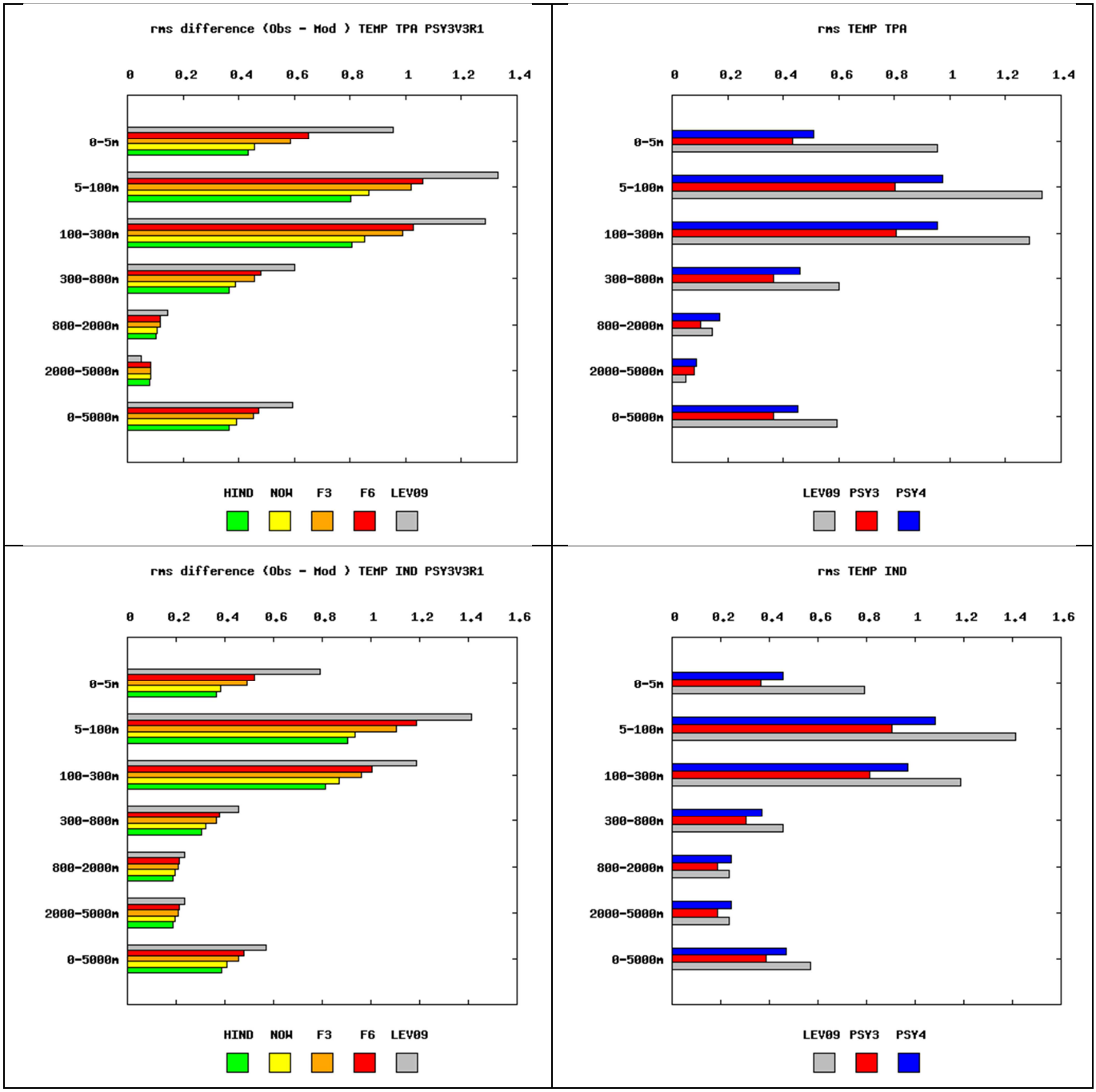
rms difference (Obs - Mod) TEMP TPA PSY3V3R1
0 0.2 0.4 0.6 0.8 1 1.2 1.4
0-5m
5-100m
100-300m
300-800m
800-2000m
2000-5000m
0-5000m
HIND NOW F3 F6 LEV09
rms TEMP TPA
0 0.2 0.4 0.6 0.8 1 1.2 1.4
0-5m
5-100m
100-300m
300-800m
800-2000m
2000-5000m
0-5000m
LEV09 PSY3 PSY4
rms difference (Obs - Mod) TEMP IND PSY3V3R1
0 0.2 0.4 0.6 0.8 1 1.2 1.4 1.6
0-5m
5-100m
100-300m
300-800m
800-2000m
2000-5000m
0-5000m
HIND NOW F3 F6 LEV09
rms TEMP IND
0 0.2 0.4 0.6 0.8 1 1.2 1.4 1.6
0-5m
5-100m
100-300m
300-800m
800-2000m
2000-5000m
0-5000m
LEV09 PSY3 PSY4

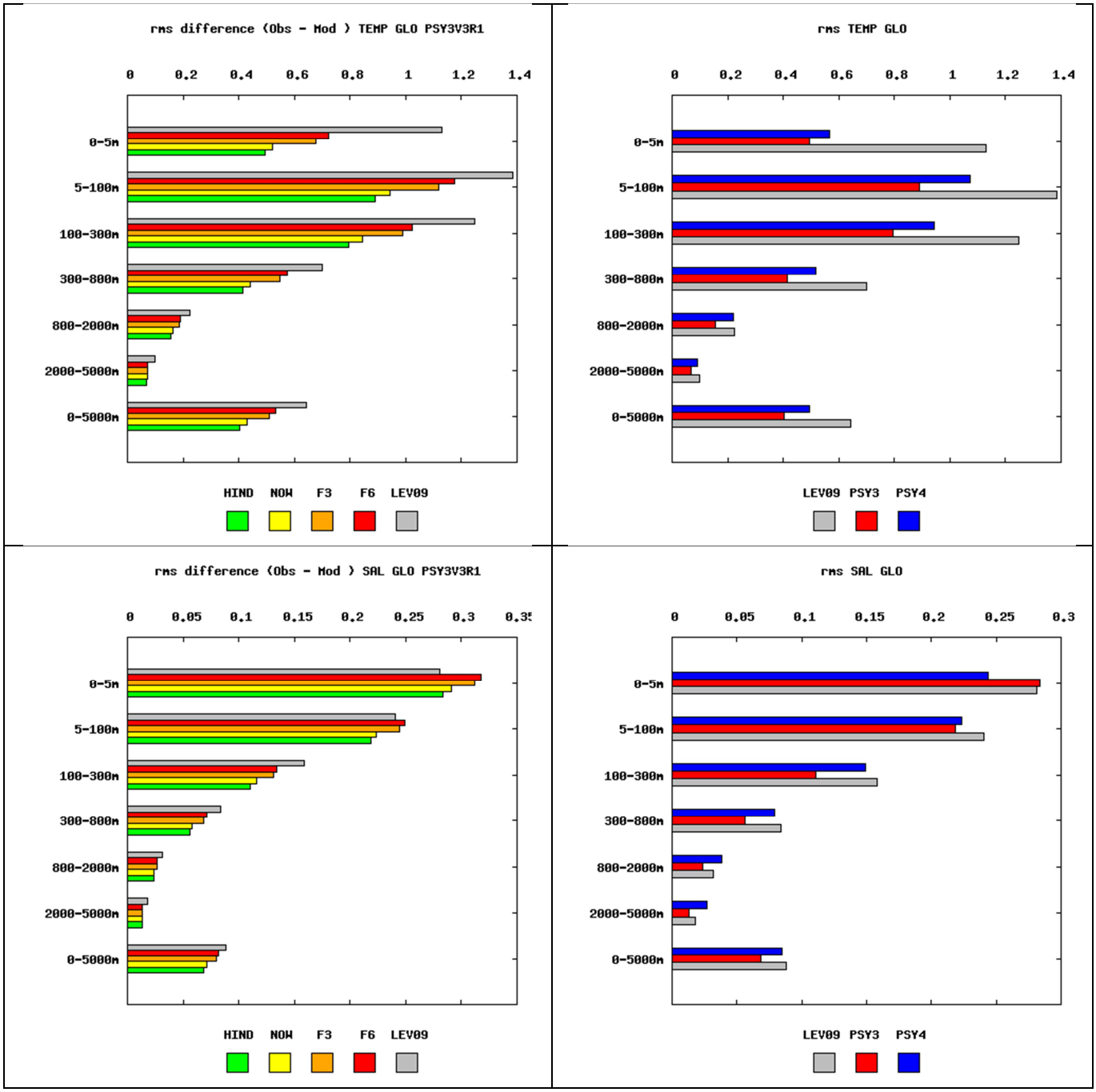

Figure 53: same as Figure 51 but for RMS statistics and for temperature (°C), PSY3V3R1 and PSY4V1R3 systems and the Tropical Atlantic (TAT), the Tropical Pacific (TPA) and the Indian Ocean (IND). The global statistics (GLO) are also shown for temperature and salinity (psu). The right column compares the analysis of the global ¼° PSY3 with the analysis of the global 1/12° PSY4 available at the end of December 2011.

VI.3. Forecast verification: comparison with analysis everywhere

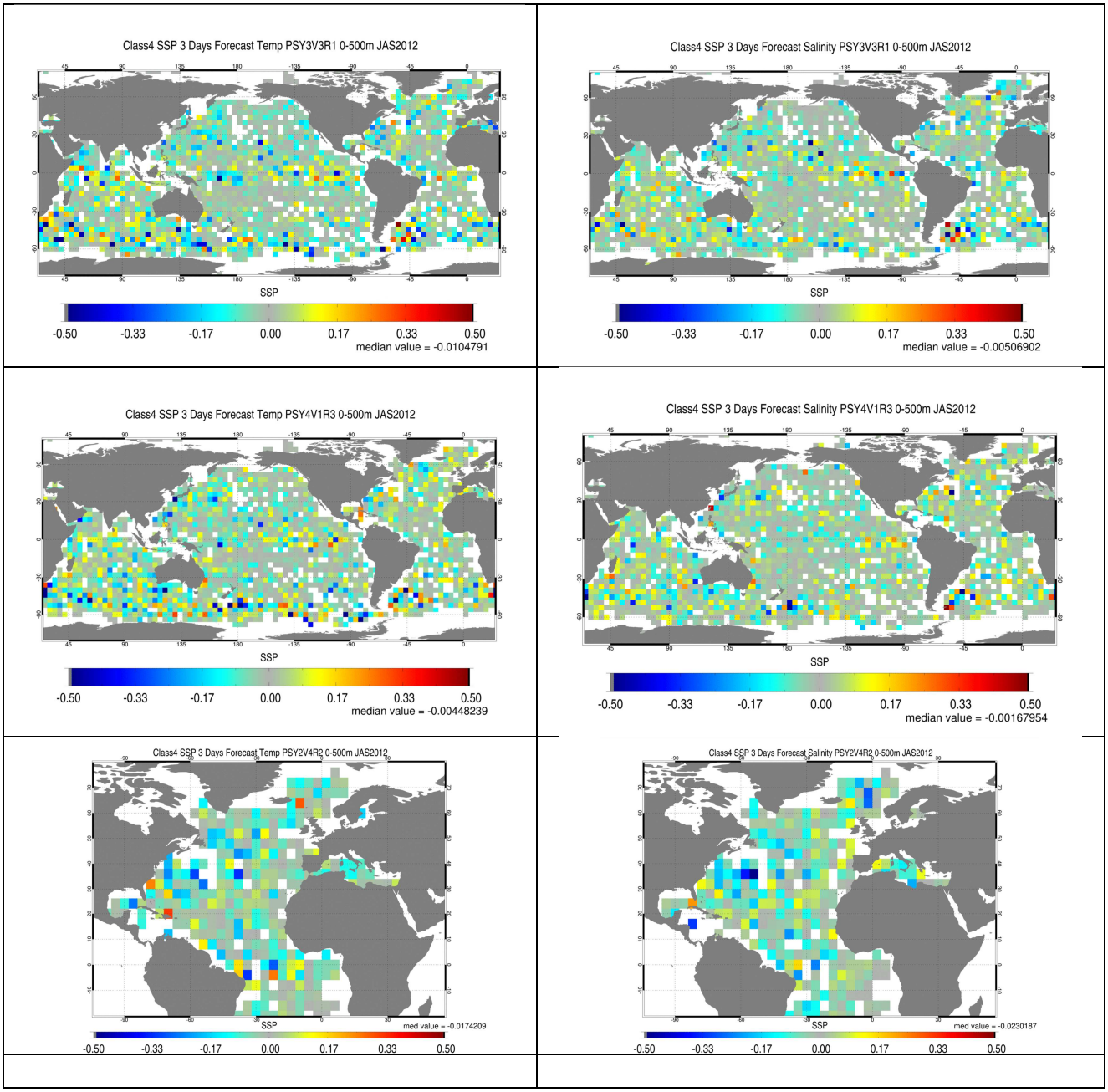

Figure 54: Temperature (left) and salinity (right) skill scores in 4°x4° bins and in the 0-500m layer in JAS 2012, illustrating the ability of the 3-days forecast to be closer to in situ observations than a reference state (climatology or persistence of the analysis, see Equation 1). Yellow to red values indicate that the forecast is more accurate than the reference. Here the reference value is the persistence of the analysis. Upper panel: PSY3V3R1; middle panel: PSY4V1R3; lower panel: PSY2V4R2.

The Murphy Skill Score (see Equation 1) is described by Wilks, *Statistical Methods in the Atmospheric Sciences*, Academic Press, 2006. This score is close to 0 if the forecast is equivalent to the reference. It is positive and aims towards 1 if the forecast is more accurate than the reference.

$$SS = 1 - \frac{\sum_{k=1}^{n}\left[\frac{1}{M}\sum_{m=1}^{M}\left(Forecast_m - Obs_m\right)^2\right]}{\sum_{k=1}^{n}\left[\frac{1}{M}\sum_{m=1}^{M}\left(Ref_m - Obs_m\right)^2\right]}$$

Equation 1

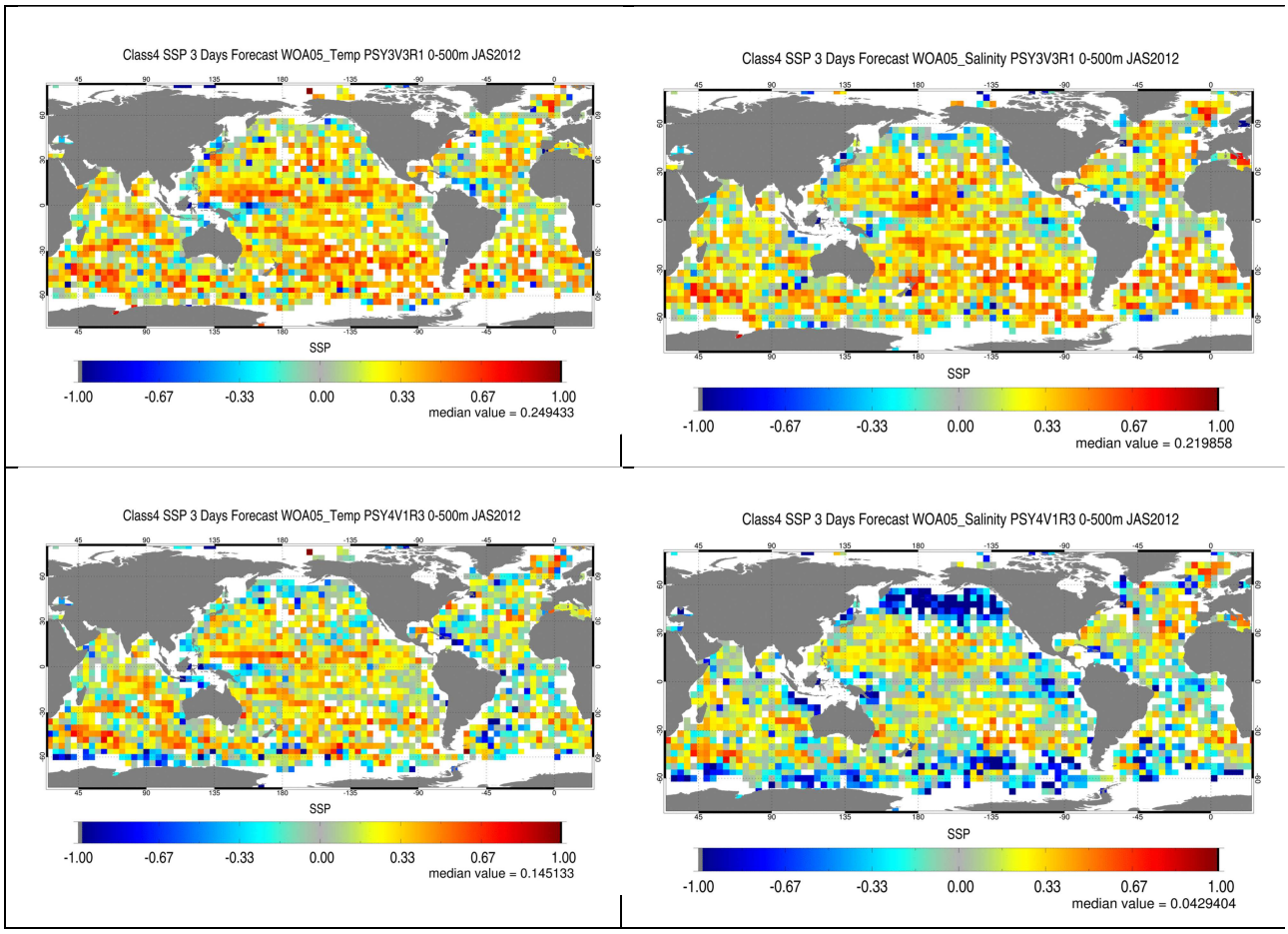

Figure 55 : As Figure 54 but the reference is the WOA 2005 climatology. Temperature (left column) and salinity (right column) skill scores are displayed, for PSY3V3R1 (upper panel) and for PSY4V1R3 (lower panel).

The Skill Score displayed on Figure 54 and Figure 55 show the added value of PSY3V3R1 forecast with respect to the climatology. All Mercator Ocean systems have a very good level of performance with respect to the climatology (see previous section). When the reference is the persistence of the last analysis, the result is noisier and the systems 3-day forecast seems to have skill in some regions in particular: North East Atlantic, central pacific, Indian basin and Tropical Atlantic. In some regions of high variability (for instance in the Antarctic, Gulf Stream, Agulhas Current, Zapiola) the persistence of the previous analysis is locally more accurate than the forecast. As expected PSY4V1R3 displays less forecast skill than the other systems with respect to the climatology, at least in terms of water masses (forecast skills with respect to other types of observations have to be computed in the future). This is especially the case in the Antarctic near the sea ice limit, in the Bering Sea, in the Zapiola anticyclone and in the Caribbean Sea.

The PSY3V3R1 "forecast errors" illustrated by the sea surface temperature and salinity RMS difference between the forecast and the hindcast for all given dates of July-August-September 2012 are displayed in Figure 56. The values on most of the global domain do not exceed 1°C and 0.2 PSU. In regions of high variability like the western boundary currents, the Circumpolar current, Zapiola eddy, Agulhas current, Gulf Stream, Japan Sea and Kuroshio region the errors reach around 3°C or 0.5 PSU. For salinity, the error can exceed 1 PSU in regions of high runoff (Gulf of Guinea, Bay of Bengal, Amazon, Sea Ice limit) or precipitations (ITCZ, SPCZ).

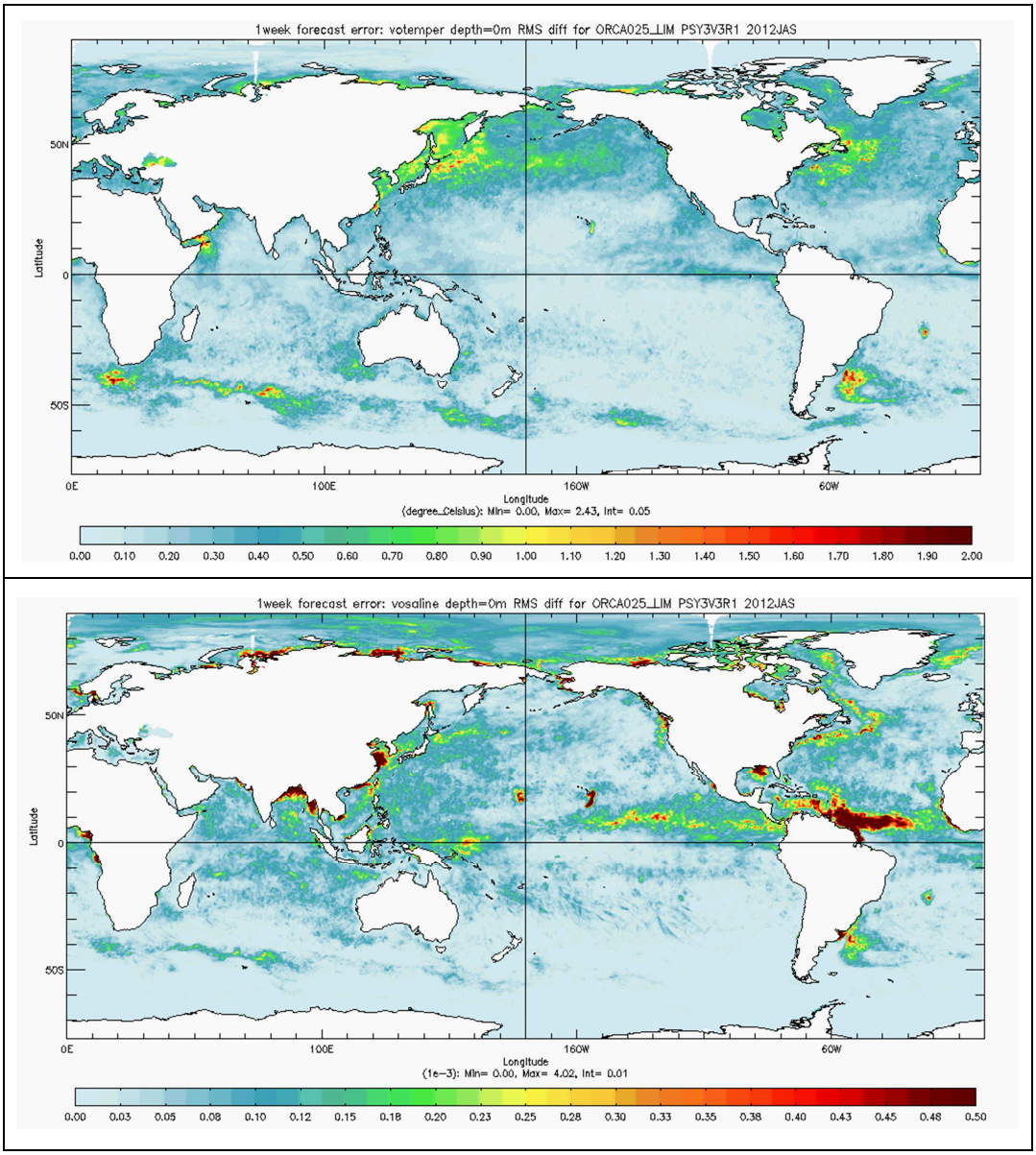

Figure 56: comparison of the sea surface temperature (°C, upper panel) and salinity (PSU, lower panel) forecast – hindcast RMS differences for the 1 week range for the PSY3V3R1 system for the JAS 2012 period.

VII Monitoring of ocean and sea ice physics

VII.1. Global mean SST and SSS

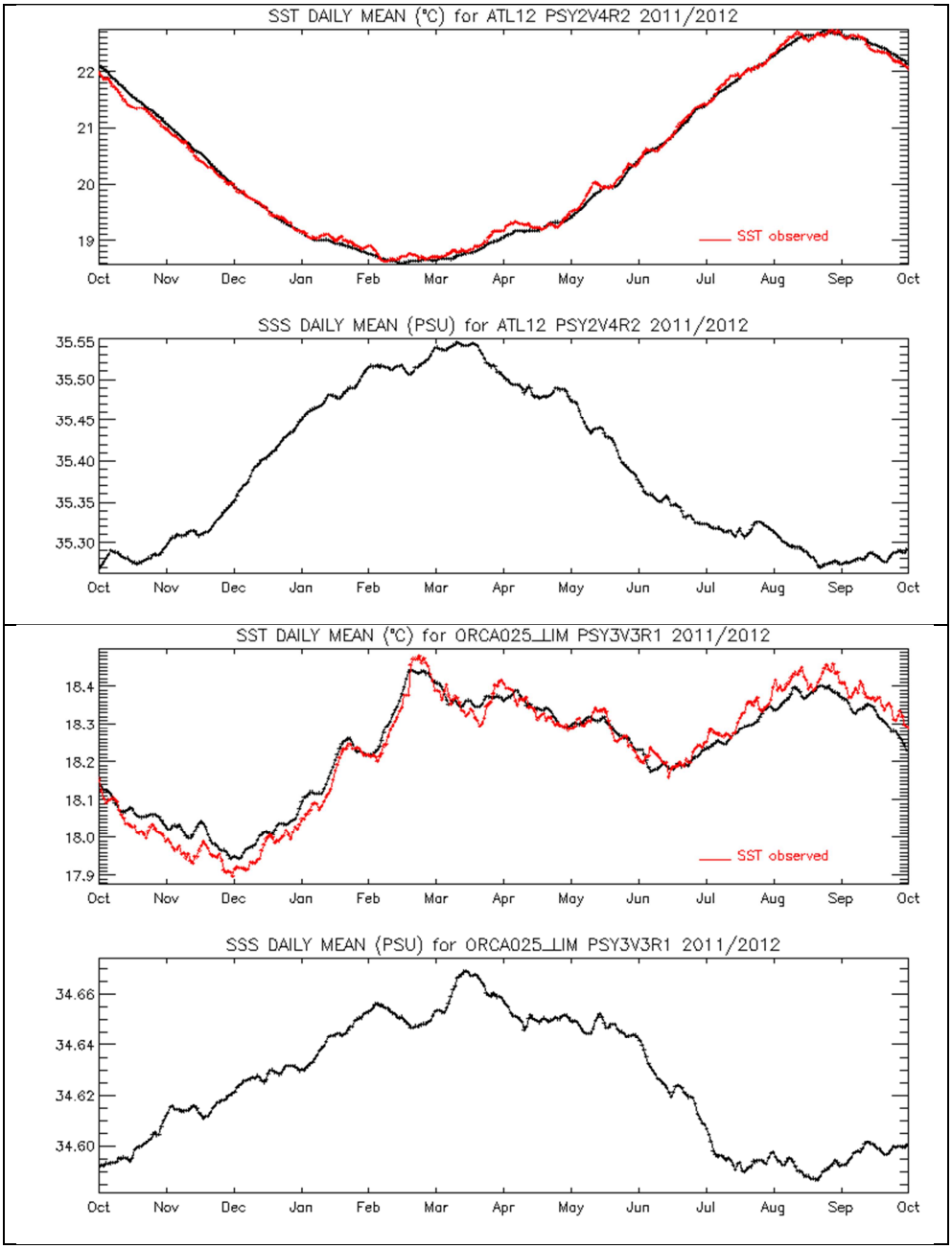

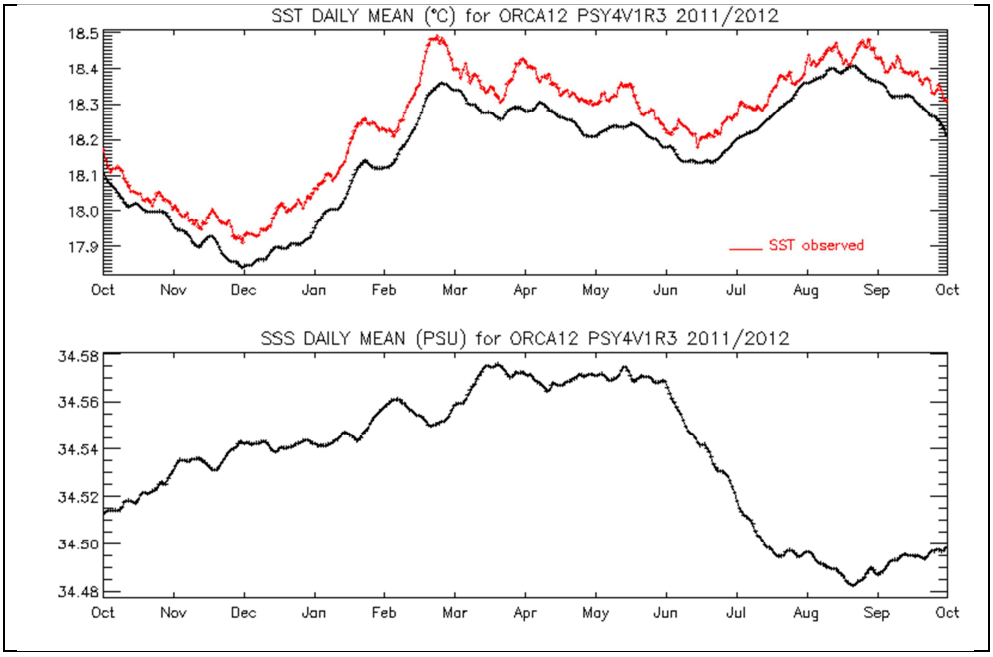

Figure 57: daily SST (°C) and salinity (psu) spatial mean for a one year period ending in JAS 2012, for Mercator Ocean systems (in black) and RTG-SST observations (in red). Upper: PSY2V4R2, middle: PSY3V3R1, lower: PSY4V1R3.

The spatial means of SST and SSS are computed for each day of the year, for PSY2V4R2, PSY3V3R1 and PSY4V1R3 systems. The mean SST is compared to the mean of RTG-SST on the same domain (Figure 57), except for PSY2V4R2 where it is compared with Reynolds AVHRR SST.

The main feature is the good agreement of PSY2V4R2 and Reynolds SST, and of PSY3V3R1 and RTG-SST on global average. On the contrary the global mean of PSY4V1R3 SST is biased of about 0.1°C all year long, consistently with data assimilation scores of section V.1.2. This bias is mainly located in the tropics which are too cold on average. Paradoxically, local departures from RTG-SST are much stronger in PSY3V3R1 (more than 2°C at the peak of the seasonal bias) than in PSY4V1R3 (not shown).

VII.2. Surface EKE

Regions of high mesoscale activity are diagnosed in Figure 58: Kuroshio, Gulf Stream, Niño 3 region in the central Equatorial pacific, Zapiola eddy, Agulhas current. The mesoscale activity is reduced in the equatorial regions with respect to the previous JFM season, especially in the Indian and Pacific basins. PSY3V3R1 at ¼° and PSY4V1R3 at 1/12° are in very good agreement. EKE is generally higher in the high resolution PSY4V1R3 system, for instance in the subtropical gyres.

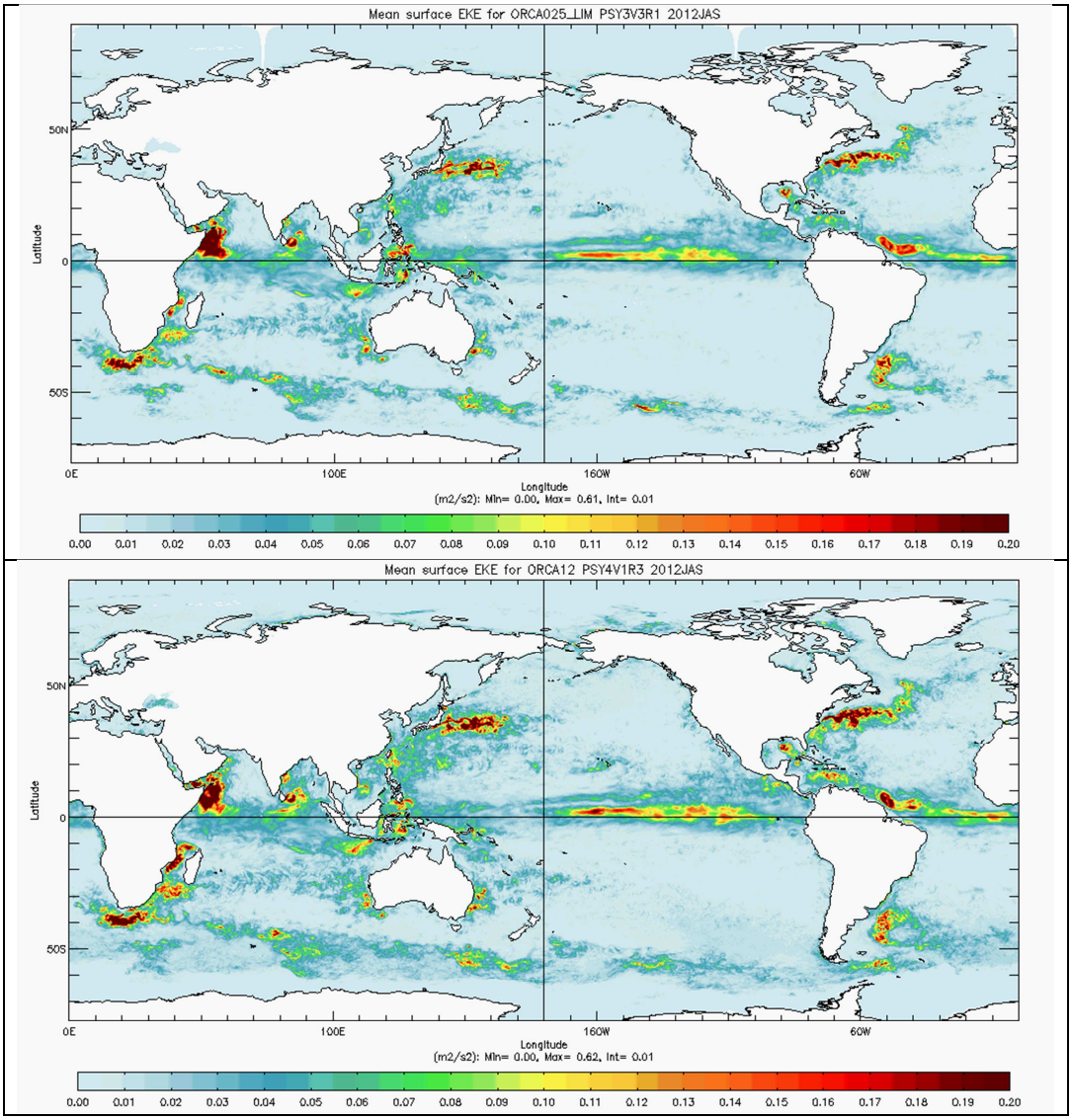

Figure 58: surface eddy kinetic energy EKE (m^2/s^2) for PSY3V3R1 (upper panel) and PSY4V1R3 (lower panel) for JAS 2012.

VII.3. Mediterranean outflow

In PSY3V3R1 the Mediterranean outflow is too shallow with respect to the climatology in the Gulf of Cadiz. Anyway, consistently with Figure 33, the outflow is better reproduced by PSY3V3R1 than by PSY4V1R3. The Mediterranean outflow of PSY2V4R2 (with high resolution and bias correction) is the most realistic of all systems.

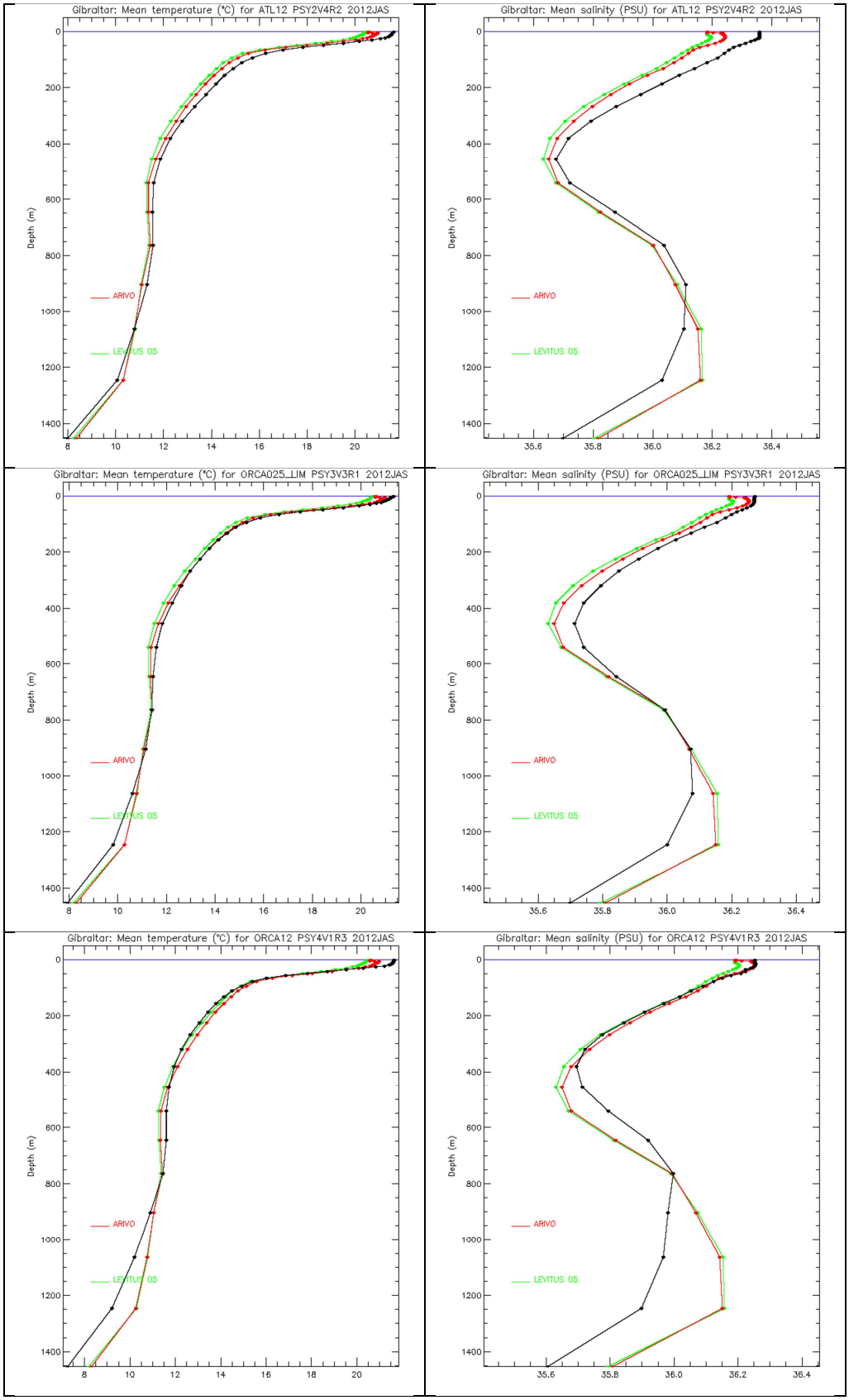

Figure 59: Comparisons between JAS 2012 mean temperature (°C, left panel) and salinity (psu, right panel) profiles in PSY2V4R2, PSY3V3R1 and PSY4V1R3 (from top to bottom, in black), and in the Levitus WOA05 (green) and ARIVO (red) monthly climatologies.

VII.4. Sea Ice extent and area

The time series of monthly means of sea ice area and sea ice extent (area of ocean with at least 15% sea ice) are displayed in Figure 60 and compared to SSM/I microwave observations. Both ice extent and area include the area near the pole not imaged by the sensor. NSIDC web site specifies that it is assumed to be entirely ice covered with at least 15% concentration. This area is 0.31 million square kilometres for SSM/I.

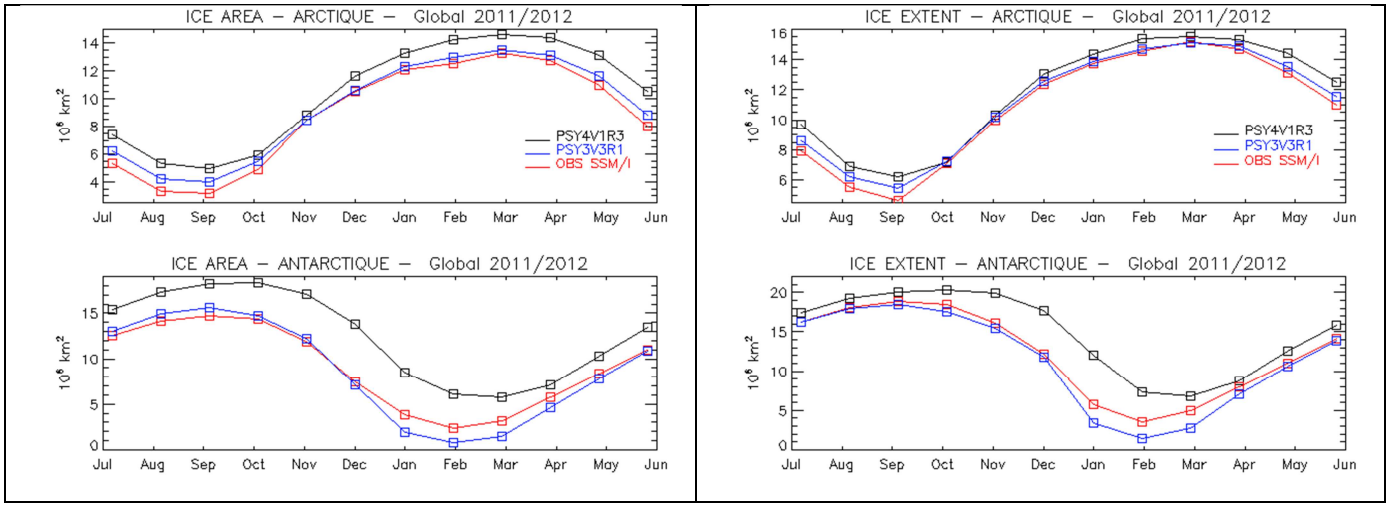

Figure 60: Sea ice area (left panel, 10^6 km2) and extent (right panel, 10^6 km2) in PSY3V3R1(blue line), PSY4V1R3 (black line) and SSM/I observations (red line) for a one year period ending in JAS 2012, in the Arctic (upper panel) and Antarctic (lower panel).

These time series indicate that sea ice products from PSY4V1R3 are generally less realistic than PSY3V3R1 products. This is partly due to the use of two different dynamics in the two models. PSY4V1R3 sea ice cover is overestimated throughout the year. The accumulation of multiannual Sea Ice in the Central arctic is overestimated by the models and especially by PSY4V1R3 all year long (see Figure 38). PSY4V1R3 overestimates the sea ice area and extent in boreal summer, while PSY3V3R1 ice area and extent are slightly underestimated. In boreal winter, PSY3V3R1 performs very well, with respect to observations.

I Annex A

I.1. Table of figures

Figure 1: schematic of the operational forecast scenario for IBI36QV1 (green) and PSY2QV4R1 (blue). Solid lines are the PSY2V4R1 weekly hindcast and nowcast experiments, and the IBI36V1 spin up. Dotted lines are the weekly 14-day forecast, dashed lines are daily updates of the ocean forecast forced with the latest ECMWF atmospheric analysis and forecast. The operational scenario of PSY3V3R1 and PSY3QV3R1 is similar to PSY2's scenario. In the case of PSY4V1R3, only weekly hindcast, nowcast and 7-day forecast are performed..... 8
Figure 2: schematic of the operational forecast scenario for BIOMER.. 9
Figure 3: bathymetry (m) of IBI36V2R1. On the left : around British isles ; on the right : zoom on the red rectangle on the left figure. The red circle points out the point where the model crashes. 10
Figure 4 :the shlat parameter is changed inside the red zone 10
Figure 5 : surface velocities (m/s) on 29 August 2012. 10
Figure 6 : Depth-time diagram of the number of observations of temperature (left column) and salinity (right column) assimilated each week in PSY3V3R1 during the JAS 2012 quarter. 11
Figure 7: Seasonal JAS 2012 temperature anomalies with respect to WOA05 (World Ocean Atlas from Levitus 2005) climatology. Upper panel: SST anomaly (°C) at the global scale from the 1/4° ocean monitoring and forecasting system PSY3V3R1. Lower panel heat content anomaly ($\rho_0 C_p \Delta T$, with constant ρ_0=1020 kg/m3) from the surface to 300m. 13
Figure 8: Arctic sea ice extent from the NSIDC: http://nsidc.org/arcticseaicenews/files/2000/11/Figure2.png..... 14
Figure 9: Comparison of SLA data assimilation scores (left: average misfit in cm, right: RMS misfit in cm) in JAS 2012 and between all available Mercator Ocean systems in the Tropical and North Atlantic. The scores are averaged for all available satellite along track data (Jason 1 G, Jason 2, Cryosat 2 and Envisat). For each region the bars refer respectively to PSY2V4R2 (cyan), PSY3V3R1 (green), PSY4V1R3 (orange). The geographical location of regions is displayed in annex A. 15
Figure 10: Comparison of SLA data assimilation scores (left: average misfit in cm, right: RMS misfit in cm) in JAS 2012 for PSY2V4R2. The scores are averaged for all available satellite along track data (Jason 1 G, Jason 2, Cryosat 2 and Envisat). See annex B for geographical location of regions. 16
Figure 11: Comparison of SLA data assimilation scores (left: average misfit in cm, right: RMS misfit in cm) in JAS 2012 and between all available global Mercator Ocean systems in all basins but the Atlantic and Mediterranean: PSY3V3R1 (green) and PSY4V1R3 (orange). The scores are averaged for all available satellite along track data (Jason 1 G, Jason 2, Cryosat 2 and Envisat). The geographical location of regions is displayed in annex B..... 17
Figure 12: Comparison of RTG-SST data assimilation scores (left: average misfit in °C, right: RMS misfit in °C) in JAS 2012 and between all available Mercator Ocean systems in the Tropical and North Atlantic: PSY4V1R3 (orange), PSY3V3R1 (green). In cyan: Reynolds ¼°AVHRR-AMSR-E data assimilation scores for PSY2V4R2. The geographical location of regions is displayed in annex B. 18
Figure 13: Comparison of SST data assimilation scores (left: average misfit in °C, right: RMS misfit in °C) in JAS 2012 for each region for PSY2V4R2 (comparison with Reynolds ¼° AVHRR-AMSR). The geographical location of regions is displayed in annex B. 18
Figure 14: Comparison of RTG-SST data assimilation scores (left: average misfit in °C, right: RMS misfit in °C) in JAS 2012 and between all available global Mercator Ocean systems in all basins but the Atlantic and Mediterranean: PSY3V3R1 (green) and PSY4V1R3 (orange). See annex B for geographical location of regions. 19
Figure 15: Profiles of JAS 2012 innovations of temperature (°C, left panel) and salinity (psu, right panel), mean (solid line) and RMS (dotted line) for PSY3V3R1 in red and PSY4V1R3 in blue in North Pacific gyre region. The geographical location of regions is displayed in annex B. 20

Figure 16: Profiles of JAS 2012 innovations of temperature (°C, left panel) and salinity (psu, right panel), mean (solid line) and RMS (dotted line) for PSY3V3R1 in red and PSY4V1R3 in blue in South Atlantic gyre region. The geographical location of regions is displayed in annex B. 21
Figure 17: Profiles of JAS 2012 innovations of temperature (°C, left panel) and salinity (psu, right panel), mean (solid line) and RMS (dotted line) for PSY3V3R1 (in red) and PSY4V1R3 (in blue) in the Indian Ocean region. The geographical location of regions is displayed in annex B. 22
Figure 18: Profiles of JAS 2012 innovations of temperature (°C, left panel) and salinity (psu, right panel), mean (solid line) and RMS (dotted line) for PSY4V1R3 in blue, PSY3V3R1 in red, and PSY2V4R2 in yellow in North Madeira region. The geographical location of regions is displayed in annex B. 23
Figure 19: Profiles of JAS 2012 innovations of temperature (°C, left panel) and salinity (psu, right panel), mean (solid line) and RMS (dotted line) for PSY4V1R3 in blue, PSY3V3R1 in red, and PSY2V4R2 in yellow in Dakar region. The geographical location of regions is displayed in annex B. 23
Figure 20: Profiles of JAS 2012 innovations of temperature (°C, left panel) and salinity (psu, right panel), mean (solid line) and RMS (dotted line) for PSY4V1R3 in blue, PSY3V3R1 in red, and PSY2V4R2 in yellow in Gulf Stream 2 region. The geographical location of regions is displayed in annex B. 24
Figure 21: Profiles of JAS 2012 innovations of temperature (°C, left panel) and salinity (psu, right panel), mean (solid line) and RMS (dotted line) for PSY4V1R3 in blue, PSY3V3R1 in red, and PSY2V4R2 in yellow in Cape Verde region. The geographical location of regions is displayed in annex B. 25
Figure 22: Profiles of JAS 2012 innovations of temperature (°C, left panel) and salinity (psu, right panel), mean (solid line) and RMS (dotted line) for PSY4V1R3 in blue, PSY3V3R1 in red, and PSY2V4R2 in yellow in Sao Tome region. The geographical location of regions is displayed in annex B. 25
Figure 23: Profiles of JAS 2012 mean (cyan) and RMS (yellow) innovations of temperature (°C, left panel) and salinity (psu, right panel) in the Algerian region. The geographical location of regions is displayed in annex B. 26
Figure 24: Profiles of JAS 2012 mean (cyan) and RMS (yellow) innovations of temperature (°C, left panel) and salinity (psu, right panel) in the Gulf of Lion region. The geographical location of regions is displayed in annex B. 27
Figure 25: Profiles of JAS 2012 mean (cyan) and RMS (yellow) innovations of temperature (°C, left panel) and salinity (psu, rightpanel) in the Rhodes region. The geographical location of regions is displayed in annex B. 27
Figure 26: RMS temperature (°C) difference (model-observation) in JAS 2012 between all available T/S observations from the Coriolis database and the daily average hindcast PSY3V3R1 products on the left and hindcast PSY4V1R3 on the right column colocalised with the observations. Averages are performed in the 0-50m layer (upper panel) and in the 0-500m layer (lower panel). The size of the pixel is proportional to the number of observations used to compute the RMS in 2°x2° boxes. 29
Figure 27: RMS salinity (psu) difference (model-observation) in JAS 2012 between all available T/S observations from the Coriolis database and the daily average hindcast PSY3V3R1 products on the left and hindcast PSY4V1R3 on the right column, colocalised with the observations. Averages are performed in the 0-50m layer (upper panel) and in the 0-500m layer (lower panel). The size of the pixel is proportional to the number of observations used to compute the RMS in 2°x2° boxes. 30
Figure 28 : JAS 2012 global statistics of temperature (°C, left column) and salinity (psu, right column) averaged in 6 consecutive layers from 0 to 5000m. RMS difference (upper panel) and mean difference (observation-model, lower panel) between all available T/S observations from the Coriolis database and the daily average hindcast PSY3V3R1 products (green) , hindcast PSY4V1R3 (red) and WOA09 climatology (blue) colocalised with the observations. NB: average on model levels is performed as an intermediate step which reduces the artefacts of inhomogeneous density of observations on the vertical. 31
Figure 29: Upper panel: RMS difference (model-observation) of temperature (°C) in JAS 2012 between all available T/S observations from the Coriolis database and the daily average PSY2V4R2 hindcast products colocalised with the observations in the 0-50m layer (left column) and 0-500m layer (right column). 32
Figure 30: Upper panel: RMS difference (model-observation) of salinity (psu) in the 0-50m layer in JAS 2012 between all available T/S observations from the Coriolis database and the daily average PSY2V4R2 hindcast products colocalised with the observations in the 0-50m layer (left column) and 0-500m layer (right column). 32

Figure 31: Water masses (Theta, S) diagrams in the Bay of Biscay (upper panel), Gulf of Lion (second panel) and Irminger Sea (third panel) and Baltic Sea (upper panel), comparison between PSY3V3R1 (left column) and PSY4V1R3 (middle column) and PSY2V4R2 (right column) in JAS 2012. PSY2, PSY3 and PSY4: yellow dots; Levitus WOA09 climatology: red dots; in situ observations: blue dots. 34
Figure 32 : Water masses (T, S) diagrams in the Western Tropical Atlantic (upper panel) and in the Eastern Tropical Atlantic (lower panel): for PSY3V3R1 (left); PSY4V1R3 (middle); and PSY2V4R2 (right) in JAS 2012. PSY2, PSY3 and PSY4: yellow dots; Levitus WOA09 climatology; red dots, in situ observations: blue dots. 35
Figure 33: Water masses (T, S) diagrams in South Africa, Kuroshio, and Gulf Stream region (respectively from top to bottom): for PSY3V3R1 (left); PSY4V1R3 (right) in JAS 2012. PSY3 and PSY4: yellow dots; Levitus WOA09 climatology: red dots; in situ observations: blue dots. 37
Figure 34 : RMS temperature (°C) differences between OSTIA daily analyses and PSY3V3R1 daily analyses (upper left); between OSTIA and PSY4V1R3 (upper right), between OSTIA and PSY2V4R2 (lower left), and between OSTIA and RTG daily analyses (lower right). The Mercator Océan analyses are colocalised with the satellite observations analyses. 38
Figure 35: Mean SST (°C) daily differences between OSTIA daily analyses and PSY3V3R1 daily analyses (upper left), between OSTIA and RTG daily analyses (upper right) and between OSTIA and Reynolds ¼° AVHRR daily analyses (lower left). 39
Figure 36: Comparison between modelled zonal current (left panel) and zonal current from drifters (right panel) in m/s. In the left column: velocities collocated with drifter positions in JAS 2012 for PSY3V3R1 (upper panel), PSY4V1R3 (middle panel) and PSY2V4R2 (bottom panel). In the right column, zonal current from drifters in JAS 2012 (upper panel) at global scale, AOML drifter climatology for JAS with new drogue correction from Lumpkin & al, in preparation (middle) and zonal current in JAS 2012 from drifters (lower panel) at regional scale. 40
Figure 37 : In JAS 2012, comparison of the mean relative velocity error between in situ AOML drifters and model data on the left side and mean zonal velocity bias between in situ AOML drifters with Mercator Océan correction (see text) and model data on the right side. Upper panel: PSY3V3R1, middle panel: PSY4V1R3, bottom panel : PSY2V4R2. NB: zoom at 500% to see the arrows 41
Figure 38: Comparison of the sea ice cover fraction mean for JAS 2012 for PSY3V3R1 in the Arctic (upper panel) and in the Antarctic (lower panel), for each panel the model is on the left, the mean of Cersat dataset in the middle and the difference on the right. 42
Figure 39: Comparison of the sea ice cover fraction mean for JAS 2012 for PSY4V1R3 in the Arctic (upper panel) and in the Antarctic (lower panel), for each panel the model is on the left, the mean of Cersat dataset in the middle and the difference on the right. 43
Figure 40: JAS 2012 Arctic sea ice extent in PSY3V3R1 with overimposed climatological JAS 1992-2010 sea ice fraction (magenta line, > 15% ice concentration) (left) and NSIDC map of the sea ice extent in the Arctic for June 2012 in comparison with a 1979-2000 median extend (right). 44
Figure 41 : Comparisons (observation-model) between IBI36V2 and analysed SST from MF_CMS for the JAS 2012 period. From the left to the right: mean bias, RMS error, correlation, number of observations 45
Figure 42 : For IBI36V2: On the left: mean “model - observation” temperature(°C) bias (red curve) and RMS error (blue curve) in JAS 2012, On the right: mean profile of the model (black curve), of the observations (red curve), and of the PSY2V4R2 model (green curve) in JAS 2012. In the lower right corner: position of the profiles. Top panel: the whole domain; bottom panel: the Bay of Biscay region. 46
Figure 43: For IBI36V2: On the left: mean “model - observation” salinity (psu) bias (red curve) and RMS error (blue curve) in JAS 2012, On the right: mean profile of the model (black curve), of the observations (red curve), and of the PSY2V4R2 model (green curve) in JAS 2012. In the lower right corner: position of the profiles. Top panel: the whole domain; bottom panel: the Bay of Biscay region. 47
Figure 44 : For IBI36V2 (top panels): Mixed Layer Depth distribution in JAS 2012 calculated from profiles with the temperature criteria (difference of 0.2°C with the surface); the model is in grey, the observations in red. Left panel: whole domain; right panel: Bay of Biscay. Bottom panel: the same for PSY2V4R2. 48
Figure 45 : For IBI36V2: RMS error (cm) and correlation for the non-tidal Sea Surface Elevation at tide gauges in JAS 2012, for different regions and frequencies. 48

Figure 46 : For IBI36V2: Bias (observation-model), RMS error (°C) and correlation of the Sea Surface Temperature between IBI model and moorings measurements in July (upper panel), August (middle panel) and September 2012 (lower panel)..... 49
Figure 47 : Chlorophyll-a concentration (mg/m^3) for the Mercator system BIOMER (left panels) and Chlorophyll-a concentration from Globcolour (right panels). The upper panel is for July, the medium panel is for August and the bottom panel is for September 2012. 50
Figure 48 : Probability Density Function (PDF) of Chl-a bias in log scale (log10(obs)-log10(model)) in North Atlantic (30-70N; 80W:20E) 51
Figure 49 : RMS difference between BIOMER and Globcolour Chl-a concentrations (mg/m^3) in JAS 2012. 51
Figure 50: Schematic of the change in atmospheric forcings applied along the 14-day ocean forecast. 52
Figure 51: Accuracy intercomparison in the North Atlantic region for PSY2V4R2 in temperature (left panel) and salinity (right panel) between hindcast, nowcast, 3-day and 6-day forecast and WO09 climatology. Accuracy is measured by a mean difference (upper panel) and by a rms difference (lower panel) of temperature and salinity with respect to all available observations from the CORIOLIS database averaged in 6 consecutive layers from 0 to 5000m. All statistics are performed for the JAS 2012 period. NB: average on model levels is performed as an intermediate step which reduces the artefacts of inhomogeneous density of observations on the vertical. 53
Figure 52: Accuracy intercomparison in the Mediterranean Sea region for PSY2V4R2 in temperature (°C, left column) and salinity (psu, right column) between hindcast, nowcast, 3-day and 6-day forecast and WO09 climatology. Accuracy is measured by a rms difference (lower panel) and by a mean difference (upper panel) with respect to all available observations from the CORIOLIS database averaged in 6 consecutive layers from 0 to 5000m. All statistics are performed for the JAS 2012 period. NB: average on model levels is performed as an intermediate step which reduces the artefacts of inhomogeneous density of observations on the vertical. 54
Figure 53: same as Figure 51 but for RMS statistics and for temperature (°C), PSY3V3R1 and PSY4V1R3 systems and the Tropical Atlantic (TAT), the Tropical Pacific (TPA) and the Indian Ocean (IND). The global statistics (GLO) are also shown for temperature and salinity (psu). The right column compares the analysis of the global ¼° PSY3 with the analysis of the global 1/12° PSY4 available at the end of December 2011. 57
Figure 54: Temperature (left) and salinity (right) skill scores in 4°x4° bins and in the 0-500m layer in JAS 2012, illustrating the ability of the 3-days forecast to be closer to in situ observations than a reference state (climatology or persistence of the analysis, see Equation 1). Yellow to red values indicate that the forecast is more accurate than the reference. Here the reference value is the persistence of the analysis. Upper panel: PSY3V3R1; middle panel: PSY4V1R3; lower panel: PSY2V4R2. 58
Figure 55 : As Figure 54 but the reference is the WOA 2005 climatology. Temperature (left column) and salinity (right column) skill scores are displayed, for PSY3V3R1 (upper panel) and for PSY4V1R3 (lower panel). 59
Figure 56: comparison of the sea surface temperature (°C, upper panel) and salinity (PSU, lower panel) forecast – hindcast RMS differences for the 1 week range for the PSY3V3R1 system for the JAS 2012 period. 60
Figure 57: daily SST (°C) and salinity (psu) spatial mean for a one year period ending in JAS 2012, for Mercator Ocean systems (in black) and RTG-SST observations (in red). Upper: PSY2V4R2, middle: PSY3V3R1, lower: PSY4V1R3. 62
Figure 58: surface eddy kinetic energy EKE (m^2/s^2) for PSY3V3R1 (upper panel) and PSY4V1R3 (lower panel) for JAS 2012. 63
Figure 59: Comparisons between JAS 2012 mean temperature (°C, left panel) and salinity (psu, right panel) profiles in PSY2V4R2, PSY3V3R1 and PSY4V1R3 (from top to bottom, in black), and in the Levitus WOA05 (green) and ARIVO (red) monthly climatologies. 64
Figure 60: Sea ice area (left panel, 10^6 km2) and extent (right panel, 10^6 km2) in PSY3V3R1(blue line), PSY4V1R3 (black line) and SSM/I observations (red line) for a one year period ending in JAS 2012, in the Arctic (upper panel) and Antarctic (lower panel). 65
Figure 61 : illustration of QC: Quality test example chosen for windage (eg. 1%) we reject or correct a drift that differs little from the windage (less than 70% of the drift angle <40 °) 73

II Annex B

II.1. Maps of regions for data assimilation statistics

II.1.1. Tropical and North Atlantic

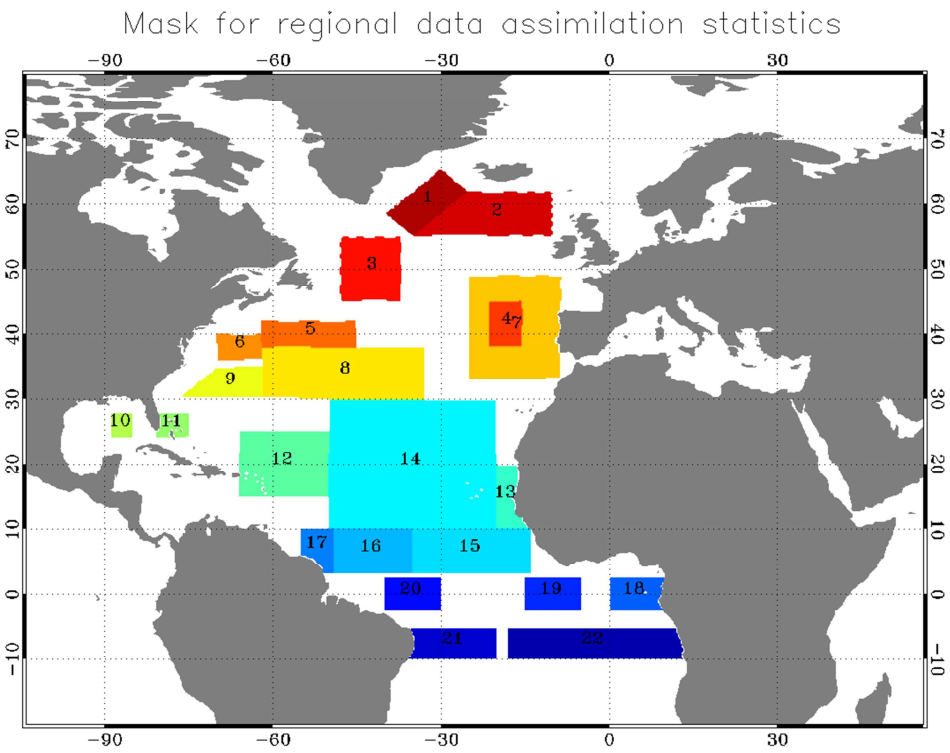

1	Irminger Sea
2	Iceland Basin
3	Newfoundland-Iceland
4	Yoyo Pomme
5	Gulf Stream2
6	Gulf Stream1 XBT
7	North Medeira XBT
8	Charleston tide
9	Bermuda tide
10	Gulf of Mexico
11	Florida Straits XBT
12	Puerto Rico XBT
13	Dakar
14	Cape Verde XBT
15	Rio-La Coruna Woce
16	Belem XBT
17	Cayenne tide
18	Sao Tome tide
19	XBT - central SEC
20	Pirata
21	Rio-La Coruna
22	Ascension tide

II.1.2. Mediterranean Sea

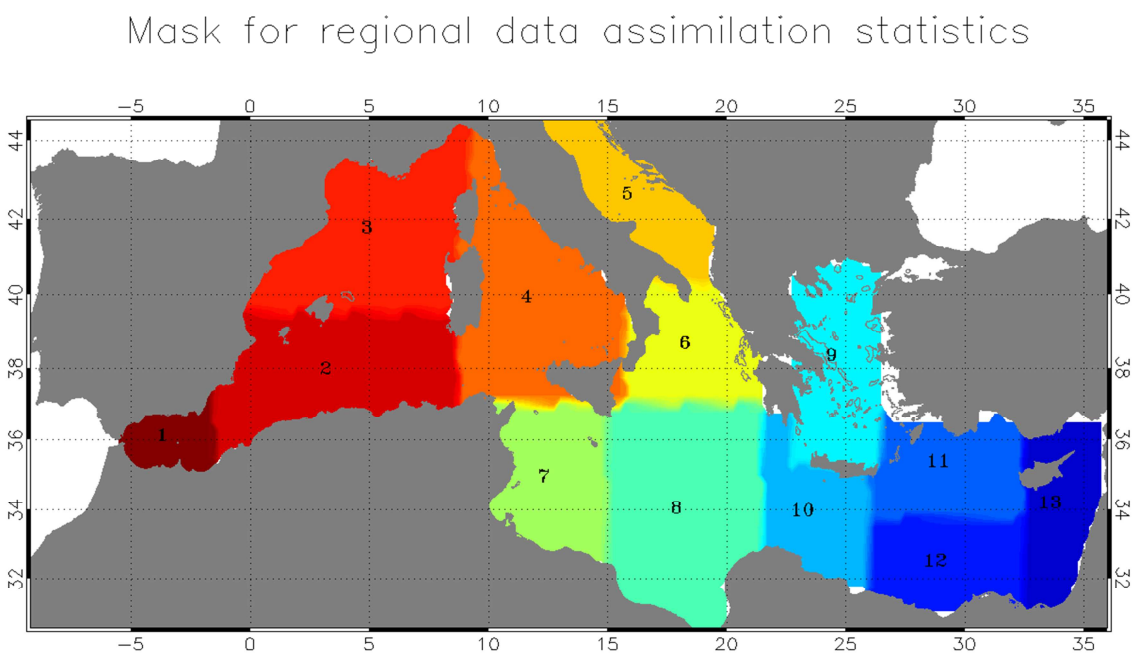

1	Alboran
2	Algerian
3	Lyon
4	Thyrrhenian
5	Adriatic
6	Otranto
7	Sicily
8	Ionian
9	Egee
10	Ierepetra
11	Rhodes
12	MersaMatruh
13	Asia Minor

II.1.3. Global ocean

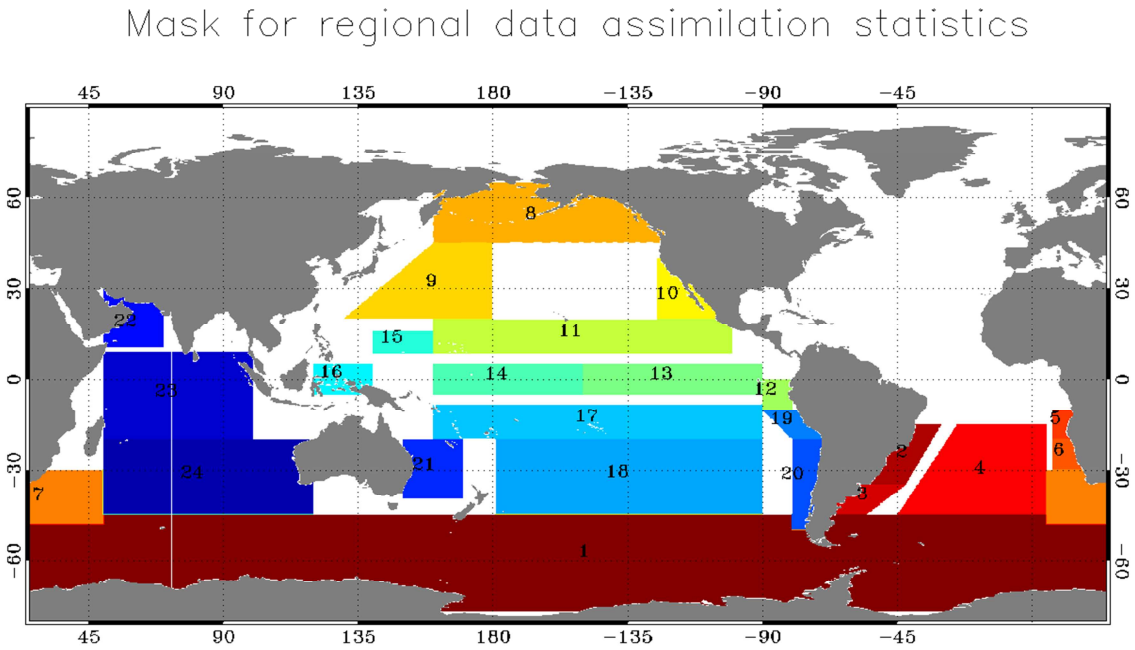

1	Antarctic Circumpolar Current
2	South Atlantic
3	Falkland current
4	South Atl. gyre
5	Angola
6	Benguela current
7	Aghulas region
8	Pacific Region
9	North Pacific gyre
10	California current
11	North Tropical Pacific
12	Nino1+2
13	Nino3
14	Nino4
15	Nino6
16	Nino5
17	South tropical Pacific
18	South Pacific Gyre
19	Peru coast
20	Chile coast
21	Eastern Australia
22	Indian Ocean
23	Tropical indian ocean
24	South indian ocean

III Annex C

III.1. Quality control algorithm for the Mercator Océan drifter data correction (Eric Greiner)

Before estimating the bias, it is essential to conduct a quality control. We must consider an individual monitoring of buoys, and a comparison with the geostrophy and windage. In real time, this is not possible, and I propose below a simple test developed by position (date by date) which involves only the mean wind (2 days) and the buoy drift. Basically, we found drifters where drift is close to argue between 0.2 and 3% of the wind (almost the same direction with a drag corresponding to a loss of drogue). For these buoys, if the contamination is real, then the error due to the wind is important with respect to current real at 15m depth. We test different values of windage (wind effect for a fraction of a given wind between 0.2% and 3%). If a questionable observation is found for a given windage, we estimate a correction. We apply at the end an average correction QC (windage among all acceptable). We although increase the error of observation. Note that in delayed time, we could correct all the data from the buoy, at least in a 10-day window. **Note however that a buoy that has lost its drogue can give a good measure if the wind is low**

- **No anomaly : slippage correction of 0.07% of the 10m wind speed**
- **Windage > 0.2% or < 3% correction of 1% of windage**

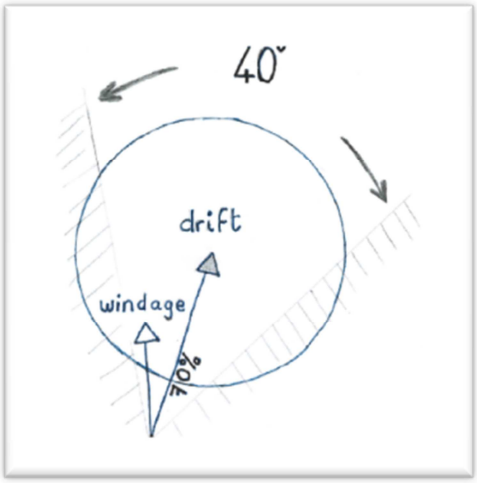

Figure 61 : illustration of QC: Quality test example chosen for windage (eg. 1%) we reject or correct a drift that differs little from the windage (less than 70% of the drift angle <40 °)

Note that a correction of more than 3% is not normally possible (construction of the buoy). This may correspond to breaking waves and swell. Between 2% and 3%, there is ambiguity between Stokes and windage. In other words, it is likely that beyond 2%, we eliminate all or part of the effect of waves and swell. If waves and swell are not aligned with the mean wind (swell remote for example), then the correction will be approximate. Ideally, you should use the Stokes drift from a wave model like Wavewatch3.

When calculating the equivalent models with AOML positions, which were filtered to remove 36h gravity waves and reduce positioning errors, we must :

- **add 0.07% wind averaged over 48h 10m : slippage correction**
- **windage correction and modify the error**